DEPARTMENT OF CHEMISTRY, UNIVERSITY OF JYVÄSKYLÄ
RESEARCH REPORT No. 209

BENEFICIATION, DESILICATION AND SELECTIVE PRECIPITATION TECHNIQUES FOR PHOSPHORUS REFINING FROM BIOMASS DERIVED FLY ASH

BY
ROSHAN BUDHATHOKI

Academic Dissertation for the Degree of
Doctor of Philosophy

To be presented, by permission of the Faculty of Mathematics and Natural Science of the University of Jyväskylä, for public examination in Auditorium KEM4, on July 6th, 2018 at 12 noon.

UNIVERSITY OF JYVÄSKYLÄ

Jyväskylä, Finland
ISBN 978-951-39-7500-5 (print)
ISBN 978-951-39-7501-2 (electronic)
ISSN 0357-346X

Academic dissertation

Author's address

Roshan Budhathoki
Department of Chemistry
Renewable Natural Resources and
Chemistry of Living Environment
P.O. Box 35, FI-40014
University of Jyväskylä
Finland
roshan.budhathoki@jyu.fi

Supervisor

Docent Ari Väisänen
Department of Chemistry
University of Jyväskylä
Finland

Reviewers

Professor Mika Sillanpää
Department of Environmental Engineering
Lappeenranta University of Technology
Finland

Professor Ulla Lassi
Research Unit of Sustainable Chemistry
University of Oulu
Finland

Opponent

Assistant Professor Mari Lundström
Department of Chemical and Metallurgical Engineering
Aalto University
Finland

Abstract

Budhathoki, Roshan

Beneficiation, desilication and selective precipitation techniques for phosphorus refining from biomass derived fly ash

Jyväskylä: University of Jyväskylä, 2018, 64 p.
Department of Chemistry, University of Jyväskylä Research Report No. 209
ISSN 0357-346X
ISBN 978-951-39-7501-2

The supply of affordable phosphorus (P), a biocritical element, is at great risk due to the utilization of limited natural phosphate minerals at an unprecedented scale. The need of phosphorus recovery to sustain the anthropogenic P-cycle was recognized and fly ash, a waste product from the combustion of renewable biofuels, was selected as the secondary resource. Increasing supply of fly ash in the future due to growing use of forest biofuels in energy production also contributes to its suitability for P-recovery. Fly ash comprises of silicates, oxides, carbonates, phosphates and hydroxides of the elements that potentially represent the entire periodic table. This only augments the complexity of the recovery process, since most of the interfering matrices need to be removed prior to the extraction of phosphorus.

Methods for separation of impurities and extraction of the phosphorus were developed and optimized. The establishment of a relationship between the particle size and mineral content enables an elevation of the phosphorus level by a factor of 1.38, while the silicon (Si) content is reduced by a factor of 3.8 for a circulatory fluidized bed derived fly ash. This was achieved by the use of sieving beneficiation with a sieve size of 125 μm.

Despite the feasibility of fly ash leaching with a lower molar concentration of acid for efficient dissolution of phosphorus, higher concentration of HCl at 8 M was employed. Aging of this leachate for 5 h facilitates the removal of silica with an efficiency of 99% from the leachate solution by precipitation of Si-particles and/or Si-gel formation. The Si removal rate was found to vary proportionally with temperature and the H^+ and Cl^- ion concentration.

Chemical equilibrium calculations (in the Medusa & Hydra software) were used to identify the phosphate species in the leachate and to draft the P-recovery strategies. Selective precipitation of $AlPO_4$ was identified as a feasible method to recover phosphorus from the leachate. Interference of Fe was limited by the use of chelation-based masking with ethylenediaminetetraacetic acid (EDTA) at [EDTA]/[Fe]=1 and pH of 4. An amorphous white precipitant was obtained that comprises 18.1 wt% of P, 16.3 wt% of Al and 2.18 wt% of Fe as major components and also trace elements in low concentrations.

$AlPO_4$ was further converted to struvite; a slow releasing fertilizer. The process involved dissolution of solids with 0.5 M phosphoric acid, removal of Al and metal ion impurities with 0.6 g/mL of Amberlite IR120H^+ (a strongly cation exchange resin), addition of Mg^{2+} and $NH_4{}^+$sources and precipitation at pH 9.5. Prospects of leachate recirculation for leaching were also investigated to lower the use of fresh

phosphoric acid. Granulated white-pure crystalline struvites containing 12.5 wt% of P were obtained. The combination of refining and extraction technologies, employed in this study, contribute to elevate the P content in the final product by a factor of the order of 10. Procuring struvite. from biomass fly ash is seen as a sustainable P recycling method which promotes conservation of the natural resources used for fertilizer production.

Keywords: phosphorus recovery, fly ash, forest fertilizer, desilication, Si-gelation, EDTA chelation, precipitation, aluminium phosphate, struvite.

Preface

This work was accomplished between 2014 and 2018 at the Laboratory of Renewable Natural Resources and Chemistry of Living Environment, at the Department of Chemistry, University of Jyväskylä.

I owe my deepest gratitude to my supervisor, docent Ari Väisänen, for his continuous support, encouragement and advice during these years. I am also grateful for the freedom and trust I have received from him.

I would like to thank Professor Jukka Konttinen for giving me the opportunity to work in his group and pursue my doctoral study. I also wish to thank all my colleagues working at the Department of Chemistry. In particular, I would like to thank Dr. Siiri Perämäki for offering guidance and assistance with ICP-OES analysis during the initial days. I also thank Esa Lehtimäki, Enni Nygrén, Sini Reuna, Virva Kinnunen, Joona Rajahalme, Suvi Kulomäki and Elmeri Lahtinen for interesting discussions and good memories. Special thanks are committed to Jukka Pekka Isoaho, Hannu Salo and Manu Lahtinen for their help with experimental work, SEM analysis and XRD measurements.

Professor Mika Sillänpää and Professor Ulla Lassi are warmly acknowledged for their valuable comments on this thesis. I also thank Matti Nurmia for language revision.

I am grateful to my parents, sister Rojeena and niece Saanvi- you have been my constant source of encouragement and strength. I owe my deepest gratitude to my loving wife and best friend, Kreetika, whose support and trust is unwavering. Thank you for your unconditional love and being my inspiration. I am also grateful to my parents in-law and my late grandfather for their prayers and support. Last but not least, I also appreciate my dear friends and relatives for their love and regards.

List of publications

This thesis is based on the following publication:

I. R. Budhathoki, A. Väisänen, "Particle size based recovery of phosphorus from combined peat and wood fly ash for forest fertilization," *Fuel Processing Technology*, 2016, vol. 146, pp. 85-89, ISSN 0378-3820.

II. R. Budhathoki, A. Väisänen, "Removal of silicon from CFB-derived fly ash leachate in the context of phosphorous recovery," *Hydrometallurgy*, 2018, vol. 179, pp. 215-221, ISSN 0304-386X.

III. R. Budhathoki, A. Väisänen, and M. Lahtinen, "Selective recovery of phosphorus as $AlPO_4$ from silicon-free CFB-derived fly ash leachate," *Hydrometallurgy*, 2018, vol. 178, pp. 30–36, ISSN 0304-386X.

IV. R. Budhathoki, A. Väisänen, and M. Lahtinen, "Sustainable conversion of $AlPO_4$ derived from biomass fly ash into struvite by hydrometallurgical methods," -*Manuscript*, 2018

In all papers, the author has a major role in planning, method development, design and execution of experimental works, measurements, analysis of data and manuscripts preparation. Manu Lahtinen performed the XRD characterization, while Hannu Salo performed SEM-EDS analysis of solid samples in publication [III] and [IV].

Contents

List of abbreviations and symbols

AIR-120H	Amberlite® IR120 H^+
ANOVA	Analysis of variance
ATP	Adenosine triphosphate
ATR-IR	Attenuated total reflection Infrared
AxF	Auxiliary gas flow
BFB	Bubbling fluidized-bed
CCD	Central composite design
CER	Cation exchange resin
CFAP	Carbonate fluorapatite
CFB	Circulating fluidized-bed
CHN	Carbon Hydrogen Nitrogen
CHP	Combined heat and power
DFA	Discarded/rejected fly ash
DNA	Deoxyribonucleic acid
DOE	Design of experiment
EDS	Energy-dispersive X-ray spectroscopy
EDTA	Ethylenediaminetetraacetic acid
ER	Ratio of EDTA to sum of iron and aluminium concentration
FA	Fly ash
FFA	Fractionated fly ash
GHG	Greenhouse gas
ICP	Inductively coupled plasma
LS	Liquid to solid ratio (mL/g)
LTE	Local thermodynamic equilibrium
MIBK	Methyl isobutyl ketone
NbF	Nebulizer gas flow
NF	Nano-filtration
OES	Optical emission spectrometry
PgF	Plasma gas flow
PSD	Particle size distribution
RfP	Radio frequency power
RNA	Ribonucleic acid
RO	Reverse osmosis
RSM	Response surface methodology
RSS	Relative supersaturation
SEM	Scanning Electron Microscopy
SMN	Sodium metasilicate nonahydrate
SpF	Sample aspiration rate

TBP	Tri-butly phosphate
WPA	Wet phosphoric acid
XRD	X-ray diffraction
ZVI	zero-valent iron

β	Separation factor
β_{0-n}	Coefficient of function
b	adsorption energy (Langmuir isotherm)
C	Concentration
C_p	Center point
D	partition coefficient
K_f	adsorption capacity (Freundlich isotherm)
K_p	Equilibrium constant
K_{sp}	Solubility product
$1/n$	Intensity of sorption (Freundlich isotherm)
Q	Ionic product
q_e	Quantity of solute adsorbed per weight unit of adsorbent at equilibrium
q_{max}	Adsorption capacity (Langmuir isotherm)
ΔR	Change in reaction rate
RSS	Relative supersaturation
T	Temperature

1. Introduction

1.1 The importance of phosphorus

Phosphorus is an essential nutrient for all life forms. It plays an essential role in all biochemical systems.[1] The genetic materials DNA and RNA are phosphodiesters. ATP, the principal biochemical energy reservoir, is a phosphate derivative. Most of the coenzymes are esters of phosphoric acid. The structural support of organisms provided by membranes consists of phospholipids, and bones are biomineral hydroxyapatite.[2] The biological productivities are contingent upon the bio-availability of phosphorus to the flora and fauna that constitute the base of the food web in our ecosystems.[3] P is frequently the most limiting element for plant growth,[4] and crop yield on 30-40% of the global arable land is limited by P bio-availability.[5] Commercialization of P-based fertilizers, along with N, K, and micro-nutrients has gained much interests in recent years.[6] Phosphorus and its derivatives are also used in consumer products such as detergents, feed & food additives, pesticides & medicines, and fire retardants.[7–10] In order to meet the global phosphorus demand, P is primarily derived from phosphate rock, usually a mixed lithology of marine sediments containing carbonate fluorapatite (CFAP) and apatite species; $Ca_5(PO_4CO_3OH)_3(F)$.[11,12] Therefore, anthropogenic activities have hugely influenced the modern P cycle and an overview of global phosphorus cycle is depicted in Figure 1.1.

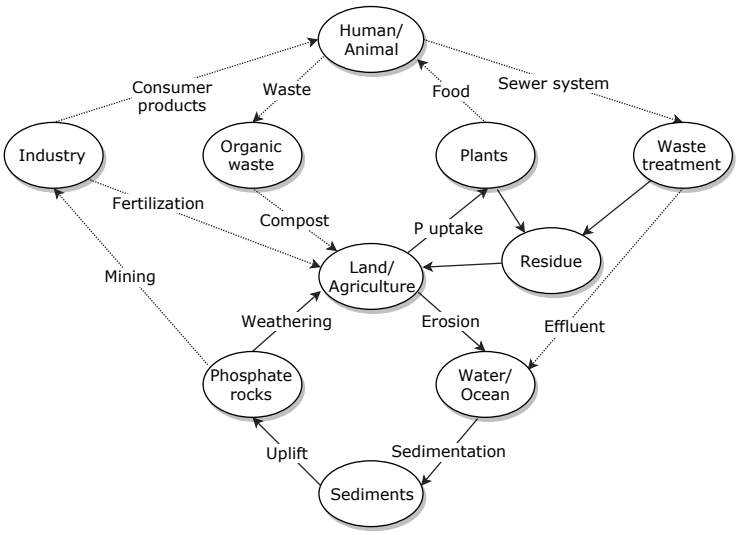

Figure 1.1: The human-intensified global phosphorus cycles (showing anthropogenic footprints by dotted lines).[13(modified)]

1.2 Global phosphorus sustainability

More than 75% of the globally and commercially used phosphate rock is surface mined. The P_2O_5 content in most mined ores ranges from 5 to over 40 wt% and its beneficiation may consist of several methods in combination. This requires significant resources of chemicals and energy. In addition, the cost of recovery and beneficiation of phosphate rock increase in relation to the decreasing grade and quality of the phosphate rocks. The demand for phosphorus is predicted to increase by 50-100% by 2050 due to growing global population and food demands.[12] 148 million tonnes of phosphate rock per year, which is 80-90% of global mined phosphorus, is used for food production, but only 40% goes to harvested crop. About 23% of that is accumulated into food products, and only 16% is consumed at the end.[9,14] This shows that a significant fraction of phosphorus is lost during the various stages of the P cycle. A net annual loss of 10.5 million metric tons of phosphorus only from the crop land is estimated,[15] and can be attributed to inefficient use of phosphorus.

Global P demand, P mining and rapid loss of P from the terrestrial ecosystem are increasing at the same time. This presents a great threat to phosphorus security and sustainability. Phosphate rock, a non-renewable mineral, is being depleted and about 50-100 years of economical mining is estimated to remain.[8,12,16] As a sustainable supply of affordable phosphorus is at risk, immediate measures are needed to reduce our use of non-renewable phosphate rock by more efficient use of phosphorus and recycling of P from secondary sources.[12,13]

1.3 Biofuel utilization and ash formation

Use of renewable resources in energy sector is expanding due to security, supply, sustainability and environmental concerns. European Union proposed a mandatory target of 20% for renewable energy's share of energy consumption by 2020, 10% of which for biofuels, in the *"Renewable Energy Road Map"*.[17] The utilization of renewable biofuels and peat, has increased in Finland in recent years. The total volume of the growing stock for extraction amounts to 2357 million m^3 over bark, 16 million m^3 being utilized annually for energy production.[18] Furthermore, the European Directive of Cogeneration (2004/8/CE) emphasizes the use of combined heat and power (CHP) for cogeneration of heat and electricity to increase energy efficiency and reduce greenhouse gas (GHG) emissions in EU.[19] CHP technology allows to convert the chemical energy stored in the biofuels into heat and power simultaneously with an efficiency of over 80%.[20] About 31% of the total electricity production and about 70% of the total heat production in 2015 were contributed with CHP technology.[21] Fixed-bed (grate) furnaces, bubbling and circulating fluidized-bed furnaces (BFB and CFB) are some examples of state of the art technologies.[22] The fluidized-bed technology utilizes an inert material bed, usually silica sand, in the reactor to assist combustion of the solid fuels. This is because sand allows efficient gas-solid interaction and improves the combustion efficiency.[23]

Solid ash residue, including bottom and fly ash, is a major waste product formed during combustion of biofuels. CHP plants in Finland produce over 150,000 t of wood ash and 450,000 t of peat ash annually.[24] With growing demands of renewable

biofuels and efficient CHP technologies, consumption of forest resources are expected to increase in forthcoming years. As a result, production of solid residual waste increases and imposes further challenges in waste management. Ash utilization is regulated by the Finnish legislation "the Decree of 12/7" and primarily depends on the concentration of trace elements with toxic characteristics.[25]

The residual inorganic ash, in general, is composed of silicates, oxides, carbonates, phosphates, sulphates, hydroxides, and halides of mineral elements that potentially represent the entire periodic table.[26,27] The phosphorus content in the ash residue depends greatly on the fuel type. In addition, the concentration of phosphorus is higher in fly ash than in bottom ash.[28] Fly ash from wood and woody biomass consists of 0.66-13.01 wt% of P_2O_5 (0.29-5.68 wt% of P) by weight, while a major fraction is composed of alkali metal oxides and silicates.[29] Therefore, fly ash from biomass-based fuel has emerged as a potential secondary resource for phosphorus recovery in recent years.

2. Objectives of the study

A growing body of literature addresses the concept of phosphorus recovery from various ash materials; sludge ash,[30–38] municipal solid-waste fly ash,[39,40] and animal manure ash.[41,42] However, P recovery from biomass-based ash is often limited to use as soil ameliorant for second-rotation conifer stands on drained peats and forest fertilization.[24,43–47] These studies clearly indicate lack of research regarding high grade phosphorus recovery from biomass-based fly ash.

Rise in production of ash residue is inevitable due to new legislation promoting use of renewable biofuels, efficient CHP technologies for energy production and increasing share of forest biofuel on the energy market. This may abet new challenges in solid waste management. On the other hand, depletion of phosphate rocks is fostering threats for phosphorus security. Therefore, the broad aspect of this study is to recover phosphorus from the biomass-based fly ash to provide an assurance towards phosphorus security and sustainability. This approach includes following aspects:

- exploring the feasibility of phosphorus recovery from low grade secondary waste materials,
- identification and development of phosphorus refining methods to acquire pure homogeneous products,
- optimization of the drafted recovery process,
- characterization and usage of the recovered P-product.

3. Inorganic phosphorus

3.1 Chemistry

Phosphorus belongs to group 15 of the periodic table, along with N, As, Sb and Bi. It has only one naturally occurring isotope (^{31}P) with an atomic number of 15 and an atomic mass of 31. In addition, variation in oxidation state of phosphorus from -3 to +5 allows compounds containing P in both low- and high-coordinate (-3 for Li_3P and +5 for PCl_5) bonding environment.[48,49] A comprehensive map of phosphorus coordination with various group elements of periodic table forming industrially important inorganic products is shown in Figure 3.1.

Phosphorus exhibits complicated allotropy, and 12 forms including crystalline and amorphous ones have been reported. White phosphorus and red phosphorus are two major forms of elemental P and widely used as precursors for synthesis of several industrial important chemical compounds. In addition, oxides (P_4O_{10}), halides (PCl_3), sulfides (P_4S_{10}), oxohalides ($POCl_3$), oxoacids (H_3PO_4) of phosphorus including phosphide (Li_3P) and phosphates ($M^{n+}_{3/n}PO_4$) of several elements are also used as precursors for various phosphate derivatives.[48 pp.493-540,50]

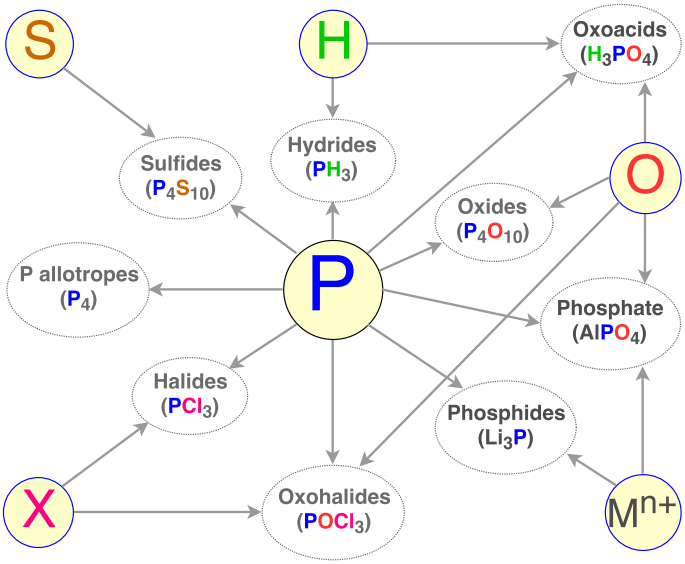

Figure 3.1: Chemistry of inorganic phosphorus with key elements of periodic table forming various industrially important chemical precursors.

3.2 Occurrence

Phosphorus is the 11th most abundant element of the earth's crust, but the existence of elemental P is very low because it is highly reactive. As a result, various forms of phosphate are the predominant species of phosphorus in natural ores. However, only a small fraction is present in high enough concentration and is physically accessible to be utilized by phosphate industry. The global phosphate rock reserves are located in only a handful of countries, mainly Morocco, China and the US.

3.2.1 Primary ores

An estimate of distribution of the world phosphate resources suggests that 75% of them are sedimentary marine deposits, 15-20% are igneous, metamorphic and weathered deposits, and 2–3% are from biogenic sources (bird and bat guano accumulations).[3,8] The most frequent and important phosphate mineral is apatite and its derivatives which coexist with other phosphorus minerals. Generally, primary P ores can be categorized into high and low grades with respective P_2O_5 values of 25-40% and 7-17%.[51] Since high-grade ore comprises impurities at low concentration, it requires less processing resources and is being mined at an unprecedented scale, leading to its depletion.

Due to increase in the demand of phosphorus products, mining of phosphorus from low-grade ores from igneous and sedimentary deposits is becoming more and more common. Low-grade phosphate ores also comprise gangue materials of several categories; siliceous, clayey, calcareous, organic matter, sulfides, magnetite, carbonates etc.[52] Low-grade ores require upgrading; which means increasing phosphorus concentration by removing gangue minerals. Several upgrading and beneficiation techniques have been implemented in the phosphate industry, and the choice of one or more of the upgrading technique depends on the type of ores as well as the gangue material present in the phosphate ore. Common phosphate minerals occurring in most of the primary ores are listed below:[53 pp. 10, 54 pp.9-11,55]

Mineral	Chemical formula
Apatite	$Ca_5(PO_4)(F,Cl,OH)$
Dahllite	$3\,Ca_3(PO_4)_2{\cdot}CaCO_3$
Francolite	$Ca_5(PO_4,CO_3OH)_3(F)$
Wavellite	$Al_3(PO_4)_2(OH)_3{\cdot}5\,H_2O$
Senegalite	$Al_2(PO_4)(OH)_3{\cdot}H_2O$
Variscite	$Al(PO_4)\cdot 2\,H_2O$
Strengite	$Fe^{3+}(PO_4)\cdot 2\,H_2O$
Barrandite	$(Al,Fe)PO_4\cdot 2\,H_2O$
Gorceixite	$BaAl_3(PO_4)_2(OH)_5\cdot H_2O$
Turquoise	$CuAl_6(PO_4)_4(OH)_8\cdot 5\,H_2O$
Rockbridgeite	$Fe^{2+}_{0.75}Mn^{2+}_{0.25}Fe^{3+}_4(PO_4)_3(OH)_5$

3.2.2 Secondary phosphorus sources

The anthropic interventions in natural phosphorus cycle and human-induced material flows in modern economies are only being intensified.[56] As mentioned earlier in

section 1.2, 80-90% of mined P is used in agriculture for food production, but only 40% goes to the harvested crop. About 23% of that is accumulated into human food products, and only 16% goes to anthropic consumption.[9,14] The phosphorus circulation, in figure 1.1 also suggests the accumulation of phosphorus into various materials at different times. For example, P consumed by humans and animals is excreted into manure wastes and some fractions are conveyed into wastewater streams. The crop harvests and forest resources also contain P accumulated via plant uptake.

Mixed wastewater streams and sludge, organic waste fractions including animal manure, urine, food waste, crop residues etc. are enriched with phosphorus. The concentration of phosphorus differs greatly; typical P concentrations in various secondary material are listed in Table 3.1. The prospect of phosphorus reuse and recovery from these secondary sources is attracting ample attention in recent years. However, high concentrations of impurities and trace elements with toxic characteristics limit its direct use as fertilizer and require several processes to remove the impurities and enrich P into single fractions.

Table 3.1: Typical phosphorus concentration in secondary sources.[29,57]

Secondary material	Phosphorus content (wt%)
Sewage sludge	1.4
Biogas digester sludge	0.48-0.77
Human urine, excreta	0.02-0.52
Compost material	0.16-0.44
Poultry manure	0.88-1.27
Animal manure	0.04-0.07
Meatmeal	1.09
Bonemeal	8.73-10.91
Crop residues	0.04-0.33
Fly ash/deposit ash	0.28-5.6

Thermochemical conversion of dry organic waste materials and crop residues having significant heating values via combustion combine energy production with phosphorus recovery; since the P concentration is elevated in the inorganic ash residues. Therefore, these solid ash residues can be seen as low-grade phosphorus ore. Efficient methods of P recovery are constantly being studied and developed from several ash materials; sewage sludge ash[30–37], municipal solid-waste fly ash,[39,40] and animal manure ash.[41,42]

3.3 Process overview in phosphate industry

Figure 3.2 shows an overview of the phosphate industry. This process commences with phosphate rock of high grade (P_2O_5 of 25-40 wt%) as source of phosphorus. Apatite derivatives are processed into various phosphate products either via wet (acid) route (hydrometallurgy); predominantly for fertilizer production, or dry (thermal) route for industrial and feed phosphate or for direct application as fertilizer. In the wet process, sulfuric acid (H_2SO_4) is reacted with phosphate rock to yield wet phosphoric acid which is further processed to obtain pure grade phosphoric acid. In the thermal process, phosphate rock is mixed and heated with coke and sand to

above 1400°C with the aid of graphite electrodes. This releases white phosphorus (P_4) which is used in synthesis of various phosphorus derivative products, such as agrochemicals, pharmaceuticals, food grade phosphoric acid, and so on.[50 pp. 26-67] In the recent decades, wet process acid has gained interest due to its low energy demand compared to the thermal process, which significantly reduces the processing cost. Despite the differences in these methods, the primary and common objective is to obtain phosphorus products with highest possible purity, either as phosphoric acid or phosphate salts. Pure phosphoric acid (100% H_3PO_4), for example, consists of 72.45 wt% P_2O_5 or 31.61 wt% P, while anhydrous $AlPO_4$ consists of 58.18 wt% P_2O_5 or 25.4 wt% P. Simplified chemical equations are also presented below for the principle phosphate products.

$$\mathrm{Ca_3(PO_4)_2 + 3\,H_2SO_4} \xrightarrow{wet} \mathrm{2\,H_3PO_4 + 3\,CaSO_4}$$

$$\mathrm{2Ca_3(PO_4)_2 + 6SiO_2 + 10C} \xrightarrow{\Delta(dry)} \mathrm{P_4\uparrow + 10CO\uparrow + 6CaSiO_3}$$

$$\text{White phosphorus}\quad \mathrm{P_4\uparrow} \longrightarrow \mathrm{P_4}\quad \text{Red phosphorus (s)}$$

$$\mathrm{P_4\,(s) + 5\,O_2} \longrightarrow \mathrm{P_4O_{10}}$$

$$\mathrm{P_4O_{10} + 6\,H_2O} \longrightarrow \mathrm{4\,H_3PO_4}$$

$$\mathrm{P_4 + 6\,H_2} \longrightarrow \mathrm{4\,PH_3}$$

$$\mathrm{P_4 + 6\,Cl_2} \longrightarrow \mathrm{4\,PCl_3}$$

$$\mathrm{P_4 + 8\,Fe} \longrightarrow \mathrm{4\,Fe_2P}$$

$$\mathrm{4\,Fe_2P + 18\,S} \longrightarrow \mathrm{P_4S_{10} + 8\,FeS}$$

$$\mathrm{2\,NH_3 + H_3PO_4} \longrightarrow \mathrm{(NH_4)_2HPO_4}$$

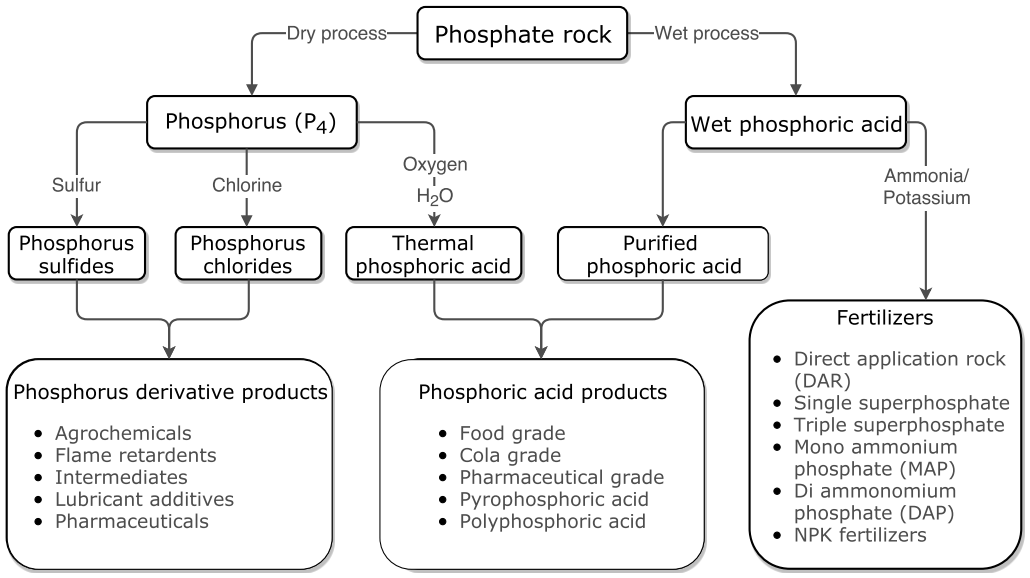

Figure 3.2: Processing of phosphate rock to obtain various consumer grade phosphorus products in phosphate industries.[50 pp. 27]

4. Pertinent refining technology

The phosphate industry has advanced phosphorus refining technology, especially from primary ores. As previously mentioned, the use of low-grade ores and secondary sources of phosphorus is rapidly growing due to scarcity of primary high-grade ores. Despite well established and developed technologies, pursuit for new efficient and economical methods still continues for the recovery of phosphorus from secondary sources. As these minerals contain various impurities in high concentration, they require one or more processes in combination to remove the impurities. The additional cost of phosphate processing is often combined with a decline in quality of the secondary source. The selection of refining methods thus depends on the concentration of phosphorus and as well as that of the impurities.

This section emphasizes some key technologies that have been established or are under development for refining and recovery of phosphorus from various grades of phosphate ores.

4.1 Beneficiation of phosphate minerals

Beneficiation is any method that improves the economic value of the ore by removing the impurities. This simply results in a higher grade product with enriched mineral content. The beneficiation process of phosphate rock allows an increment in concentration by a factor of 1.5-9. The several beneficiation techniques for upgrading phosphorus source are dependent on the nature of ores as well as that of the associated gangue minerals. However, these methods commence with crushing of the ore into a wide spectrum of particle sizes. Some key beneficiation techniques are listed below:

4.1.1 Physical methods

This technique utilizes the differences in physical (friability, density, electrostatic, magnetic, etc) properties between the phosphate mineral and the gangue matrix to separate them. Examples of physical separation methods are listed below:

- **Screening**: In most cases, phosphates are more friable than the gangue minerals which are typically hard. Screening, therefore, allows to recover the phosphate product in the fine fraction; this is already in practice in some beneficiation plants.[58]
- **Attrition scrubbing and classification**: This method is advantageous when the gangue minerals are clays. Thus, attrition in water liberates and disperses the clay which is then removed by desliming and/or classification.

- **Electrostatic separation**: Calcareous and siliceous ores have been upgraded successfully using this method mostly on laboratory scale. Large-scale production is limited due to the low capacity of electrostatic separators.[59]

- **Magnetic separation**: This method is useful for igneous phosphate minerals where one of the major gangue mineral is magnetic.[60]

4.1.2 Flotation techniques

In this method, either valuable mineral or gangue material has to float quicker than its counter part. Collecting reagents (fatty acids and amines) are used when phosphate minerals are being floated, while in case of flotation of gangue materials, depressants (phosphoric acid, fluorosilisic acid, etc.) are used so that the sink fraction contains phosphate minerals.[61] Particle size, degree of liberation and the hydrophobicity of mineral surfaces dictate its recovery rate during flotation. The efficiency decreases in a relation with decreasing particle size.[62] The Crago "Double Float" plant in Florida is one beneficiation plant that uses flotation to upgrade phosphate minerals.[63]

4.1.3 Chemical methods

This method uses leaching of carbonate minerals from phosphate ores with organic acids. The most common organic acids used are: acetic acid, lactic acid, formic acid and succinic acid. Acetic acid leaching of phosphate deposits with 10 wt% P_2O_5 at 15% w/w acid, 15% w/v solids at 40°C raised the P_2O_5 content to 32.1 wt%.[64] The concentration and type of acid are determined by the nature and concentration of gangue minerals.

4.2 Thermal treatment

Thermal treatment involves heating of high-grade phosphate ore (mostly fluorapatite) to a certain temperature to obtain phosphorus products with specific properties. The processes are categorized into drying of ores at temperatures of 120-150°C, removal of organics and carbonates by calcination at 650-1000°C, and defluorination up to 1350°C. Calcination of phosphate ores allows collecting defluorinated phosphates with P/F ratios of over 100. The principal reactions involved are shown in section 3.3. However, high capital cost of calcination plants and their energy-extensive operation are drawbacks of these methods.[59]

4.3 Chemical extraction of phosphorus

4.3.1 Leaching of phosphorus from solid phase

Chemical extraction of phosphorus ores has emerged as an economical option in comparison to the thermal process. This approach utilizes suitable reagents to leach phosphorus from the solid into solution media; it has no strict requirements for

particle size.[65] The principal objective of leaching is to extract phosphorus from solid to a liquid phase with high efficiency.

Chemical leaching

Alkali leaching with NaOH and acid leaching with HCl, H_2SO_4 and HNO_3 are common methods for extraction of phosphorus from P ores. The selection of leaching solution depends on the mineralogy of the phosphate ore. Alkali leaching (1M NaOH) is ineffective in leaching P from iron ores with an efficiency lower than 30%, while acid leaching (1% H_2SO_4) has an efficiency of over 91%.[66] Organic acids (acetic and succinic acid) have also proven their strength in leaching of calcareous and carbonate P minerals.[64,67–70] These studies also conclude that the kinetics of chemical leaching is relatively fast and can range between minutes and days.

In case of ash residue leaching, H_2SO_4 and HCl yield higher recovery for phosphorus extraction than HNO_3 and organic acids. However, the concentration of acid and other leaching parameters primarily depend on phosphorus and matrix (Ca, Fe, Al) content.[41,71]

Bioleaching

Bioleaching of phosphate in hydrometallurgy is a novel technology that uses microorganisms to mobilize phosphorus from the source. Studies using *Burkh-olderia caribensis* and *Aspergillus niger* for dephosphorization of iron ores with 0.23-0.26 wt% P indicated an efficiency of up to $33\%_{(wt)}$.[72,73] Higher dephosphorization degrees can be achieved at the cost of longer treatment times, ranging from weeks to a few months.[36,72–75] Despite the drawbacks of bioleaching against chemical leaching in terms of extraction time, these studies suggest the applicability of bioleaching for long-term treatment of marginal high-phosphorus iron ores in heaps or ponds.

4.3.2 Recovery and separation methods

$H_nPO_4{}^{(3-n)-}$ derivatives are considered to predominate in the solution phase; its efficiency is a function of pH and metal concentration.[50,76] Key differences in the recovery methods appear in their approach to mobilize the $H_nPO_4{}^{(3-n)-}$ phase.

The mobilization of phosphorus from solid to liquid phase is followed by one or more separation and recovery steps in the phosphate hydrometallurgy. Most frequently used technologies are solvent (liquid-liquid) extraction, precipitation, ion exchange and adsorption, which have been applied either to recover P products or to remove impurities. Prospects of phosphorus recovery will be primarily discussed in this section.

Precipitation

Chemical precipitation is a process where cations and anions in aqueous solution combine fo form an insoluble ionic solid/salt, also called precipitate. This only occurs when the ionic product (Q) of the given cations and anions exceed the solubility product constant (K_{sp}) of their salts (Figure 4.1). The precipitation mechanism comprises a series of fundamental processes: saturation → nucleation → Ostwald

ripening → agglomeration → particle formation. The particle size of precipitates is inversely proportional to the relative supersaturation (RSS) of the solution; a high RSS value yields many small particles while a low value forms fewer larger crystals.

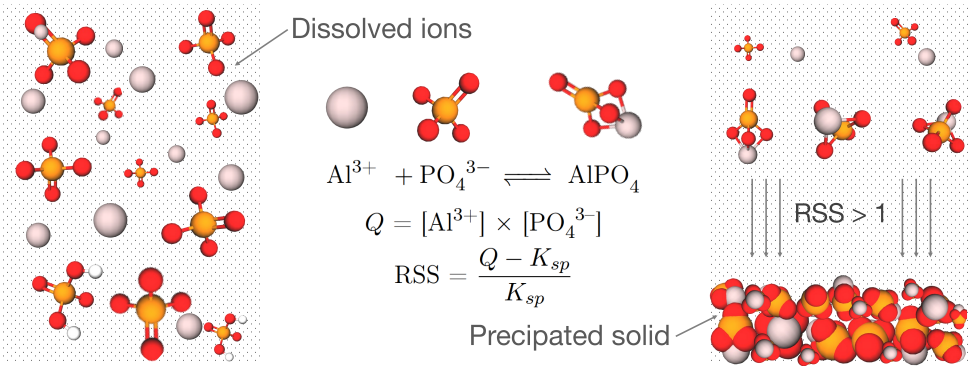

Figure 4.1: Simplified illustration of precipitation mechanism.

Precipitation is practiced in hydrometallurgy to separate metal ions as hydroxides, sulphides, or carbonates from the solution. It is also used in the phosphate industry for fertilizer production. Furthermore, waste water treatment plants extensively use precipitation to remove and recover phosphorus from waste streams. The technologies for phosphorus removal from waste water have advanced since their inception during 1950s in response to the issue of eutrophication. Various salts of phosphate have been identified, as listed in table 4.1. This bring opportunity to recover phosphorus from the solution via its precipitation using a metal source with a suitable stoichiometric concentration in the pH range where its precipitation is favorable, since the nature of metal phosphate salts is a function of pH.[76] Precipitation mechanisms have poor selectivity for the separation of particular cations or anions. Unwanted compounds often co-precipitate due to their supersaturation along with the compound of interest. Thus, co-precipitation of unwanted solids is a major challenge in precipitation technology.

Table 4.1: Various phosphorus compounds with solubility constant values.

Compounds	$\log(K_{sp})$
$MgHPO_4 \cdot 3\,H_2O$	18.18
$CaHPO_4$	19.28
$AlPO_4$	20.48
$MgNH_4PO_4$	21.84
$FeNH_4PO_4$	22.24
Mg_3PO_{42}	23.28
$Ca_2HPO_4OH_2$	25.73
$FePO_4 \cdot 2\,H_2O$	26.40
$Ca_3(PO_4)_2$	28.92
$Fe_3(PO_4)_2 \cdot 8\,H_2O$	37.76
$CaH_2(PO_4)_2 \cdot H_2O$	40.30
$Ca_4(HPO_4)_3 \cdot 3\,H_2O$	47.08
$Ca_5(PO_4)_3(OH)$	58.33
$Ca_{10}(PO_4)_6F_2$	118.00

Metal (Al, Fe, Mg, Ca) sources/salts are commonly used in phosphorus precip-

itation and coagulation as means of post-treatment of wastewaters. Phosphorus removal of 30-45% was obtained after aluminium coagulation.[77] Removal efficiency of over 90% was reported in case of iron use.[78,79] Precipitation of calcium phosphate is also explored by addition of Ca.[80,81] A growing literature suggests that struvite precipitation via Mg addition is also gaining attraction due to the product value in agriculture.[82–85]

A limited number of studies have explored the prospects of phosphorus precipitation from acid leachate of ash residue.[30,38,39,41] These studies have emphasized precipitation of phosphorus with calcium because the Ca-P solid has better solubility in water than Al or Fe-P solids, and its use as fertilizer. Moreover, iron is considered an impurity due to the low commercial value of iron phosphate and is removed via precipitation at pH 3 prior to phosphate precipitation at pH higher than 4.[39,41]

Solvent extraction

Solvent extraction is a principal technique for partitioning dissolved compounds between two immiscible solvents; one being aqueous (also termed feed) and the other typically organic in nature. Use of a third organic liquid as diluent to disperse the solvent is also a common practice. Solvent extraction of wet phosphoric acid (WPA) commences with mobilization of H_3PO_4 from aqueous to organic solvent. Use of a scrubbing agent is a viable option to remove impurities present in the organic phase. Subsequently, H_3PO_4 is conveyed back to aqueous phase from the organic solvent with a stripping solution.[50] The mechanism of H_3PO_4 immobilization during solvent extraction can be written as:

$$\begin{aligned} \mathrm{H_3PO_{4(aq)}} + \mathrm{S_{(org)}} &\longrightarrow \mathrm{S \cdot H_3PO_{4(org)}} + \mathrm{R(raffinate)_{(aq)}} \\ \mathrm{S \cdot H_3PO_{4(org)}} + \mathrm{A(strip)_{(aq)}} &\longrightarrow \mathrm{S_{(org)}} + \mathrm{A \cdot H_3PO_{4(aq)}} \end{aligned}$$

The efficacy of organic solvent is expressed with its separation factor (β). It denotes the selectivity of organic solvent to extract the ion of interest; a value higher than unity indicates good separation of the ionic species and high purity of the extracted product. The separation factor can be estimated as:[86]

$$\beta = \frac{D_{\mathrm{PO_4}^{3-}}}{D_{m^{-or+}}} \;\&\; D_i = \frac{x_{i,org}}{x_{i,aq}}$$

where D is the partition coefficient, x_i is the molar concentration of species i, and m is any matrix ion of interest.

Many organic solvents, including isoamyl alcohol, 2-ethyl-1-hexanol, dibutyl ether, tributyl phosphate (TBP) and methyl isobutyl ketone (MIBK) are used for the purification of the WPA in phosphate industry.[87–89] Unfortunately, ideal solvents highly selective to phosphoric acid do not exist. This requires purification in several steps with a strong negative impact on the economy of the process. Separation factors ($\beta^{\mathrm{H_3PO_4}}_{matrix}$) in a decreasing order were identified for TBP, mixture of 55 vol% MIBK & 45 vol% TBP, and MIBK solvent during purification of wet phosphoric acid obtained by H_2SO_4 leaching of phosphate ore (54 wt% P_2O_5). In terms of matrix selectivity, the order Mg>Al>Fe>SO_4^{2-} was observed for the above mentioned solvents.[90] The separation factor of phosphoric acid depends on the nature of matrix

ion and its concentration, and also on the phosphoric acid concentration. The presence of Fe^{3+} and Al^{3+} reduce the extraction of phosphoric acid with isoamyl alcohol in nitrate media.[91] Chloride separation is also important for solutions digested with HCl because most solvents have a low chloride separation factor.[86] Temperature and pH of the solution are other fundamental parameters that also dictate the efficiency of solvent extraction.[92]

An extraction process starting with leaching of waste-activated sludge ash (26 wt% P_2O_5) with 1 M HCl followed by solvent extraction with 1-butanol and stripping with distilled water reported a recovery of 76% of phosphorus. In addition, increasing concentration of Al resulted in a decrease in the P-recovery rate; purity of the recovered product was not reported.[31] Solvent extraction is challenging for low-grade phosphate source and requires further development.

Ion exchange

Ion exchange is a reversible chemical process for removing dissolved ions from the solution and replacing them with other ions of similar characteristics. An anion exchanger adsorbs negatively charged ions in the exchange resin, while a cation exchanger adsorbs positively charged ions. An anionic resin is typically favorable in the separation and purification of aqueous solutions with a low concentration of phosphate. On the other hand, cationic resin is also a viable option for metal ions at low level of concentration. After the extraction process, the ion exchanger can be regenerated by eluting desired ions in excess concentration.

Cheeseman et. al. reported a process that uses a cation exchanger to remove metal impurities followed by evaporation of sludge ash leachate (0.98-1.07 wt% of H_3PO_4) to concentrate H_3PO_4 up to an essay of 85 wt%.[33] Ion exchange for recovering phosphate from sludge ash and sludge is used in the BioCon, KREPRO and Rim-Nut processes.[93,94] However, the main disadvantage of these processes is that the volume of chemicals used to regenerate the resins is rather large.[95]

Adsorption

Adsorption is a form of sorption similar to ion exchange where one or more solutes are distributed between a fluid phase and particles. The key difference is in the mobility of ions. In adsorption, adhesion of ions or molecules takes place on the surface of a solid.

Study of phosphorus adsorption from incinerated sewage sludge ash leachate using Ze (IV)-loaded orange waste gel showed the possibility of selective P adsorption from solution containing 38 mg/L of P.[32] Various materials such as activated biochar, activated iron systems (zero-valent iron (ZVI), Fe_2O_3 and Fe^{2+}) and zeolite have also been used in phosphorus recovery technology. Studies indicate that the adsorption isotherms of the adsorbate depend on the P concentration, pH of the solution, and anion (SO_4^{2-}, NO_3^-) concentration.[96–99] Therefore, phosphorus recovery via adsorption is limited to solutions with low concentration of phosphorus.

Chelation and masking

Chelation involves the incorporation of metal/cation into a complex structure of an organic molecule, the chelating agent. Typically, electron-donor atoms (sulphur, nitrogen, and/or oxygen) on the chelating molecule form a coordinate bond to the metal ions and form a stable complex. Chelation is used in various fields of chemistry including food industry, as a stabilizing agent, in chelation therapy to detoxify heavy metals, and as masking agents to remove some particular metals in the desired product.[100]

Ethylenediaminetetraacetic acid (EDTA) is a versatile chelating agent forming four or six coordinate bonds with both transition-metal ions and main-group metal ions. The interference of unwanted metals in the solution can be masked by EDTA; it is used as a chelating agent in chemical recovery processes such as struvite precipitation by Ca-masking,[101] Ni recovery by masking of Fe,[102] Cu recovery from electronic waste,[103] and separation of Ni and Co from emulsion liquid membranes.[104]

4.4 Desilication methods

Silica scaling on internal surfaces of equipment is one of the most problematic issues in many industrial operations. It is extremely difficult and costly to remove. When the Si concentration increases above the saturation level at a given temperature and pH in a solution, silica scale is formed.[105]. Silica co-precipitation via polymerization, agglomeration and aggregation possesses a great threat to the purity of any product being recovered. Yokoyama et. al. reported the inhibiting effect of silicic acid on the precipitation of $CaCO_3$,[106] while the risk of silica co-precipitation with iron during Zn recovery was discussed by Dyer et. al.[107]

Desilication includes various methods for removal of dissolved Si; they can be categorized into precipitation (with and without addition of seeds and/or metal hydroxides), adsorption, flocculation (addition of flocculants, coagulants and/or antiscalants), inorganic ion-exchange, lime-soda softening, nano-filtration (NF) and reverse osmosis (RO) strategies.[108–112]

Most of the desilication treatments are performed in mildly acidic or neutral to basic pH regimes, while limited processes are carried out below pH 2[113]. In addition, these strategies possess some major limitations; coagulation mostly occurs at high pH and requires high dosages of coagulants and flocculants.[108,114] NF and RO processes are associated with fouling problems and high energy consumption.[115]

Depending on the pH of the solution, Si can exist in many forms; as monomeric to polymeric dissolved species, colloidal and/or precipitated forms. However, monosilicic acid, $Si(OH)_4$ (also expressed as H_4SiO_4), is presumed to exist at lower pH's. In acidic conditions, the monosilicic acid tends to polymerize, yielding oligomeric and polymeric units. These polymeric silica units grow by addition of monomeric silicic acid to yield primary particles ($\sim$20-50 nm) that aggregate to form particulates of silica followed by gel formation and precipitation.[116]

Leaching of fly ash with higher molar concentrations of acid seems to be a promising approach to achieve better phosphorus leachability and simultaneous removal of Si by aging of leachate that facilitates Si-gel formation.

5. Experimental methods

5.1 Samples

Seven samples of fly ash, originating from different combinations of peat and wood as fuel, were received from three CHP plants of Finland. The fuel composition varied from 100 wt% peat (P) to 100 wt% wood-based biomass fuel (B). P_{100}, $P_{80}B_{20}$, $P_{70}B_{30}$, $P_{65}B_{35}$, $P_{50}B_{50}$, $P_{30}B_{70}$ and B_{100} are labeled on the basis of their fuel composition; subscripts indicate the fuel composition percentage by weight. P_{100} is received from Keljonlahti CHP, while $P_{80}B_{20}$, $P_{70}B_{30}$, $P_{65}B_{35}$, $P_{50}B_{50}$ and $P_{30}B_{70}$ are from Rauhalahti CHP and B_{100} is from Alholmens Kraft CHP.

- For Paper I, seven samples were investigated in the context of phosphorus beneficiation.
- For Papers II-III, samples from Alholmens Kraft CHP (B_{100} or FA) were used in studies of phosphorus recovery via the hydrometallurgical method.

5.2 Reagents

All concentrated acids and chemical reagents used were of analytical grade. Ultrapure water of 18.2 MΩ cm resistivity was produced using Elga PURELAB Ultra Analytic and used throughout this study.

5.3 Design of experiment

Design of experiment (DOE) is a systematic, rigorous approach to problem solving that applies principle and technique at the data collection stage to acquire valid, supportable and defensible conclusions. An experiment that is strategically planned and executed provides a great deal of information about the effect of one or more variable on the measured data. DOE techniques are widely employed for comparison, screening, modeling and optimization processes in various fields of science such as analytical chemistry, pharmaceuticals, bio-processing and engineering.[117,118]

"RcmdrPluging.DoE" plugin[119,120] in R software[121] was used to design the experiment and analyze the results. Definitions of some key terms in design of experiment approach are presented below:

- **Experimental domain** is the region of interest where experiment is performed.

- **Factors** are the experimental variables that can be independently altered. Typical independent variables comprise pH, reaction time, reagent concentration, flow rate and others.

- **Levels of a variable** are values of a variable at which the experiment must be performed. For example, the variable pH can be studied at five levels: 2, 3, 4, 5 and 6 during precipitation optimization.

- **Experimental design** is a set of experiments defined by a matrix composed by a combination of different values of the variables.

- **Response** is the measured dependent value from the experiment.

5.3.1 Response surface methodology

Response-surface methodology (RSM) involves mathematical and statistical techniques based on the fit of polynomial equations to the experimental data obtained. The most important factors (either identified after screening or known from experience) that have significant effect on the measured values are examined in detail using response-surface design. Due to inclusion of linear, interaction and quadratic terms in the polynomial function, RSM method is able to produce surfaces of linear, curve, minimum or maximum point, and saddle nature. It is one of the most relevant multivariate techniques used in analytical optimization.

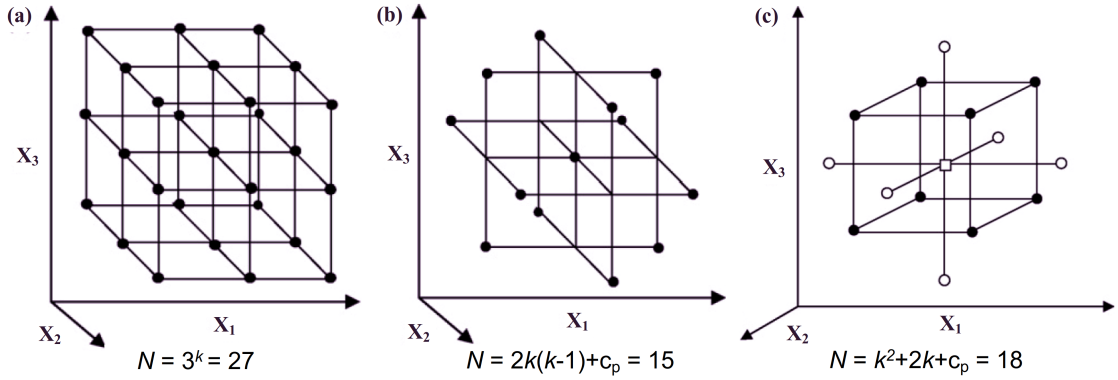

Figure 5.1: Rectangular symmetrical designs used in RSM; (a) three-level factorial design, (b) Box-Behnken design and (c) central composite design for three variables (k) and three center points (c_p).[117]

Figure 5.1 illustrates experimental domains for a three variables systems; three-level full factorial, Box-Behnken, and central composite designs (CCD) are examples of symmetrical designs. They differ primarily in the selection of experiment points in the domain that are typically selected at -1, 0 and +1 level.[122]

The flow chart (Figure 5.2) illustrates the systematic procedure in the DOE approach. After choosing the suitable experimental design, data are collected at specified points. This is followed by fitting of the polynomial function to the experimental data as described in Eq.5.1 for two factors. This equation is solved by using the method of least-square regression and the coefficients of functions (β) related to

linear, interaction and quadratic terms are estimated. Then, the surface of response is generated using the fitted model/function.

$$y = \beta_0 + \beta_1 x_1 + \beta_2 x_2 + \beta_{12} x_1 x_2 + \beta_{11} x_1^2 + \beta_{22} x_2^2 \tag{5.1}$$

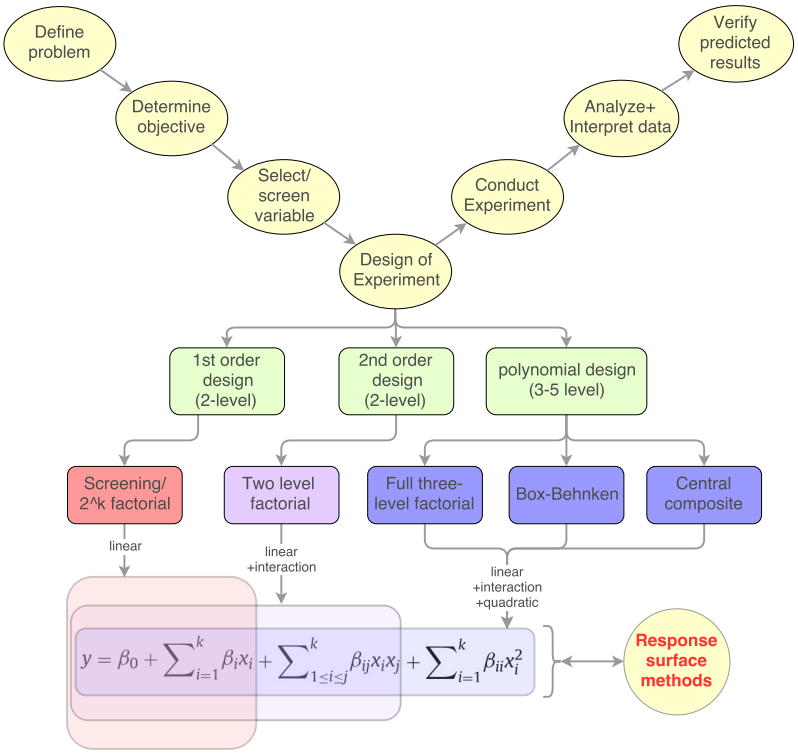

Figure 5.2: Common strategy for implementation of DOE approach and most used design in analytical chemistry. (RSM equation contains: y as response, β_0 as constant term, β_i, β_{ij} and β_{ii} represent coefficients of the linear, interaction and quadratic parameters, and k indicates the number of variables x.)

5.4 Optimization of ICP-OES parameters

Inductively coupled plasma-optical emission spectrometry (ICP-OES) instrument (PerkinElmer Optima 8300) was used in this study for elemental characterization of samples and recovered products and efficiency determination of the proposed recovery methods.

ICP is a widely used radiation source in analytical spectrometry. A high kinetic temperature of the plasma is the characteristic feature of the ICP that contributes to low levels of physical and chemical interference and lower detection limits.These features depend on the local thermodynamic equilibrium (LTE) of the plasma. Instrument operational parameters, nature of solution injected to the plasma, and matrices in the solutions have a significant effect on the LTE of plasma.[123,124] Estimation of the plasma LTE follows a heuristic approach, the departure from LTE being measured with the ionic (II) to atomic line (I) intensity ratio of magnesium (Mg), since most ionic intensities are sensitive to changes in operating parameters,

Table 5.1: Experimental domain of the operating parameters used in orthogonal factorial design.

ICP-OES parameter	Abbr.	Unit	Lower value	Upper value
Plasma gas flow	(PgF)	L/min	8	16
Auxiliary gas flow	(AxF)	L/min	0.2	0.4
Nebulizer gas flow	(NbF)	mL/min	0.4	0.8
Sample aspiration rate	(SpF)	mL/min	0.8	2
RF power	(RF)	W	1300	1500

in contrast to atomic intensities.[125] An MgII/MgI ratio above 8 (in axial view) and 10 (in radial view) indicates proximity to LTE conditions of plasma. This ratio is used to compare the LTE of plasma and to optimize the operating parameters in this study.

Five operating parameters were considered in this study: plasma gas flow, auxiliary gas flow, nebulizer gas flow, RF power and sample aspiration rate. Statistical approach based on design of experiments was employed to identify and optimize the operating parameters. Orthogonal factorial design was created to screen the factors with significant effect (experimental domain summarized in Table 5.1), while central composite design (CCD) was used to optimize the selected variables.

5.5 Sample characterization

5.5.1 Particle size distribution analysis

The particle size distribution (PSD) profiles for all seven samples were evaluated with a Fritsch Analysetter 22 Economy particle-size analyzer using wet dispersion in a saturated sodium chloride solution. The use of a saturated solution is presumed to mitigate the problems with the dissolution of fly ash particles in water.[I]

5.5.2 Elemental analysis

The elemental composition of solid samples was determined with an Elementar vario EL(III) for CHN (Carbon, Hydrogen and Nitrogen) determination and an ICP-OES PerkinElmer Optima 8300 instrument for determination of major elements and trace elements.[I-III]

Digestion

This study employs a modified version of ultrasound-assisted digestion of solid fly ash samples developed by Ilander and Väisänen.[126] 0.25 g of solid samples were dissolved in 3-5 ml of aqua-regia with 3–4 drops (up to 0.5 mL) of hydrofluoric acid. The digestion was further assisted by ultrasound for 18 min with sonication procedure divided into six equal steps (3 min) at 60°C. All samples were shaken in between and the evolved gas was released.

The extraction process was followed by filtration (with Whatman No. 41 filter paper) of the solution samples, which were diluted to 50-100 ml in plastic volu-

metric flasks with ultrapure water of 18.2 MΩ cm resistivity produced using Elga PURELAB Ultra Analytic. Trace element concentrations were determined from this fraction of sample solution. Major element concentrations were determined after a further dilution factor of 1:10. 10 vol% and 5 vol% (wt.%) of acid matrix (aqua regia or HCl or HNO_3) in the diluted samples were maintained during determination of trace and major elements.

5.6 Beneficiation of fly ash

5.6.1 Fractionation by sieving

A Retsch vibratory sieve shaker (AS 200 basic) was used for beneficiation of fly ash samples via sieving-based fractionation. Sieve sizes of 45, 63, 125 and 250 μm were used. Five ash fractions [(0–45), (45–63), (63–125), (125–250), (>250) μm] were collected and weighed. Samples representing each fraction were digested and elemental compositions were determined with ICP-OES to study the correlation between fly ash phosphorous content and its particle size.[I] 20 g of fly ash samples were sieved in this study, while 100 g of samples were sieved in the context of fly ash beneficiation via sieving at 125 μm.[II-III]

5.7 Chemical leaching

Acid concentration, liquid to solid (LS) ratio, time, temperature, particle size, stirring, and sample morphology are some of the critical leaching parameters in hydrometallurgy.[31–33,41] Acid concentration, LS ratio and leaching time were selected as critical factors in this study and optimization was performed employing RSM methods; the CCD design was chosen. 5 levels were selected for each factors: HCl concentration (0.69, 1.5, 2.5, 3.5, 4.3 M), LS ratio (5.47, 7.5, 10, 12.5, 14.5) and time (5.47, 7.5, 10, 12.5, 14.5 min). This design matrix comprises of 20 experimental runs including 5 replicates of center point. The required concentration and volume of acid was added to 50 mL centrifuge tubes containing 1±0.001 g of fractionated fly ash sample. Leaching was assisted with ultrasound and periodic shaking of the tubes. After extraction, the samples were filtered and diluted to 100 mL for phosphorus determination by ICP-OES.

Acid concentration and type were varied in order to study the effect of acid type on P extraction and its synergistic removal of Si impurities. For this, 2M, 5M and 8M of HCl and HNO_3 were selected.[II] 20 g of fractionated fly ash sample was dissolved in 240 mL of acid. The optimal LS ratio was used in scaled-up leaching process and the ultrasonic digestion was assisted with mechanical stirring (500 rpm) for 20 min to prevent sedimentation. The undissolved residues were separated with centrifugation for 20 min.[II-III]

5.8 Precipitation

In this study, precipitation was employed to remove the silica from leachate solution via aging,[II] to recover phosphorus with aluminium by raising pH[III] and recover phosphorus as struvite by addition of Mg and NH_4 salts to refined aluminium phosphate leachate solution.[IV] TitroLine easy unit from SCHOTT Instruments GmbH (automatic titration unit) was used to adjust the pH to target value in titration. Freshly prepared 1M or 3M NaOH was used in this study.[III]

5.8.1 Impact of Si on P precipitation

Prior the removal of silica, the influence of silicon concentration on P precipitation was examined using synthetic solutions where the Si concentrations were maintained at 0, 50, 200 and 850 mg/L, while concentrations (mg/L) of P(1650±100), Al (1100±50), Fe (1140±60), Ca (15000±200) and Mg (500±50) were kept constant; this also represented the fly ash leachate matrix. Phosphorus was precipitated at pH 2-4 by adding 1 M NaOH. The concentration of phosphorus in the supernatant was measured with ICP-OES. The supernatants were separated via centrifugation and the precipitates were washed several times with ultra pure water followed by oven drying. Concentrations of phosphorous and silica in the dry precipitate were measured with Bruker Quantax 400 EDS.

5.8.2 Silica removal

The addition of coagulants or other antiscalant products to promote coagulation and aggregation of silica are not considered in this study due to high quantities of coagulants demanded by high Si concentration in leachate solutions and to avoid further contamination and complexity during phosphorous recovery, the primary objective of this study. The formation of Si-gel particulates under acidic condition is seen as an advantage in this study, since the acid leachates of fly ash are highly acidic and contain silica in high concentration. Since gelation is a bonding phenomenon between the aggregates forming particulate networks, it is affected by process parameters such as pH, supersaturation, temperature and ions in the solution. Therefore, high molar concentrations of mineral acids were used in this study to facilitate the removal of silica via precipitation of Si-gel particulates. The effect of temperature on silica precipitation was also studied.

10 mL of each acid leachate solution obtained were transferred to 15 mL centrifuge tubes and left for aging of silica gel in an unstirred condition at room temperature and also at 40 and 60°C with an accuracy of ±3°C, for examining the influence of temperature. These sample tubes were centrifuged after a certain time interval (0 to 75 h) to separate the precipitated Si-gel. 1 ml of supernatant was extracted and diluted to 100 mL to quench further polymerization of Si and precipitation. The concentration of dissolved or soluble silica and other analytes were determined from the quenched fraction with ICP-OES as a function of time. The concentration of precipitated Si-gel at given times was determined by subtraction from the known initial soluble silica concentration in the solution.[II] In case of scaled-up Si-removal, the leachates were transferred to 50 mL centrifuge tubes and left for aging at room

temperature for 5 h. The obtained Si-gel was removed from the leachate by centrifugation for 20 min. The supernatants were mixed together before precipitation experiments.[III]

5.8.3 Phosphorus precipitation

Silicon-free leachate solutions were used in this study. Phosphorus was precipitated by addition of 3 M NaOH. Co-precipitation of iron was prevented by addition of EDTA as Fe chelating agent. The optimal pH region and molar ratio of EDTA to iron and aluminium (ER=[EDTA]/[Fe+Al]) were identified using the RSM method by creating a CCD design. The designed level for pH was 3.8, 4, 4.5, 5, 5.2 and 0.29, 0.5, 1, 1.5, 1.71 for ER.[III] For this study, 10 mL of Si-free leachate solution was taken and the required weight of EDTA was added. Freshly prepared 3M NaOH was used to raise the pH to target value.

5.8.4 Synthetic phosphate compounds

Several synthetic phosphate solids were precipitated from controlled samples. Table 5.2 shows the nature and function of synthetic solids used in this study.

Table 5.2: Preparation method of synthetic phosphate compounds and their uses.

Compound	Preparation method	Use	Paper
$AlPO_4$ (A)	50 mL solution containing 0.1 M Al^{3+} and PO_4^{3-} was precipitated at pH 4 by addition of 1 M NaOH	Comparison with recovered $AlPO_4$	III
$AlPO_4$ (B)	1 L solution consisting of 0.2 M Al^{3+} and PO_4^{3-} and 9mM Fe^{3+} was precipitated at pH 4 by addition of 1M NaOH	Leaching studies and removal of Al and Fe by cation exchange resin	IV
$MgNH_4PO_4$	100 mL solution containing 0.5 M Mg^{2+}, NH_4^+ and PO_4^{3-} was precipitated at pH 9.5 by addition of 1 M NaOH	Comparison with precipitated struvite	IV

5.8.5 Conversion of $AlPO_4$ to struvite

In this study,[IV] feasibility of conversion of $AlPO_4$ to struvite ($MgNH_4PO_4$) was studied. This included leaching of $AlPO_4$ with phosphoric acid solution followed by removal of Al^{3+} and Fe^{3+} ions with cation exchange resin (CER) and precipitation of struvite by addition of Mg^{2+} and NH_4^+ sources. Leaching with phosphoric acid limits addition of foreign anions/impurities and also facilitates recirculation of refined leachate (Al^{3+} and Fe^{3+} free leachate after CER adsorption) for dissolution of solid $AlPO_4$. This method, using refined leachate for leaching, is seen as clean, sustainable and economical approach to recover phosphorus from the leachate solution. Therefore, effect of phosphoric acid concentration on leachability of phosphorus and CER dosage on removal of Al^{3+} and Fe^{3+} were investigated.[IV]

Leaching with phosphoric acid

0.1, 0.5 and 1 M of phosphoric acid were prepared from an analytical grade 85 wt% H_3PO_4 from EMSURE®. Synthetic $AlPO_4$(B) containing 18.9 wt% P, 16 wt% Al and 1.5 wt% Fe (concentration in similar range to that of precipitated $AlPO_4$) was used in leaching studies. 40 mL of 0.1, 0.5 and 1 M H_3PO_4 were added to 1 g of $AlPO_4$(B) and mixed with a magnetic stirrer at 500 rpm for 1 h. 50 mL of optimal acid concentration and refined leachate (Al^{3+} and Fe^{3+} free) were added to 1.25 g of recovered $AlPO_4$[III] at LS ratio of 40 mL/g, and used in struvite precipitation experiment. 1 ml of each leachate was filtered through 0.45 μm syringe filter and diluted for elemental analysis with ICP-OES.[IV]

Removal of metal ions with CER

Amberlite® IR120 H^+ form (AIR-120H), a strongly acidic cation exchanger, was used to remove metal cations from the leachate solution and CER dosage of 0.01 to 0.5 g/mL was investigated. Required mass of CER was added to 10 mL of leachate solution obtained from 0.5 M H_3PO_4 during optimization studies, while 50 mL of leachate solution was used during removal of Al^{3+} and Fe^{3+} ions followed by struvite precipitation. The slurry was stirred with a magnetic stirrer at 200 rpm for 1 h.[IV]

Struvite precipitation

Two batch experiments were performed to recover phosphorus as struvite. 0.5 M of phosphoric acid prepared from analytical grade (85 wt%) H_3PO_4 was employed in batch 1. Meanwhile, the refined leachate after Al and Fe exchange with AIR-120H was diluted such that phosphoric acid concentration was 0.5 M and used during leaching in batch 2. In both cases, metal ions were removed with CER dosage of 0.6 g/mL. First, the pH of leachates were adjusted between 7 and 8 by addition of 1 M NaOH, then Mg^{2+} and $NH_4{}^+$ sources were added such that Mg^{2+}:$NH_4{}^+$:$PO_4{}^{3-}$=1:1:1. Precipitates were obtained at pH 9.5 with continuous mixing of the solutions at 200 rpm for 2h. The precipitates were separated by filtration (Whatman filter 42) and rinsed twice with ultrapure water to remove loosely bound Na and Cl.[IV]

5.9 Characterization of P products

The precipitated products[III] were characterized with ICP-OES and Bruker Quantax 400 EDS for the determination of major components and trace elements. Digestion of solid products followed the procedure described in section 5.5.2 without the use of hydrofluoric acid. In addition, infrared characteristics for all recovered products[III,IV] were obtained with Bruker Alpha Platinum-ATR. An X–ray powder diffraction analysis of aluminium phosphate and struvite were done with a PANalytical X'Pert Pro alpha 1 diffractometer using Johansson monochromatized Cu $K_{\alpha 1}$ radiation ($\lambda = 1.5406$; tube settings: 45 kV, 40 mA). The samples were prepared on a silicon-made zero-background holder[III] and a sample cavity of routine steel-made sample holder.[IV] The data was recorded from a spinning sample by X'Celerator detector with a step size of 0.017° and counting times of 120[III] and 60[IV] s per step.

5.10 Chemical equilibrium modeling

Equilibrium modeling of phosphorous species and other major solids in acidic media was performed in the Medusa and Hydra program (version: 18 Aug. 2009)[127]. The components considered were Fe, Al, Ca, P as PO_4 and EDTA. Concentrations of analytes similar to the leachate solution were used in the equilibrium calculation; with a PO_4 concentration of 24 mM and PO_4:Fe:Al:Ca = 1:1:1:10 (molar fraction). The ionic strength of the solution is set at 1, unless otherwise stated. All the soluble and solid complexes available in the database were allowed.[III]

6. Results and discussion

6.1 Optimization of ICP measurement

6.1.1 Selection of factor

The effect of PgF, AxF, NbF, SpF, RF on the performance of ICP-OES instrument was studied. Figure 6.1 shows the mean effect plot of five variables to the responses; radially and axially viewed MgII/MgI ratio and wavelength for phosphorus at 213.618 nm. The LTE of plasma (as indicated by MgII/MgI) changed significantly from 14 to 10 (radial view), and 10 to 5 (axial view) when the operating parameters were changed. Higher values of the MgII/MgI ratio were obtained with lower values of plasma gas flow, which is also economically favorable. Auxiliary gas flow does not have a significant effect on the LTE of plasma and intensity of phosphorus lines. Nebulizer gas flow has both linear and quadratic effect on the MgII/MgI ratio and P intensity. The linear effect of increasing RF power is due to rising ionizing power of plasma and is reflected in a higher MgII/MgI ratio. The sample aspiration rate seems to have a significant effect on the P intensity, while its effect on the LTE of the plasma was not significant. Therefore, nebulizer gas flow and sample aspiration rates were selected as significant variables that will be quantitatively optimized using a central composite design.

6.1.2 Parameter optimization

Figure 6.2 displays the optimal region for LTE of plasma and highest analyte intensities obtained with the cross flow nebulizer connected to Scott spray chamber for nebulization of liquid samples. A nebulizer flow rate of 0.6 L/min yields the highest value of MgII/MgI ratio and Mg (II) ionic intensity lines which imply that the plasma is in LTE. These observations are valid for both axial and radial views. In the case of selected analytes (P, As, Pb), highest intensities were observed at a lower nebulizer gas flow of 0.4-0.5 L/min; however, the MgII/MgI ratio in this region is below 8, thus indicating deviations from LTE of plasma. A sample aspiration rate of 1.5 mL/min resulted in the highest intensities for all axial observations. Similar relationships with different values were observed with the GemCone low flow nebulizer connected to Cyclonic spray chamber; the optimal ICP parameters are listed in Table 6.1. These values were used throughout this study.

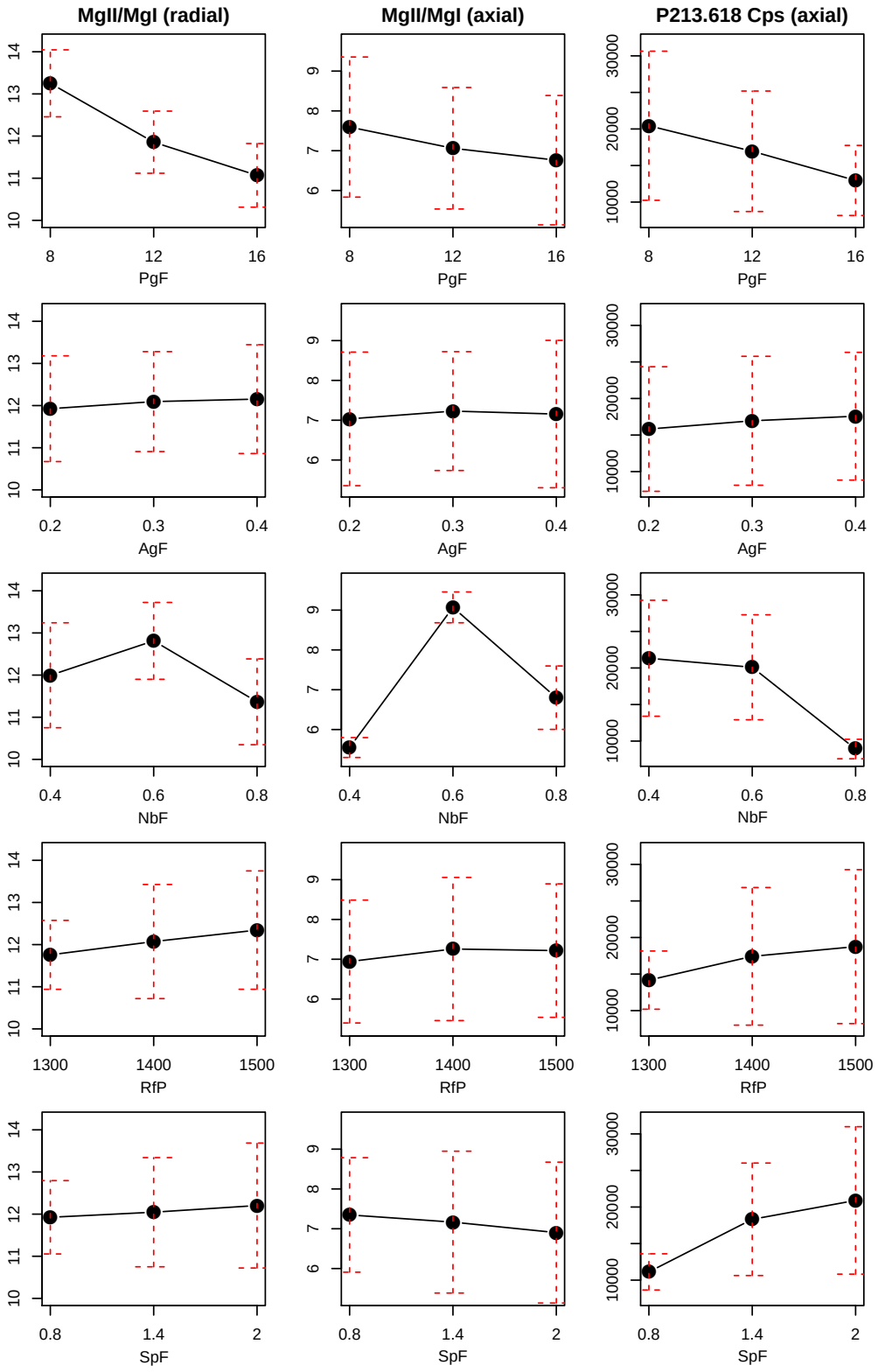

Figure 6.1: Mean effect plot of five variables (PgF, AxF, NbF, SpF, and RfP) on selected response (MgII/MgI radial and axial, and P intensity).

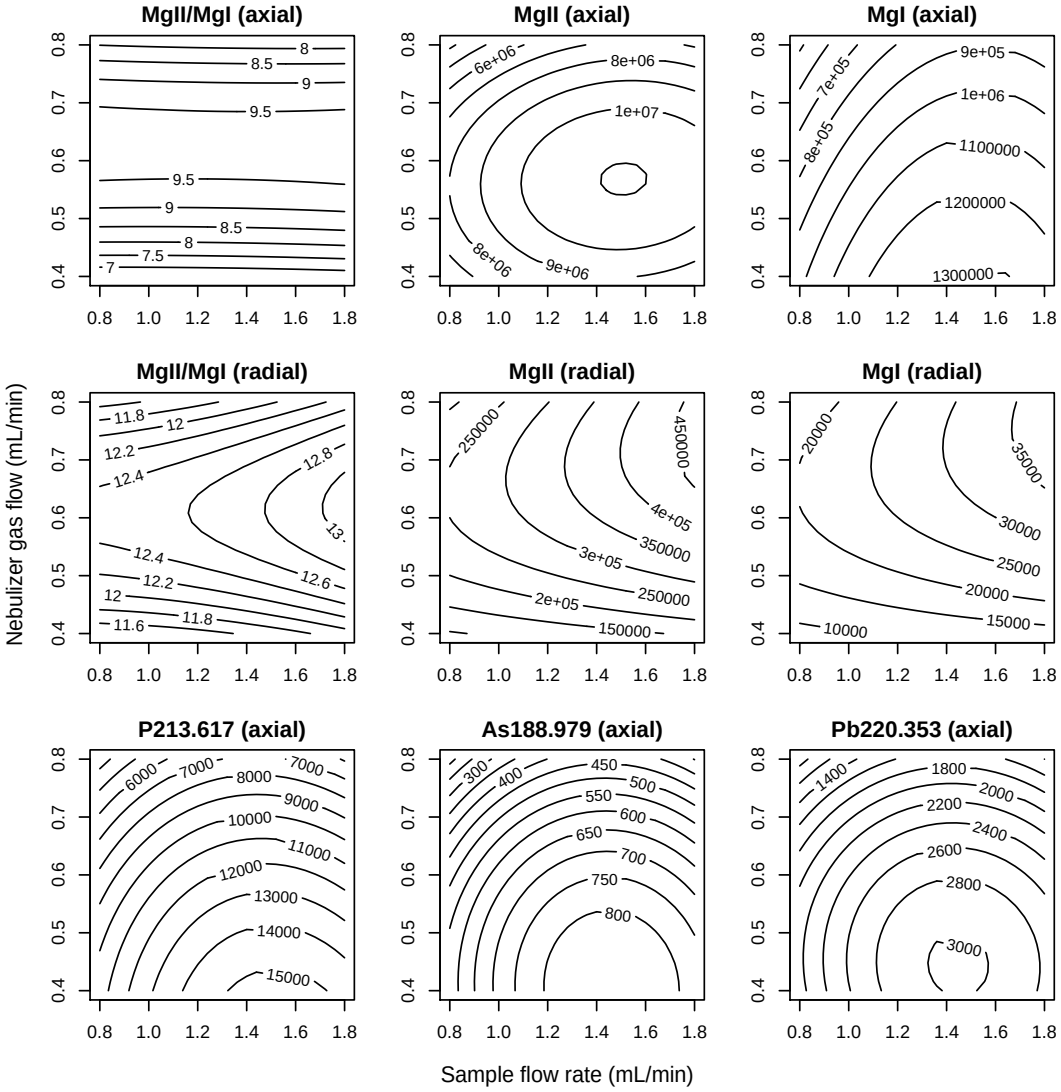

Figure 6.2: Optimization of nebulizer gas flow and sample flow rate for highest MgII/MgI ratio and highest analyte intensities (at PgF=8, AxF=0.2, and RfP=1500) with Scott spray chamber.

Table 6.1: Optimized operating parameters for Scott and Cyclonic spray chambers, thereafter used during ICP-OES measurement.

ICP-OES operating parameter	Unit	Spray chamber	
		Scott	Cyclonic
Plasma gas flow	L/min	8	8
Auxiliary gas flow	L/min	0.2	0.2
Nebulizer gas flow	mL/min	0.6	0.5 - 0.6
Sample aspiration rate	mL/min	1.5	1.3
RF power	W	1500	1500

6.2 Sieving based beneficiation of fly ash

A number of studies have focused upon the correlation of ash mineralogy with its particle size distribution and found that heavy metals such as As, Cd, Cr, Cu, Ni,

Pb and Zn are more concentrated in smaller particle size (< 75 μm) fractions than in the larger ones.[128–131] However, correlations of phosphorus content with particle sizes were not explored. This study aimed to investigate the correlation between P concentration and particle size from seven fly ash samples.

6.2.1 Fly ash properties

Seven fly ash samples originated from different fuel mixtures from three power plants of Finland were compared in terms of particle size distribution. Figure 6.3 shows the variation in the PSD profile. Fly ash originating from 100 wt% peat contains a large number of small particles, while ash from woody biomass in CFB boiler consists of larger particles. However, the quality of fly ash including PSD profiles are highly affected by power plant processing conditions in the CHP boiler and ash collection system.[130] Figure 6.4 elucidates the sand, silt and clay grain-size distribution of ash samples.

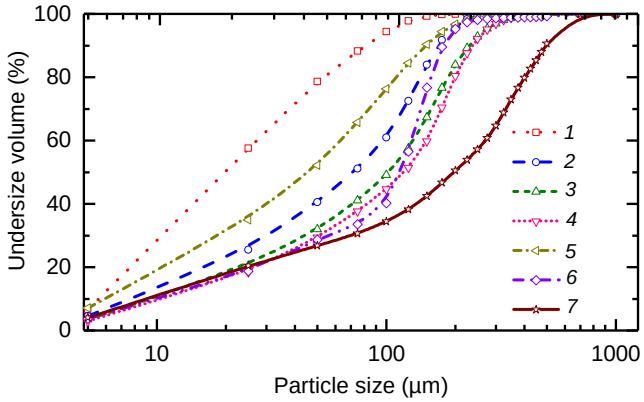

Figure 6.3: Particle size distribution (PSD) profile of seven fly ash samples. (1=P_{100}, 2=$P_{80}B_{20}$, 3=$P_{70}B_{30}$, 4=$P_{65}B_{35}$, 5=$P_{50}B_{50}$, 6=$P_{30}B_{70}$, 7=B_{100})

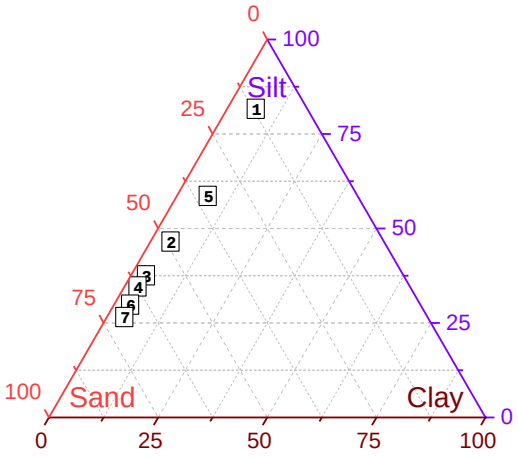

Figure 6.4: The ternary diagram of sand, silt and clay grain-size distribution for seven ash samples. (1=P_{100}, 2=$P_{80}B_{20}$, 3=$P_{70}B_{30}$, 4=$P_{65}B_{35}$, 5=$P_{50}B_{50}$, 6=$P_{30}B_{70}$, 7=B_{100})

A comprehensive elemental analysis of seven fly ash samples revealed significant variations in the distribution of elements in samples originating from different fuel mixtures; the results are listed in Table 6.2. The phosphorus composition varies from 0.49 to 1.72 wt% of ash. Si and Ca were most abundant components with respective concentrations from 14.56 to 29.64 and 8.64 to 30.43 wt%. Arsenic (As) concentration for $P_{80}B_{20}$ and $P_{50}B_{50}$ samples exceeded its limit value of 40 mg/kg, being therefore unsuitable for forest application. The rest of the samples can be used as fulfilling the requirements of the Decree on fertilizer products.

Table 6.2: Major elemental composition in wt% and trace elements concentration (mg/kg) of seven fly ash samples determined with ICP-OES.[I] The given limit value indicates the maximum concentration of trace elements that is allowed for forest fertilization use and comply with "the Decree of 12/7" on fertilizer products.[25]

Element	P_{100}	$P_{80}B_{20}$	$P_{70}B_{30}$	$P_{65}B_{35}$	$P_{50}B_{50}$	$P_{30}B_{70}$	B_{100}	
	Major component in wt%							
C	1.08	0.26	0.82	0.68	2.21	2.08	1.36	
H	0.29	-	-	-	0.16	0.11	0.20	
N	-	-	-	-	-	0.04	-	
P	1.01	1.33	0.90	0.95	1.72	0.49	1.21	
Al	7.93	9.14	9.99	8.61	6.01	4.77	3.38	
Ca	30.43	9.22	8.17	8.64	13.11	4.75	15.40	
Fe	10.73	14.28	10.67	8.03	6.04	3.17	2.00	
K	1.44	1.98	2.24	1.91	2.17	1.43	3.10	
Mg	2.35	1.65	1.35	1.26	1.69	0.85	2.16	
Na	1.03	1.10	1.45	1.10	0.73	0.65	0.90	
Si	14.56	18.91	20.74	19.00	18.78	29.64	17.31	
	Trace element concentration (mg/kg)							Limit value
As	33.4	$78.9^{\oplus}$	34.5	33.1	$61.6^{\oplus}$	24.3	6.7	30
Cd	1.1	2.7	1.1	2.2	7.4	4.0	8.6	17.5
Cr	36.2	67.6	53.7	35.3	57.8	34.7	45.1	300
Cu	84.2	100.0	93.5	130.4	125.7	112.6	89.6	700
Ni	29.0	31.8	23.2	28.0	37.5	26.5	24.6	150
Pb	40.4	82.4	39.6	43.9	69.9	38.2	26.3	150
Zn	114.9	274.7	188.5	224.4	675.7	239.2	1704.8	4500

$-$ = <LOD, $\oplus$ = concentration exceeding limit value

6.2.2 Impact of fractionation on fly ash chemistry

Sieving of all fly ash samples indicated that a large proportion of the particles belong to the smallest size range, 0-45 μm for most of samples except B_{100}, where the weight is distributed uniformly to all particle size range as seen in Figure 6.5. The elemental composition of each five fractions was determined; major elements in each fraction are shown in Figure 6.6. The relative composition of phosphorus and other major components in the respective weight fraction ($F_1 - F_5$) is estimated as:

$$M_{F_i} = C^M_{F_i} \cdot {F_i}^{wt\%} \text{ and } M_{F_i}\% = \frac{M_{F_i}}{\sum_{i=1}^{5} M_{F_i}}$$

where M_{F_i} is the relative concentration of element in F_i weight fraction, $C_{F_i}^{M}$ is the concentration of element in F_i determined with ICP-OES and $F_i^{wt\%}$ is the weight proportion of the F_i fraction.

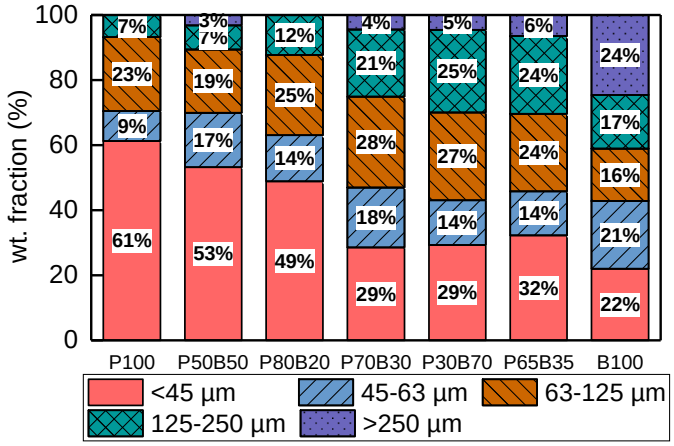

Figure 6.5: Weight fractions of each fractionated ash of seven fly ash samples.

This study emphasized the effect of fractionation on the distribution of phosphorus and other major components to different size fractions. Figure 6.6 shows that P and also Fe, Al, Ca, and K are concentrated in the small size fractions. Meanwhile, the Si concentration seems to have a nonuniform distribution. This indicates a huge scope for sieving in the manipulation of fly ash chemistry and P recovery. This study also found a correlation between elevated trace element content and smaller particle size fraction, which was in agreement with findings of other studies.[130,131]

6.2.3 Usability of fractionated fly ash

The fertilizing effect of wood ash lasts for 30-40 years; this is 5-15 years longer than that of chemical fertilizers.[132] Increased P, K, Ca and Mg concentrations in smaller-size fractions increase their value as forest fertilizer due to fertilizing effects of P and K and liming effects of Ca and Mg.[133] However, the content of heavy metals in fly ash solely regulates its use as forest fertilizer, according to the Decree on fertilizer products. The concentration of trace elements in each sieved fraction, including their maximum allowed concentration for use as forest fertilizer, is shown as a radar plot in Figure 6.7. This illustrates the potential use of fractionated ash samples whose concentrations do not exceed the limit values.

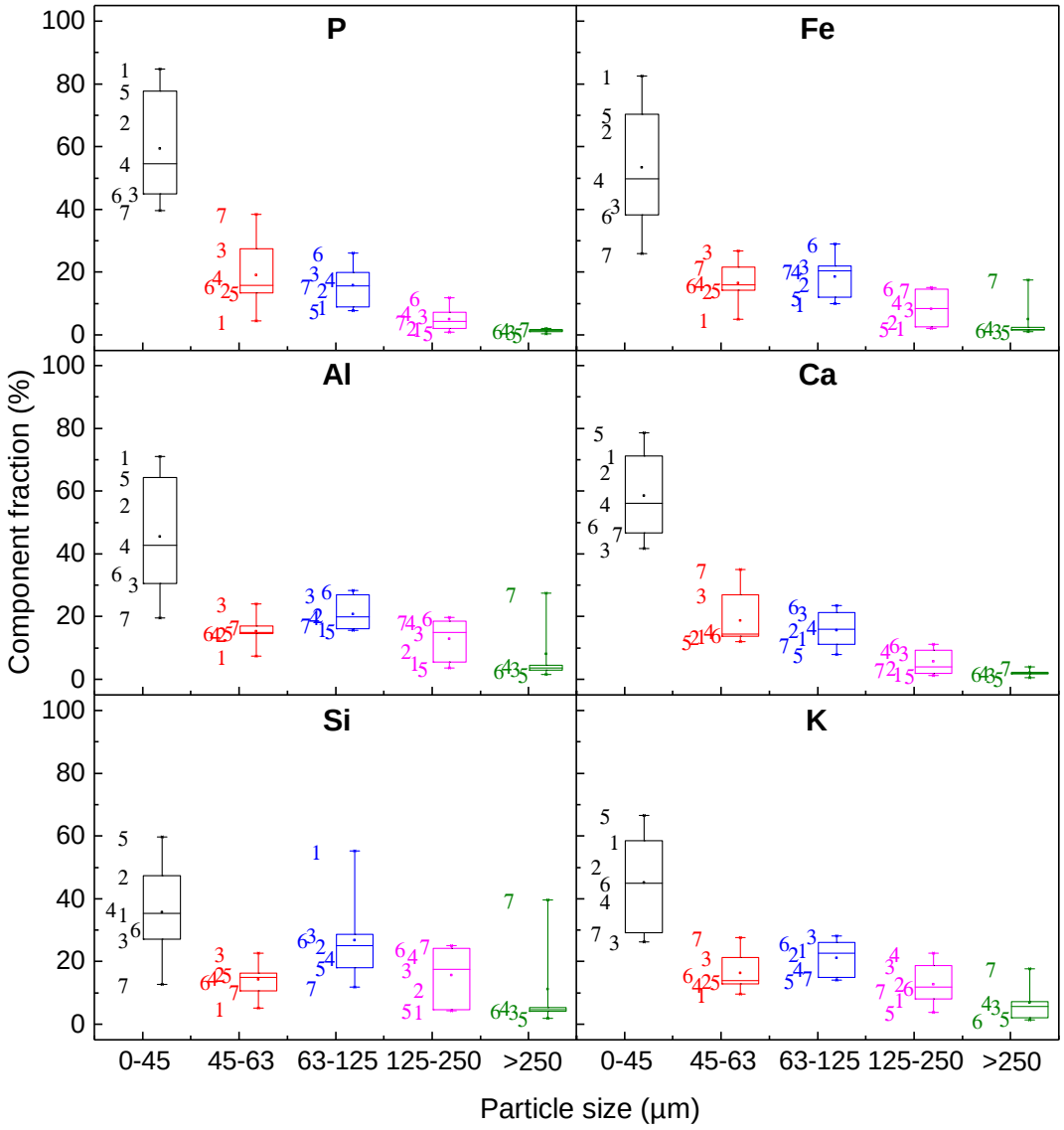

Figure 6.6: Distribution of components (P, Fe, Al, Ca, Si and K) on different size groups obtained via fractionation and its impact on fly ash chemistry. (1=P_{100}, 2=$P_{80}B_{20}$, 3=$P_{70}B_{30}$, 4=$P_{65}B_{35}$, 5=$P_{50}B_{50}$, 6=$P_{30}B_{70}$, 7=B_{100})

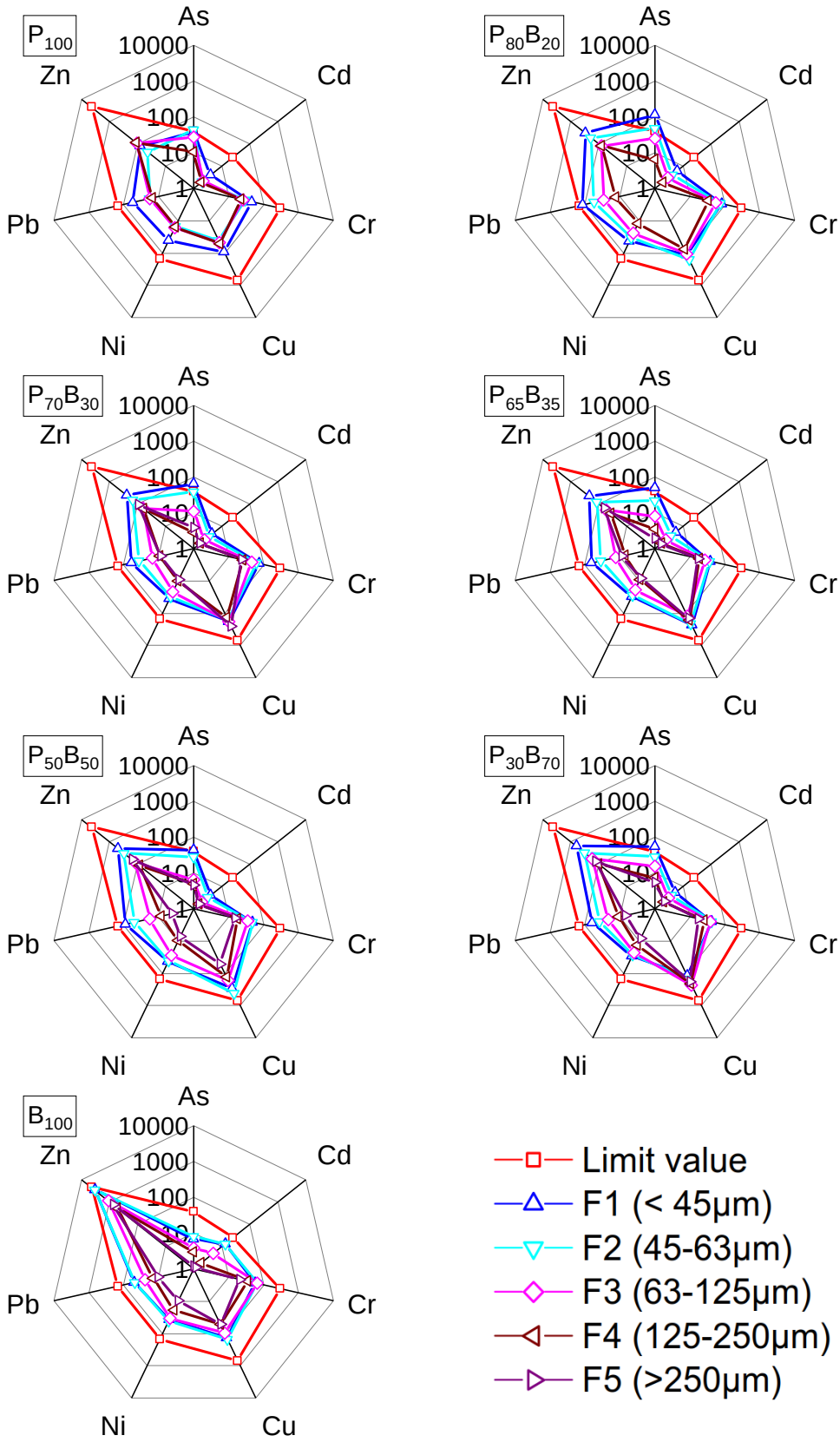

Figure 6.7: Concentration of trace elements on each set of fractionated ash showing their usability (concentration of As exceeds the limit value for F1 and F2 fractions for all samples except B_{100}).

6.2.4 Phosphorus refining via sieving

In this study, B_{100} was selected as a secondary P resource in the context of recovery of high-grade P-products. B_{100} is the residual ash obtained after combustion of renewable wood-based biofuels in CFB boiler from Alholmens Kraft CHP, the largest bio-fuelled power plant in the world. Hereafter, B_{100} is labeled as fly ash FA.

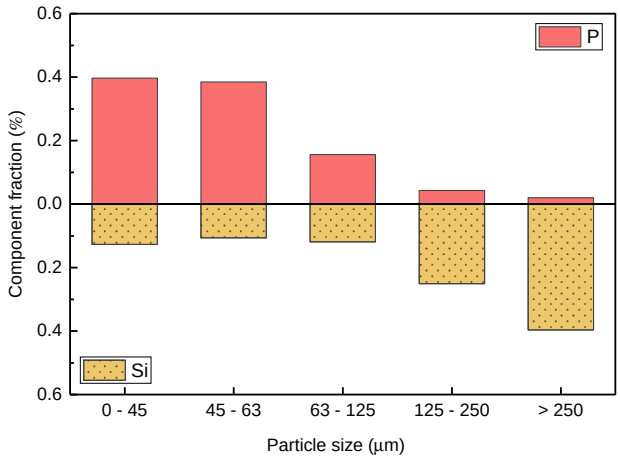

Figure 6.8: Correlation between fractions of P, Si and particle size.

The relation between P, Si and the range of particle size can be seen from Figure 6.8, showing that most of P is present in smaller particles (0–125μm) while the trend is quite opposite for Si, with higher fractions associated with larger particles (>125 μm). Fractionation at 125 μm facilitates the rejection of 41 wt% of fly ash, further affording lower consumption of chemical resources in the recovery process. In addition, P content in the fly ash is increased by a factor of 1.38 while the Si content is decreased by a factor of 3.8. Concentrations of major and trace elements in pristine (FA), fractionated (FFA) and rejected/discarded (DFA) fly ash are presented in Table 6.3.

Table 6.3: Elemental composition and heavy metal content of FA (pristine fly ash), FFA (< 125μm) and DFA (>125μm) measured by ICP-OES after extracting with *aqua regia* and 4-5 drops of HF.[II]

	Major element (wt%)						Trace elements (mg/kg)						
	P	Al	Fe	Si	Mg	Ca	Zn	Cu	Cr	Pb	Ni	As	Cd
FA	1.21	3.38	2.01	17.3	2.16	15.4	1704	89.6	45.1	26.3	24.6	6.7	8.6
FFA	1.67	3.11	2.03	4.54	2.83	21.7	2595	99.7	50.4	35.2	33.7	11.7	11.5
DFA	0.47	4.16	2.15	30.3	1.03	5.4	475	82.5	44.8	12.8	12.4	–	–

– = value lower than LOQ.

6.3 Leaching of fly ash

6.3.1 Correlation between leaching parameters

Correlation between acid concentration, LS ratio and leaching time was studied using RSM method and CCD design with a viewpoint of analyzing their linear, two-factor interaction, and quadratic effects: it is depicted in Figure 6.9. This study suggests that a minimum leaching time of 12 minutes, LS ratio of 12, and acid concentration of 2.5 M are required for total recovery of phosphorus from fly ash to an acid solution. The contour plot for phosphorus recovery against the acid concentration and leaching time also indicates that higher acid concentrations significantly lower the leaching time. On the other hand, a prolonged leaching would go against dephosphorization because of re-precipitation of phosphorus with other metal ions released during the leaching.[66]

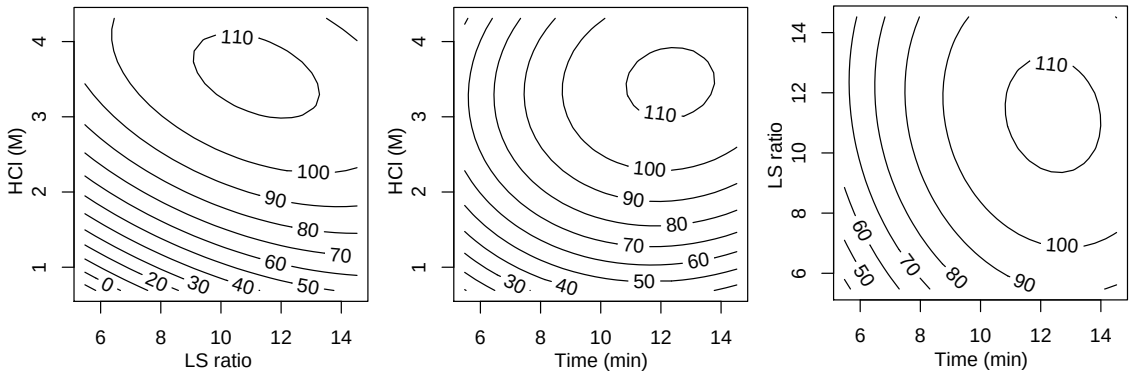

Figure 6.9: Correlation between molar concentration, LS ratio and time for phosphorus recovery from fly ash using HCl.

Therefore, use of high molar acid concentration with lower leaching time is used in this study. In addition, high acidity in the solution favors the polymerization of silicic acid and promotes the precipitation of Si-particle.[134,135]

6.3.2 Phosphorus leachability

Details of the fly ash leaching with 2, 5, 8 M of HCl and HNO_3 are summarized in Table 6.4. Phosphorus leaching was more efficient with HCl than with HNO_3, while varying the acid concentration between 2M and 8M had only a small effect on P leachability. Lower concentrations of acid showed the highest Si leachability, the order of leaching feasibility being 2M>5M>8M for both HCl and HNO_3. A similar behavior of Si leaching from zeolite analcime and sodium metasilicate nonahydrate (SMN) with HCl was also reported by Fogler et al.[135]. The low dissolution of silicon in concentrated acid may be attributed to the low availability of OH^- groups that assist the formation and stabilization of orthosilicic acid ($Si(OH)_4$) in the leachate solution and simultaneous precipitation of silica gel particles.

Table 6.4: Leachability and recovery of P, Si, Fe, Al Mg and Ca in HCl and HNO_3 acids at concentration of 2, 5 and 8 M.[II]

Element		Concentration (mg/L) of major components					
		P	Si	Fe	Al	Mg	Ca
HCl (M)	2	1407 (100.9)[a]	2403 (63.6)	760 (44.8)	1346 (52.1)	2162 (91.7)	18831 (103.9)
	5	1388 (99.5)	2135 (56.5)	911 (53.7)	1319 (51.1)	2097 (88.9)	17410 (96)
	8	1425 (102.2)	1947 (51.5)	1154 (68.0)	1380 (53.4)	2181 (92.4)	17324 (95.6)
HNO_3 (M)	2	1298 (93.1)	2472 (65.4)	673 (39.7)	1343 (52)	2123 (90)	18301 (101)
	5	1355 (97.2)	2179 (57.6)	767 (45.2)	1347 (52.1)	2100 (89)	18098 (99.8)
	8	1288 (92.3)	1811 (47.9)	760 (44.8)	1234 (47.8)	1950 (82.6)	16701 (92.1)

[a] values in "( )" indicates leaching recovery %

6.4 Role of silica in phosphorus refining

The correlation between the purity of precipitated phosphorous product and dissolved silica concentration was studied. Figure 6.10(a,b) shows the effect of pH and Si concentration on the recovery of phosphorus from the synthetic solution. At the given stoichiometric concentration of analytes, total dissolved phosphorus was precipitated at pH 4. Upon an increment in dissolved silica concentration, the phosphorus recovery slightly decreases which indicates inhibition of phosphorus precipitation due to the formation of silica particles. The inhibition mechanism is attributed to the adsorption of silicic acid on the precipitated particles which hinders their growth.[106]

Figure 6.10(c,d) depicts the relation between Si in the precipitated solids, pH and dissolved Si concentration in the solution. It also suggests a linear relation between the dissolved and precipitated silica. The co-precipitated silica simply decreases the value and use of recovered phosphorus compounds. Poon et al. also reported that Si co-precipitation with P in a single-step and two-step extraction methods account Si content up to 8.15 and 2.5 wt%, respectively in the precipitates.[71] Therefore, removal of silica from the leachate solution improves the product quality and the economy of the overall operation by limiting silica scaling.

6.5 Desilication

Removal of silica from leachate solution obtained from various molar concentrations of mineral acid was studied in unstirred conditions to avoid an adiabatic temperature rise due to stirring. The effect of acid matrices, their concentration and temperature was emphasized, since previous studies have shown that solubility of silica varies proportionally with pH and temperature.[116,136,137]

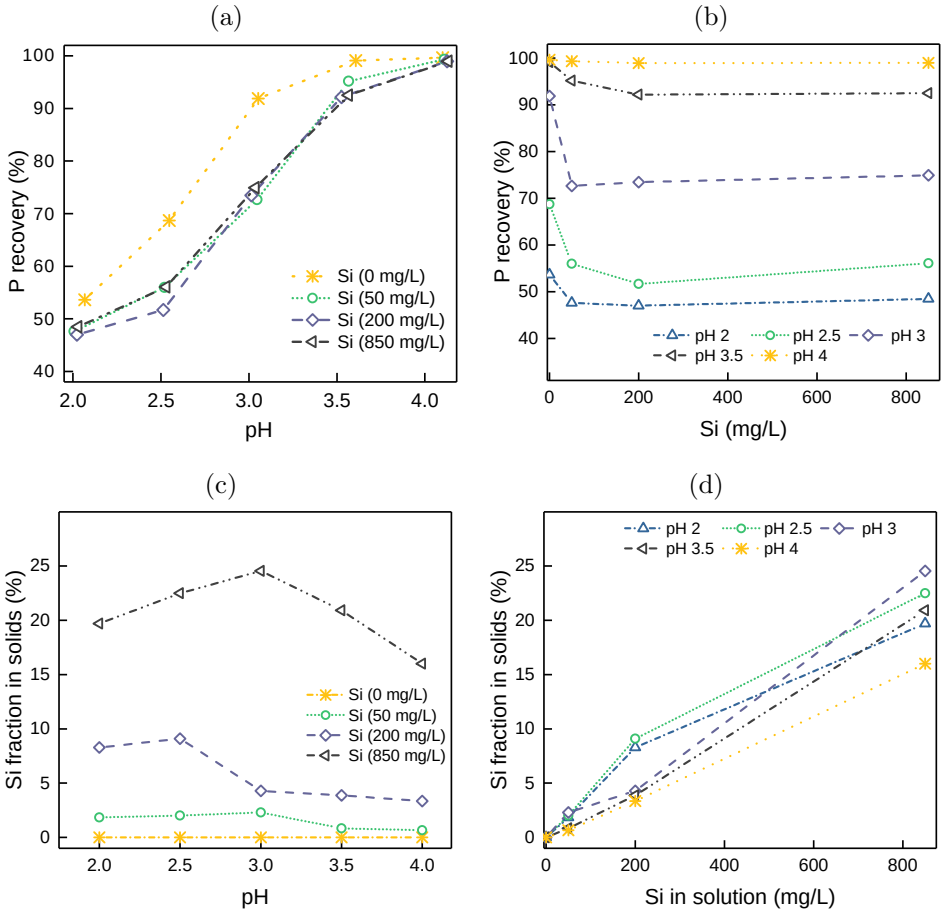

Figure 6.10: Effect of pH (a) and Si concentration in solution (b) on the recovery of phosphorus, and correlation between wt. fraction of Si (wt%) in precipitated solids with pH (c), and Si concentration in solution (d)

6.5.1 Effect of acid concentration and matrix

The concentration of dissolved Si was measured as a function of time (see Figure 6.11(a)) from leachate solution obtained from 2, 5 and 8M solutions of HCl and HNO_3. The disappearance of dissolved silica is in good agreement with a 1st order kinetic model and exhibits two kinetic regimes; (i) first regime with slow consumption and (ii) second regime with rapid depletion of soluble silica. The earlier phase is called induction time/period, while the later is called polymerization zone.[138–140] In order to evaluate the effect of H^+ ions on Si removal, the remaining H^+ ion concentration was estimated by Eq.6.1:[II]

$$H^+_{leachate} = H^+_{added} - 1.1 \times \Big(2 \times [Ca] + 2 \times [Mg] + 2 \times [Si]\Big) + 3 \times [P] \qquad (6.1)$$

where H^+_{added} is the molar concentration of acids used during leaching and [Ca], [Mg], [Si] and [P] are the concentrations (mol/L) of Ca, Mg, Si and P in the leachate solution.

At a low (0.72 mol/L) concentration of H^+ ions, removal of dissolved silica amounts to less than 10%. Increasing the H^+ ions concentration to 6.9 mol/L in HCl matrices results in the removal of 99% of Si in only 5 h (Figure 6.11(a)).

H^+ affects the silica removal in two ways; more acidic conditions (i) reduce silica solubility, thus increasing the supersaturation and promoting its precipitation,[136,137] and (ii) catalyze the polymerization of silicic acid that promotes growth in polymer and particle size.[141,142]

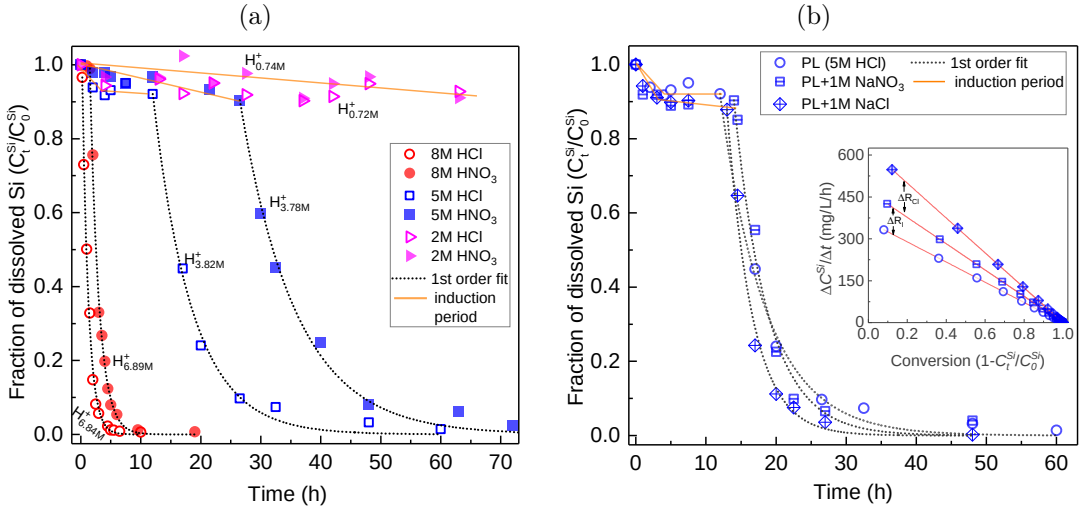

Figure 6.11: Disappearance of dissolved silica as a function of time showing (a) effect of H^+ concentration and (b) effect of Cl^- concentration. The dotted line indicates the best-fitted first order modeled data to the measured data.[II]

Despite the parity in their H^+ ion concentration, there is a clear discrepancy between the leachates obtained with similar molar concentration of HCl and HNO_3. However, there is significant difference in their anion (Cl^-) concentration. Previous studies have reported that F^-, being a small single-charged ion with a low polarizability, promotes the coordination number of silicon(IV) from four to six[143] and reduces the electron density on unsaturated tetravalent Si, making it more susceptible to nucleophilic attack from another coordinatively unsaturated Si[144]. This linkage of two monomeric Si species forming a siloxane bond (Si−O−Si) is critical in increasing silica polymer length and particle growth. Cl^- ions, sharing the same group in the periodic table, possess characteristics similar to F^- ions and catalyze the polymerization reaction. Figure 6.11(b) supports the notion of catalysis by Cl^-, where addition of 1M of NaCl shows an increment in the instantaneous reaction rate up to two-fold. 1 M of $NaNO_3$ was added to a separate batch to differentiate the effect of ionic strength from Cl^-, since 1 M of both salts induce equal increases in the ionic strength. However, no significant effect was observed on the induction period due to the added salts.

6.5.2 Effect of temperature

Due to the presence of two kinetic regimes, temperature dependence of silica precipitation is examined only on the leachate obtained with 5 M HCl solution. Figure 6.12(a) reflects the proportional variation in silica precipitation rate due to a rise in temperature. The induction time was significantly reduced from approximately 15 h to less than 1 h when the temperature was raised from 20°C to 60°C. In addition, the polymerization and precipitation of silica follow the Arrhenius relationship

(K_p=Ae$^{-E_a/RT}$) between the temperature (T) and the first order polymerization reaction constant (K_p). A plot of ln(K_p) vs. (1/T) gives an estimate of the activation energy, as the slope, which is 39.25 kJ/mol.[II] The calculated value from this study is also in agreement with the reported activation energy of 37.6 kJ/mol for highly acidic gel prepared in 1.65 M of hydrochloric acid.[145]

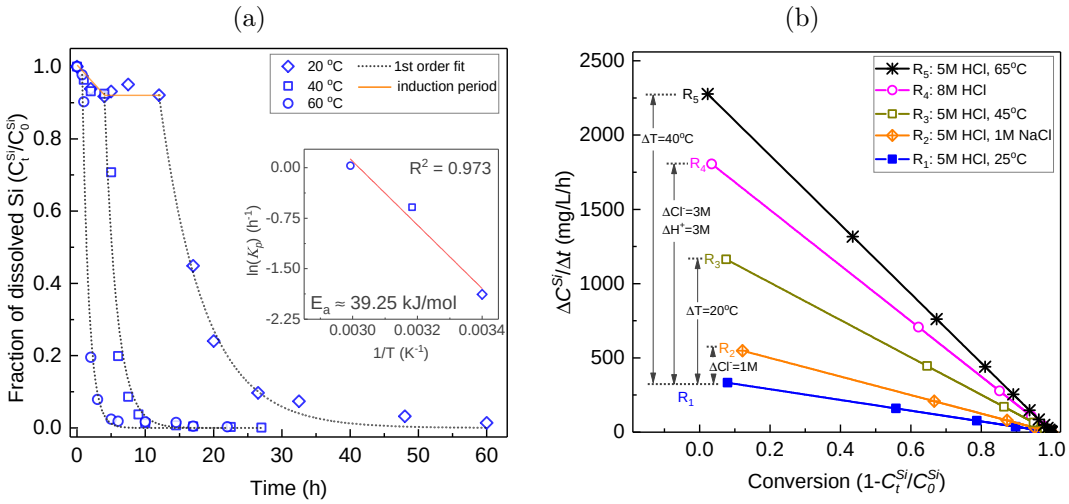

Figure 6.12: (a) Disappearance of dissolved silica in a leachate as a function of time at various temperatures showing Arrhenius relationship between the temperature (T) and the first-order polymerization reaction constant (K_p), (b) Instantaneous reaction rate for Si precipitation induced by H^+, Cl^- and temperature.[II]

6.5.3 Efficacy of silica removal

A high concentration of HCl benefits the dissolution of P during leaching and escalates the removal of silica from the leachate solution in comparison to HNO_3 (see Figure 6.11(a)). Figure 6.12(b) shows the comparison of instantaneous silica precipitation rate induced by H^+, Cl^- and temperature in the leachate obtained with 5 M HCl. A rise in temperature by 40°C increased the reaction rate approximately 7-fold, while changes in H^+, Cl^- concentration by 3 M elevated the rate ca. 5-folds. Both treatment methods, temperature and HCl concentration, result in the removal of 99% of silica in only 5 h. Higher efficiency of Si-removal can be achieved with longer aging times. However, the earlier retained more leachate solution in the gel structure and reduced the volume of recovered leachate, thereby decreasing the separation efficiency (see Table 6.5). This was due to the formation of gel with a large volume, since earlier studies have shown development of a stiffer, stronger gel network with lower shrinking tendency at elevated temperature.[142]

Hence, leaching of the fractionated fly ash (FFA) with 8 M HCl followed by aging for 5 h was selected as desilication method. This silicon-free leachate was employed for the selective precipitation of phosphorus.

Table 6.5: Initial and final (after 5 h of aging) concentration of major and trace elements for 8 M HCl leachate at 20°C and 5 M HCl leachate at 60°C.[II]

Element	8 M HCl leachate, 20°C			5 M HCl leachate, 60°C		
	Initial (t=0) (mg/L)	Final (t=5h) (mg/L)	Retained in Si-gel (wt%)[⊗]	Initial (t=0) (mg/L)	Final (t=5h) (mg/L)	Retained in Si-gel (wt%)
P	1450	1490	10.6	1522	1509	25.6
Si	1950	21	99.1	2435	8	99.8
Al	1320	1340	11.7	1355	1377	23.8
Fe	1095	1110	11.8	1038	1058	23.5
Mg	2150	2180	11.8	2453	2482	24.1
Ca	17700	17400	14.5	16191	16188	25.0
Zn	227	226	13.4	195	198	23.8
Cu	7.6	7.4	15.3	7.1	7	26.1
Cr	3.4	3.3	15.6	2.9	2.95	23.7
Pb	3.1	3.2	10.2	2.6	2.8	19.2
Ni	2.5	2.3	20.0	2.3	2.4	21.7
As	1.1	0.7	44.6	1	0.8	40.0
Cd	1	1	13.0	0.9	1	16.7

6.6 Speciation of phosphorous species in leachate

Oxides and metal salts of phosphorus are considered to exist in ash residue.[146–148] When these oxides and phosphates react with either acid or base, $H_nPO_4^{(3-n)-}$ derivatives are generally assumed to predominate in the solution phase.[50] Its fraction in solution is also a function of pH and various salts of such phosphate derivatives may precipitate at different pH.[39,41,76] Fe, Al, Ca and Mg are some of the major cations present in the leachate with concentrations above 1 g/L; they have higher affinity to form stable phosphate compounds in acidic regimes.

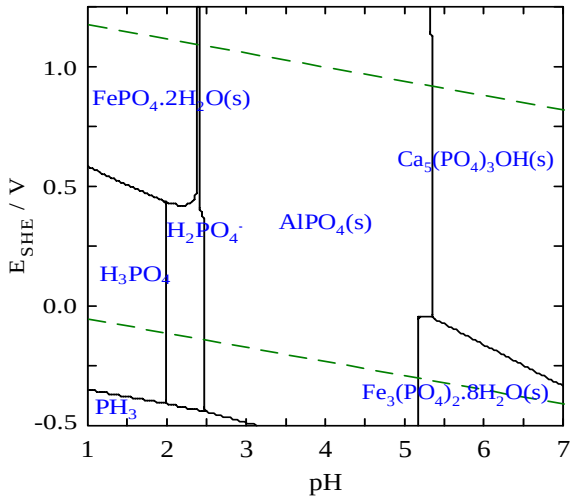

Figure 6.13: Eh-pH diagram representing predominant phosphorus species in solution. Equilibrium calculations were made using the Medusa and Hydra program at 24 mM of PO_4 and PO_4:Fe:Al:Ca = 1:1:1:10 (molar fraction).[III]

Equilibrium calculations were performed in the Medusa and Hydra program to identify the predominant phosphate species in the leachate solution. The model-

ing result is presented in Figure 6.13 and used as guide for developing strategies for phosphorus recovery. This reveals a predominance of $FePO_4$ below pH 2.5, $AlPO_4$ between pH 2.5-5.5, and $Fe_3(PO_4)_2$ and $Ca_5(PO_4)_3OH$ above pH 5. Moreover, it strongly implies the possibility of P-precipitation as $FePO_4$, $AlPO_4$ and $Ca_5(PO_4)_3OH$ at pH's where they predominate, if present in an adequate concentration.

$AlPO_4$ is more dominant phosphorus compound than $FePO_4$ and $Ca_5(PO_4)_3OH$ in acidic media. $FePO_4$ precipitation is influenced by ferrous (Fe^{2+}) and ferric (Fe^{3+}) iron equilibrium and is therefore susceptible to reduction potential of solution in comparison to other phosphates. In addition, $FePO_4$ precipitation is challenging because of akaganéite ($Fe(OH)_{1-x}Cl_x$) co-precipitation in chloride media below pH 2.[149,150]

6.7 Selective P precipitation

6.7.1 Chelation masking strategy

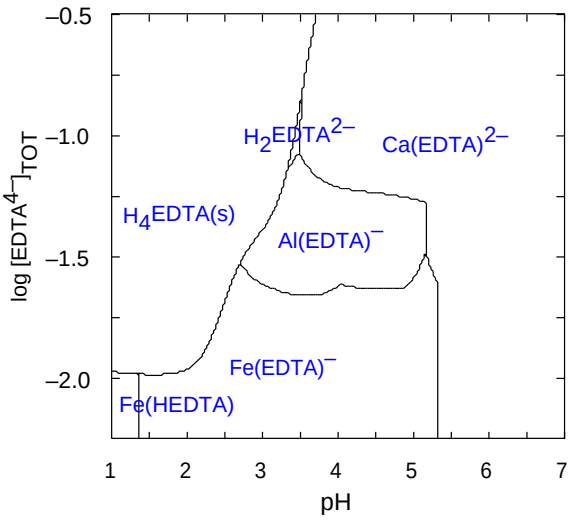

Figure 6.14: Speciation of EDTA complexes as a function of pH and EDTA concentration in the leachate solution using Medusa and Hydra program.[III]

Due to lack of commercial value as a raw material for the phosphate industry and its low solubility, recovered or recycled $FePO_4$ and $AlPO_4$ are less favoured for P recovery from secondary resources.[38] Masking of Fe and Al by the use of a chelating reagent is seen as a feasible and economical method, in contrast to its removal via precipitation. The equilibrium between Fe, Al, Ca (at respective concentrations of 24, 24 and 240 mmol/L) and varying EDTA concentrations in acidic regime is shown in Figure 6.14. It also suggests that the selectivity of EDTA is in the order Fe > Al > Ca between pH 3.5 and 5.4. Therefore, EDTA was employed for the chelation of the trivalent metal cations; the possibility of P-precipitation with Ca was explored by employing the RSM method.

6.7.2 Selective phosphorus precipitation

The relation of pH and EDTA concentration with phosphorus recovery were tested using CCD experimental design. In this study, [EDTA]/[Fe+Al], termed as ER, was adopted instead of actual EDTA concentration. An ER value of 0.29 indicates a stoichiometric equilibrium between Fe and EDTA; this was used as minimum value in the RSM approach. Similarly, an ER of 1 indicates equilibrium of EDTA with Fe and Al combined. A central composite design consisting of 12 runs was created and the experiments were run on the sequential order as provided by the program (RcmdrPlugin.DoE plug-in in R environment).

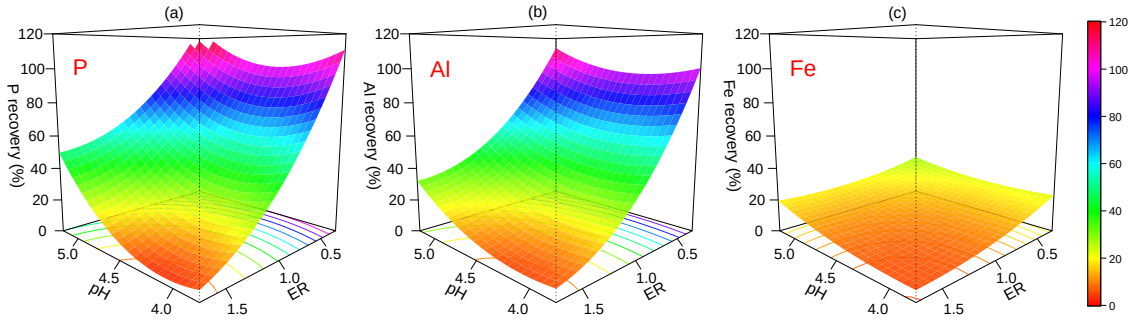

Figure 6.15: Response-surfaces for recovery of phosphorus (a), aluminium (b), and iron (c) as a function of pH and ER ($=\frac{[EDTA]}{[Fe+Al]}$). The experimental matrices are based on the central composite design.[III]

The surface profiles for P, Al and Fe recovery are presented in Figure 6.15. Use of ER values greater than 1, i.e. [EDTA] > [Fe+Al], did not improve the recovery of phosphorus (as expected with Ca) and shows a minimum recovery value of 5% at ER of 1.5 and pH of 4. P recovery increases with increasing pH at higher ER values; however, Fe precipitation also accelerates. Parity in the response surface of P and Al recovery evince the precipitation of $AlPO_4$. Fe precipitation is limited throughout the experimental domain with values between 5 and 30%. Figure 6.16,

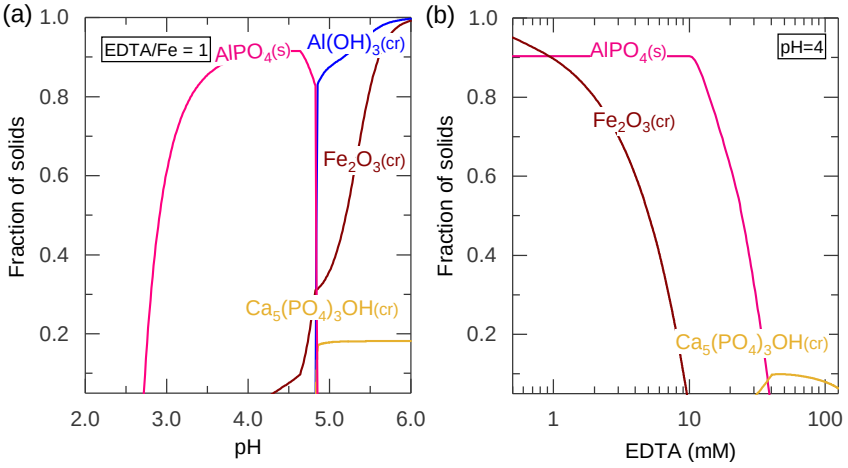

Figure 6.16: Speciation of solids as a function of pH (a) and EDTA concentration (b) in the leachate solution using the Medusa and Hydra program.[III]

a equilibrium modeling approach, explicates the response surface of P, Al and Fe recovery. The decrement of phosphorus recovery (see Figure 6.15) with increasing EDTA concentration is in agreement with declining solid fraction of $AlPO_4$ (see Figure 6.16) due to formation of stable $Al(EDTA)^-$ complex (see Figure 6.14). Although precipitation at higher pH (>5) leads to higher P recovery, rise in Fe (Fe_2O_3) co-precipitation is also foreseen.

The effect of pH on the purity of precipitated compounds was inspected with the objective of retrieving a phosphorous precipitant with lower concentration of impurities.[III] Figure 6.17 shows the recovery of analytes as a function of pH from the leachate and the elemental composition of precipitants obtained at [EDTA]/[Fe]=1. Precipitant acquired between pH 3.5 and 4 contained the highest fraction of phosphorus, 21.2-20.2 wt%. However, precipitation at pH 4 enables a complete recovery of phosphorus from the leachate solution. In addition, Figure 6.17 shows similarities between the infrared spectra of the precipitant at pH 4 and precipitated pure $AlPO_4$. The shift in v(P-O) bands among the precipitants is due to (i) decrease in the force constant for the P-O and P-OH bands with decreasing protonation, and (ii) weakening of the P-O bonds due to adsorbed impurities.[151,152]

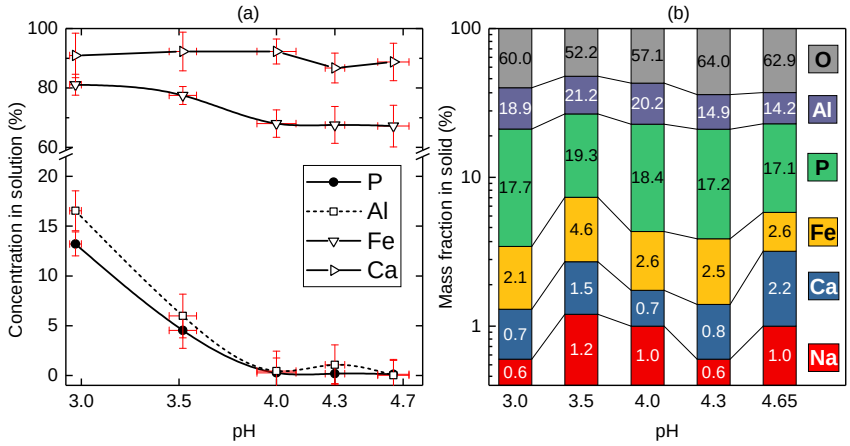

Figure 6.17: Effect of pH on (a) recovery of phosphorus and other major analytes from solution, (b) fractions of major elements in precipitate.[III]

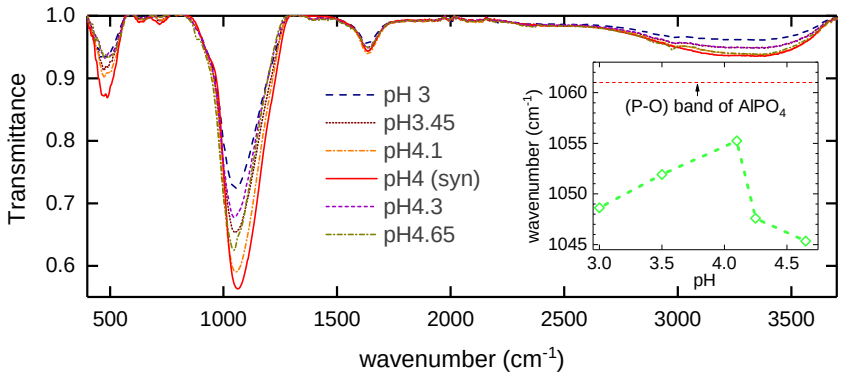

Figure 6.18: Comparison of infrared spectra of precipitated P-compounds to that of synthetic $AlPO_4$(A). Sub-figure shows the shift in the position of v(P-O) bands.[III]

Table 6.6 summarizes the recovery of major and trace elements during precipitation. This shows recoveries of over 60% for Cr and Pb while Zn, Cu, Ni, As and Cd recoveries are less than 30%. Therefore, precipitation of phosphorus as $AlPO_4$ at pH of 4 and EDTA concentration in a stoichiometric relation to Fe (i.e. [EDTA]/[Fe]=1 or ER=0.29) is found feasible. In the case of leachates with an inadequate concentration of Al with respect to PO_4^{3-}, addition of Al source enables its complete precipitation.

Table 6.6: Concentrations of major and trace elements before and after precipitation of desilicated leachate at pH 4 and $\frac{[EDTA]}{[Fe]}$=1.[III]

Element	Leachate	Filtrate		Recovery
	(mg/L)	(mg/L)	SD	%
P	1491	3.91	0.52	99.92
Al	1337	6.07	0.66	98.52
Fe	1106	230.46	11.38	31.93
Si	20.95	<LOQ		
Mg	2176	574.76	21.90	13.71
Ca	17370	4358.48	204.36	18.03
Zn	225.50	50.59	0.88	26.72
Cu	7.36	1.95	0.03	13.48
Cr	3.34	0.27	0.02	73.32
Pb	3.15	0.37	0.03	61.88
Ni	2.34	0.52	0.01	27.64
As	0.74	0.17	0.03	23.98
Cd	0.98	0.25	0.01	18.00

6.7.3 Characterization of precipitant

The elemental composition of the recovered phosphorus product (see Table 6.7) reveals Al and P in high concentration, respectively 16.3 wt% and 18.1 wt%, giving an Al/P ratio of 0.9. This closely resembles the theoretical ratio of 0.87 in pure $AlPO_4$. In addition, the diffuse peak in the range of 28-29^o in the X-ray diffraction pattern (see Figure 6.19) is comparable to that of amorphous aluminium phosphates precipitated from aluminium sludge[153] at 50-100°C[154]. The Al/P ratio, XRD pattern and the infrared spectra indicate that the precipitated compound is $AlPO_4$.

The amorphous white $AlPO_4$ still contains some impurities, 2.18 wt% Fe being a major contaminant, and traces of EDTA as indicated by the CHN analysis. Despite containing trace elements with toxic characteristics in low concentrations (below limit values imposed by "the Decree of 12/7" on fertilizer products[25]), its use as fertilizer is limited due to aluminium toxicity to plants. The industrial use of $AlPO_4$ recovered from the secondary sources, including ash residues, is limited. Therefore, new uses and/or further refining and conversion of the recycled aluminium phosphate to more usable phosphorus products need to be developed.[155]

Table 6.7: Elemental composition of the precipitate obtained at pH=4 and [EDTA]/[Fe] = 1.[III]

	P	Al	Fe	Ca	Mg	C	H	N
(wt%)	18.08	16.31	2.18	0.63	0.12	1.26	3.13	0.15
	Zn	Cu	Cr	Pb	Ni	As	Cd	
(mg/kg)	1323	19.4	258	104	8.14	37.9	1.19	

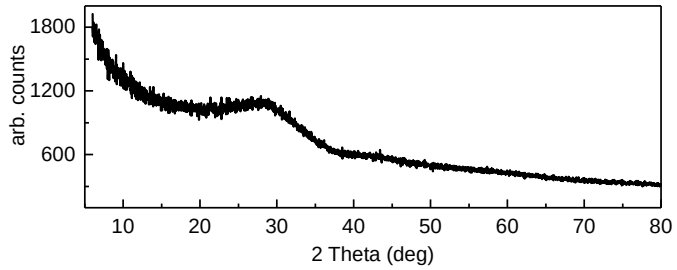

Figure 6.19: X-ray diffraction pattern showing the amorphous nature of the P-product obtained at pH 4.[III]

6.8 Conversion of $AlPO_4$ to struvite

In recent years, precipitation of magnesium ammonium phosphate (MAP)/struvite, a slow release fertilizer, is seen as a sustainable method for phosphorus recovery from waste water, sewage sludge, anaerobic digester effluent, etc.[156–158] Equimolar concentration (1:1:1) of Mg^{2+}, NH_4^+ and PO_4^{3-} at alkaline pH (8-10) and stirring/mixing (speed of 70 – 200 rpm) are required to precipitate struvite.[159–161]

6.8.1 Extraction of P with phosphoric acid

This study explores the dissolution behavior of $AlPO_4$(B, synthetic compound) in phosphoric acid solution. The effect of acid concentration at LS ratio of 40 on extraction efficiency is presented in Figure 6.20. LS ratio of 40 ensured the Al concentration in the range of 3-5 g/L; for this range styrene based cation exchanger is known to exhibit favorable adsorption for Al.[162] 0.5 M of phosphoric acid was found sufficient for complete dissolution of $AlPO_4$(B) and the measured pH was 1.6. The dissolution efficiency (η) was estimated with Eq.6.2.

$$\eta_{\mathrm{A}}(\%) = \frac{\mathrm{C}^{\mathrm{L}}_{(\mathrm{mg/L})}}{\mathrm{C}^{\mathrm{A}}_{(\mathrm{mg/kg})}} \times \frac{\mathrm{V}^{\mathrm{L}}_{(\mathrm{mL})}}{\mathrm{W}^{\mathrm{AlPO_4}}_{(\mathrm{g})}} \times 100 \tag{6.2}$$

where $\mathrm{C}^{\mathrm{L}}_{(\mathrm{mg/L})}$ is concentration of analytes A (Al, Fe and P) in leachate solution, $\mathrm{C}^{\mathrm{A}}_{(\mathrm{mg/kg})}$ concentration of analytes A in solid, $\mathrm{V}^{\mathrm{L}}_{(\mathrm{mL})}$ volume of leaching reagent and $\mathrm{W}^{\mathrm{AlPO_4}}_{(\mathrm{g})}$ is the weight of solid used during dissolution. A known concentration of P (from leaching reagent) was subtracted from the measured P concentration for determination of its dissolution efficiency.

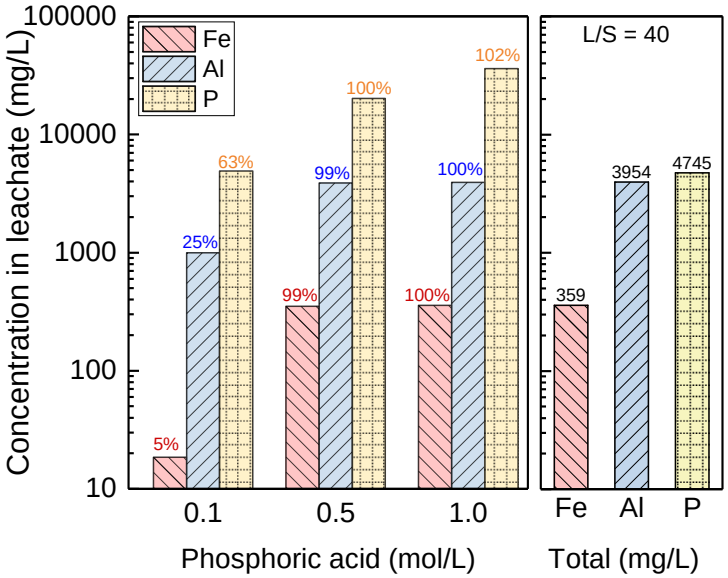

Figure 6.20: Leaching behavior of $AlPO_4$(B) with varying phosphoric acid concentration at LS ration of 40 mL/g.[IV]

6.8.2 Removal of Al and Fe with cation exchange resin

Goher et. al. suggested that AIR-120H, a strongly cation exchange resin, is an excellent, effective and inexpensive material to remove high amounts of Al and Fe ions from waste water.[163] AIR-120H was also shown to be capable of removing heavy metals (Cr, Cu, Ni, Pb and Zn) from aqueous solution.[164–166] Therefore, the feasibility of metal ion removal with AIR-120H from leachate obtained with 0.5 M H_3PO_4 was studied with varying CER dosage and retention time of 1 h (see Figure 6.21(a)). A CER dosage of minimum 0.5 g/mL was required to remove 99% of Al and 95% of Fe ions from the P-rich solution.

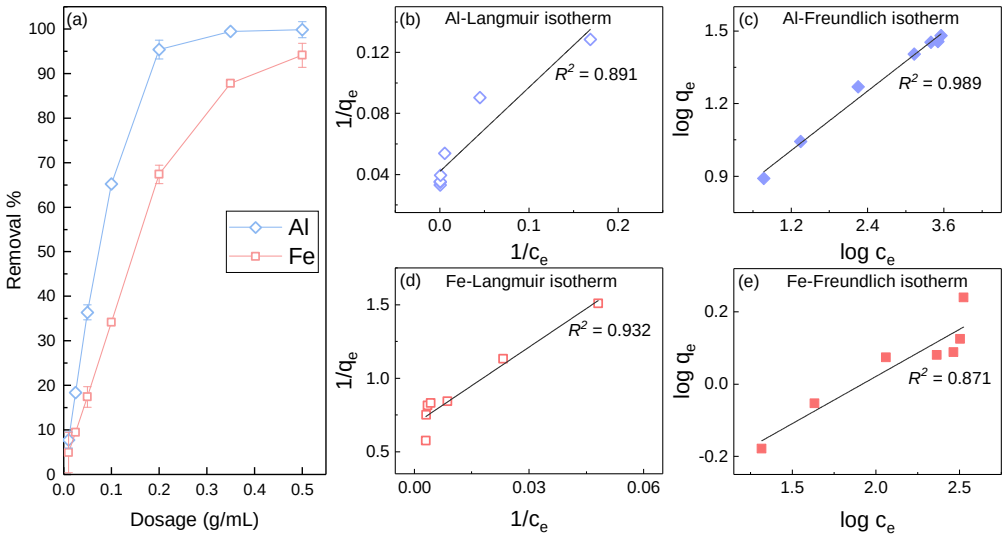

Figure 6.21: Effect of AIR-120H dosage on the removal efficiency of Al and Fe (a), Langmuir and Freundlich isotherm plot of aluminium (b-c) and iron (d-e).[IV]

The adsorption mechanism of Al and Fe ions on AIR-120H resin was also studied using Langmuir and Freundlich adsorption isotherms. The Langmuir isotherm is based on theoretical principle that assumes uptake of metal ions on a homogeneous surface by monolayer sorption, while the Freundlich isotherm assumes sorption in a heterogeneous surface of adsorbate's monolayer.[164]

Eq. 6.3 and 6.4 represent a general and linear form of the Langmuir and Freundlich isotherm, respectively;

$$q_e = \frac{x}{m} = \frac{q_{max} b C_e}{(1 + bC_e)} \;\Rightarrow\; \frac{1}{q_e} = \left(\frac{1}{q_{max} b}\right)\frac{1}{C_e} + \frac{1}{q_{max}} \;\leftarrow \text{(linear form)} \tag{6.3}$$

$$q_e = K_f C_e^{1/n} \;\Rightarrow\; \log q_e = \left(\frac{1}{n}\right)\log C_e + \log K_f \;\leftarrow \text{(linear form)} \tag{6.4}$$

where q_e (mg/g) is the quantity of solute adsorbed per weight unit of adsorbent at equilibrium, C_e (mg/L) is the concentration of solute remaining in the solution. q_{max} and b are Langmuir adsorption capacity and energy, while K_f and $1/n$ are Freundlich constant for adsorption capacity and intensity of sorption.

Linear form ($y = mx + c$) of Langmuir and Freundlich isotherm provide insight on the behavior of metal ions sorption on the adsorbate (see Figure 6.21(b-e)). The results depict that Langmuir and Freundlich isotherm models were well fitted for Al and Fe ions sorption in AIR-120H. However, Freundlich isotherm provides a better fit to experimental data for Al adsorption with correlation regression coefficient (R^2) value of 0.989, while Langmuir isotherm provides better fit for Fe ions with R^2 value of 0.932. Therefore, at the given concentrations, 3.9 g/L of aluminium and 0.35 g/L of iron in the leachate solution, adsorption of Al ions occurred in a heterogeneous surface of AIR-120H resin, while uptake of Fe ions proceeded by monolayer sorption on homogeneous surface of the adsorbate. The Langmuir and Freundlich constants and correlation coefficients are listed in Table 6.8.

Table 6.8: Langmuir and Freundlich isotherm parameters for Eq. 6.3 and 6.4.[IV]

Metals	Langmuir isotherm				Freundlich isotherm		
	b	q_{max}	R_L	R^2	n	K_f	R^2
Al	0.076	23.87	0.0033	0.891	4.89	5.765	0.989
Fe	0.039	1.45	0.0672	0.932	3.83	0.316	0.871

The separation factor (R_L) gives an estimate on affinity between the adsorbate and sorbent which can be derived from Langmuir isotherm parameters as; $R_L = 1/(1 + bC_0)$. The R_L value indicates the behaviour of Langmuir adsorption isotherm to be irreversible (R_L=0), favorable (0<R_L<1), linear (R_L=1) or unfavorable (R_L<1).[167] On the other hand, the model parameter n in Freundlich isotherm, at 1<n<10, suggests the beneficial sorption behavior[168] Therefore, styrene divinylbenzene based resin, Amberlite IR120 H^+, shows favorable and beneficial sorption behavior and was found suitable to remove metal ions in high concentrations form the phosphoric acid leachate solution.

Recirculation of reagents

The $H_3PO_{4(wt.)}$ content in fresh 0.5 M phosphoric acid and purified P-rich solution were 2.9 vol% and 3.5 vol%. This is an increment by a factor of 1.21 at LS ratio of 40

and demands 84 vol% of refined P-rich solution for recirculation. This efficacy can be improved by lowering LS ratio during P-extraction and using CER with higher sorption capacity. However, lower LS ratio also requires high CER dosage during Al and Fe removal. The P-extraction and metal removal efficacy from purified P-rich solution were akin to fresh 0.5 M phosphoric acid solution (see Table 6.9). Concentrations of trace elements were below the detection limit, thus are not presented in the table. Therefore, recirculation of refined leachate for leaching (see Figure 6.22) in combination with regeneration of CER in highly acidic medium (not presented in this study) provide a green-economical scheme to lower the consumption of pristine phosphoric acid solution and CER.

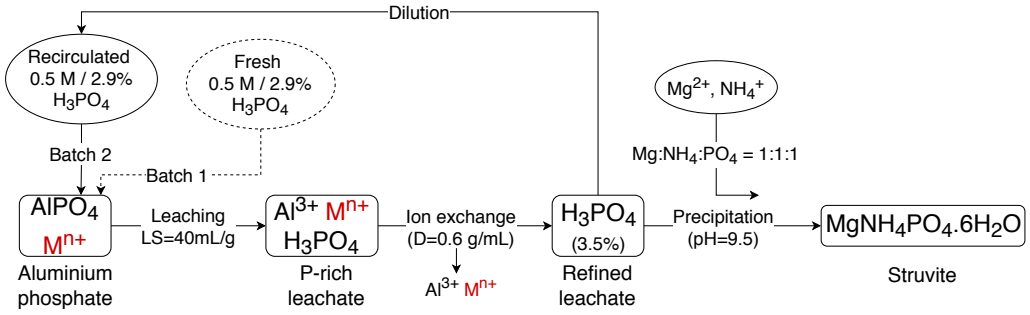

Figure 6.22: Process flow sheet for precipitation of struvite from P-rich solution obtained with fresh and recirculated 0.5 M phosphoric acid. M^{n+} represent metal impurities.

6.8.3 Struvite precipitation

The prospect of struvite recovery from precipitated P-products was investigated in two batch (see Figure 6.22); each differing only in the origin of leaching reagent. Two phosphorus-rich solutions (pristine and recirculated solution) obtained after adsorption of Al and Fe ions on CER (at 0.6 g/mL of dosage) were precipitated after addition of Mg^{2+} and NH_4^+ sources at pH 9.5 using Mg^{2+}:NH_4^+:PO_4^{3-}=1:1:1. In the absence of co-existing ions in the refined solutions, stoichiometric concentration of Mg, N and P ensures efficient and impurities free precipitates[161]. Use of higher CER dosage is also expected to remove some fraction of heavy metals. A summary depicting the concentration of major elements in each process is presented in Table 6.9. In both batch experiments, phosphorus recovery efficiency over 99% were observed. The net efficiency of the proposed conversion process in batch 1 and 2 is estimated to be 91.3 and 91.5% respectively, which is derived with Eq. 6.5:

$$\eta_{\text{net}} = \eta_{\text{D}} \times \eta_{\text{CER}} \times \eta_{\text{PPT}} \tag{6.5}$$

where η_{D}, η_{CER} and η_{PPT} represent dissolution, ion exchange and precipitation efficiencies, respectively.

The purified P-rich solution consisted of 3.5 vol% of H_3PO_4 and minor concentration of metal impurities (see Table 6.9). Therefore, further purification of leachate and concentration by evaporation also facilitates the recovery of phosphorus as high grade phosphoric acid.

Table 6.9: Summary of conversion of aluminium phosphate to struvite showing concentration of various elements at different stages with their respective efficiencies in batch 1 (use of pristine 0.5 M phosphoric acid) and batch 2 (use of refined 0.5 M phosphoric acid) experiments.[IV]

Element	P-product	Leaching LS = 40 mL/g		Ion exchange Dosage = 0.6 g/mL		Precipitation (pH = 9.5)	
		Batch 1	Batch 2	Batch 1	Batch 2	Batch 1	Batch 2
	(mg/kg)	(mg/L)	(mg/L)	(mg/L)	(mg/L)	(mg/L)	(mg/L)
P	180090	19970 (99.5)[a]	19950 (99.1)	18420 (92.3)	18540 (92.9)	105.7 (99.4)	115.2 (99.3)
Al	160300	3990 (99.6)	3965 (98.9)	9.0 (99.8)	10.1 (99.7)		
Fe	20010	493 (98.5)	485 (99.2)	14.5 (97.1)	15.2 (96.9)		
Ca	6300	155 (98.2)	158 (100.3)				
Mg	1180	29 (98.2)	29 (96.6)				

[a] Values in "( )" represent efficiency in % of each process, empty cells = not detected (<LOD)

6.8.4 Evaluation of struvite precipitates

Elemental analysis

Elemental composition of precipitates was estimated with ICP-OES analysis (see Table 6.10). The Mg/P ratio in the precipitates from batch 1 and 2 was found to be 0.773 and 0.777, which closely resembles the theoretical ratio of 0.785 in pure struvite. A slight elevation in the concentration of Fe, Al, Zn, Cr and Pb in batch 2 precipitate is also observed and may be due to their cumulation during recirculation of refined leachate for leaching purpose.

Table 6.10: Elemental composition of batch 1 and 2 precipitates.[IV]

Element	P	Mg	Fe	Al	Zn	Cr	Pb
Batch 1 (mg/kg)	125000	96600	100.4	85.8	35.1	12.3	7.0
Batch 2 (mg/kg)	125850	97820	105.1	70.0	39.3	13.2	8.1

X-ray Diffraction

Results from XRD analysis confirm the presence of struvite ($MgNH_4PO_4 \cdot 6\,H_2O$) as a dominant crystalline phase for all precipitates as shown in Figure 6.23. Phase analysis did not reveal unambiguous match to any candidates/impurities due to the low number and intensities of the unindexed peaks. Comparison of three struvite precipitates shows similar spectral pattern to that of standard spectrum of struvite (00-015-0462). Between batch 1 and 2 struvite, the intensities observed for the (110), (020), (011) and (211) reflections differ for each other. This is attributed to preferred orientation and the elongation of crystals in respective plane.[169]

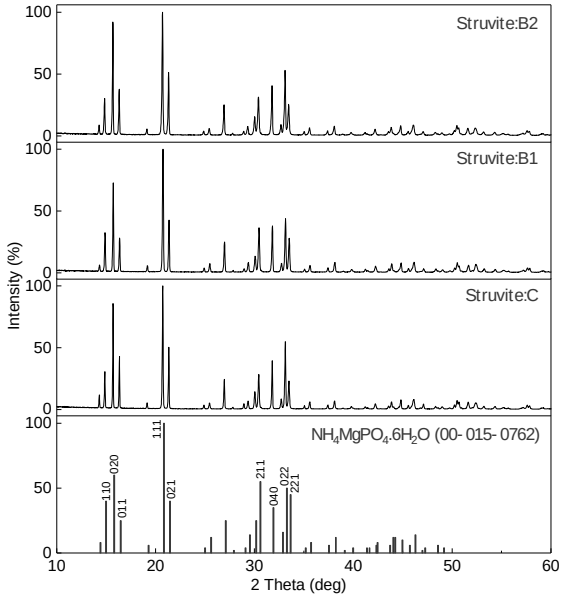

Figure 6.23: X-ray diffraction pattern showing the crystalline nature of the precipitates and standard struvite.[IV]

Infrared spectroscopy analysis

ATR IR analysis of struvite obtained from batch 1 and 2 were conducted to determine the effect of leachate recirculation on the speciation of IR-active functional groups. In addition, their spectra were also compared to struvite obtained from synthetic solution free from impurities (Figure 6.24). The spectral peaks from this study were assigned to specific functional group (Table 6.11) as reported from other study.[170] Similarities in the spectral position and their intensity suggest that precipitates obtained from both batch (1 and 2) are similar, thus recirculation of leachate do not affect the spectral properties of the struvite precipitates.

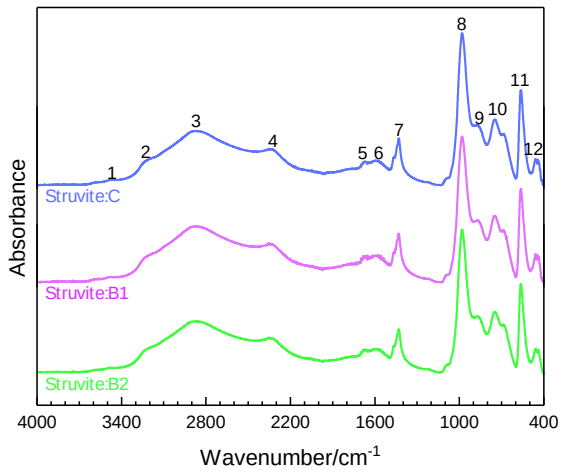

Figure 6.24: IR spectra of struvite precipitated from synthetic solution, batch 1 and 2. The numbered peaks correspond to assigned functional group (Table 6.11).[IV]

Table 6.11: Comparison of the observed and reported spectral peaks of struvite.[IV]

Peak number	Observed value (cm^{-1})	Reported value (cm^{-1})[170]	Bonds/vibrations
1	3475	3480	OH, NH stretching
2	3245	3256	OH, NH stretching
3	2870	2943	OH, NH stretching
4	2345	2353	OH, NH stretching
5	1675	1683	NH_4^+ v4 bending
6	1610	1615	NH_4^+ $v4$ bending
7	1432	1439	NH_4^+ $v2$ bending
8	980	1004	PO_4^{3-} $v3$ stretching
9	885	896	PO_4^{3-} $v4$ bending
10	755	761	PO_4^{3-} $v2$ bending
11	565	570	PO_4^{3-} $v2$ bending
12	460	459	Mg-O stretching

SEM analysis

Figure 6.25 displays photographic and SEM microscopic images of struvite particles obtained from controlled synthetic sample (Struvite:C), batch 1 (Struvite:B1) and batch 2 (Struvite:B2). The morphology of white precipitates depict orthorhombic structure that grow further into the form of tubular particles. In the absence of coexisting salts, the granulated particles form compact and hard aggregates.[161] The aggregates grow further to form fractal aggregates with elongated shapes and rougher surfaces.[171] The appearances and morphology of struvite precipitates obtained from batch 1 and 2 posses similar features. Therefore, recirculation of refined leachate do not impose any threat to morphology of the precipitates.

Figure 6.25: Photograph and SEM images of struvite obtained from controlled synthetic sample (Struvite:C), batch 1 (Struvite:B1) and batch 2 (Struvite:B2).[IV]

7. Summary and conclusion

This study attempts to explore the feasibility of phosphorus recovery from a low-grade secondary material, CFB-derived fly ash. Figure 7.1 illustrates the pertinent pretreatment and extraction methods employed in phosphorus refining and recovery. The process commences with the collection of fly ash (FA) from the combustion of forest residue and woody biomass in a circulatory fluidized-bed reactor. The FA constitutes 1.21 $wt\%_{(wt.)}$ of P, with Si and Ca at 17.3 and 15.4 wt% as the major impurities (see Table 6.2 on page 29). In addition, trace elements with toxic characteristics are also present and possess a threat to its usability. A correlation of smaller particle size with higher phosphorus content was established (see Figure 6.6 on page 31). Hence, sieving-based beneficiation was employed and the P content in the fly ash was raised to 1.67 wt%; this is an improvement by a factor of 1.38, while Si was reduced by a factor of 3.8.

An HCl matrix was found suitable for enhanced leaching and desilication treatment due to the catalyzing effect of H^+ and Cl^- ions towards Si polymerization and precipitation. Dissolution of FFA with 8 M HCl followed by aging of leachate for 5 h prompts the removal of silica with an efficiency of 99% via precipitation of the Si particulates and gel formation. A proportional relation between the precipitation

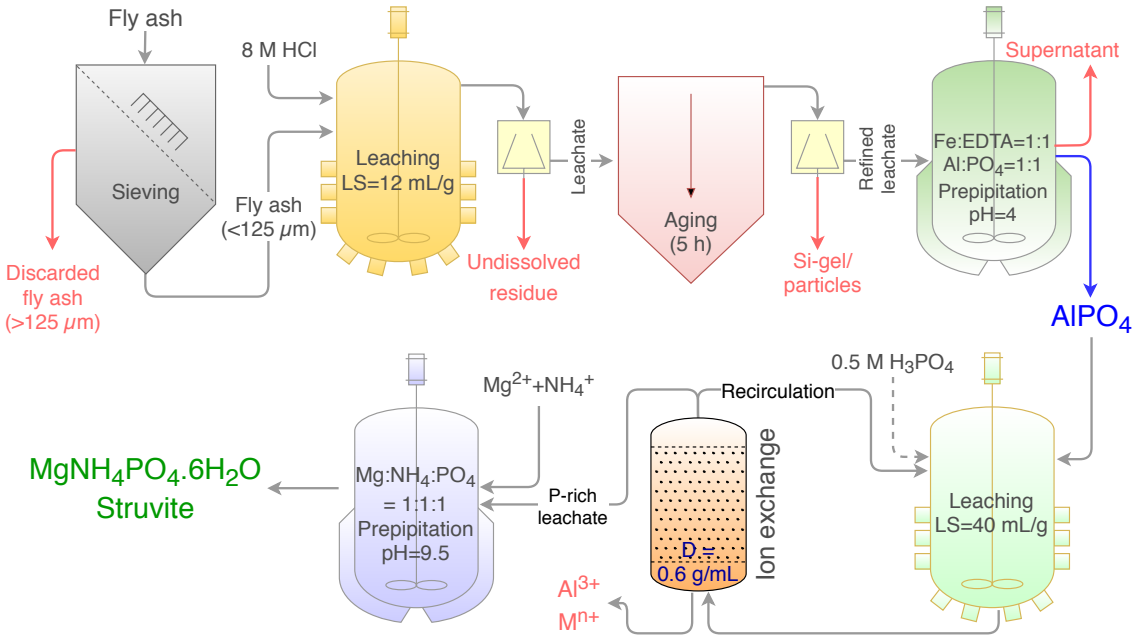

Figure 7.1: Schematic representation of phosphorus recovery method from fly ash developed in this study.

rate and temperature was also established (see Figure 6.11(a) on page 37). Thus, the objectives of identification and development of phosphorus refining were met in two different stages: (i) sieving-based beneficiation in the solid phase and (ii) desilication of the leachate solution.

The selective precipitation of phosphorus with aluminium was found feasible due to the stability and dominance of $AlPO_4$ in acidic regimes, as confirmed with chemical equilibrium calculations in the Medusa and Hydra software. The influence of Fe during phosphorus precipitation was restricted with EDTA at a stoichiometric concentration (see Figure 6.15 on page 41). $AlPO_4$ was recovered as a white amorphous solid that consisted of 16.3 wt% Al and 18.1 wt% P.

Low valued aluminium phosphate was converted into high value struvite fertilizer. 0.5 M phosphoric acid was adequate to dissolve $AlPO_4$ with an efficiency of 99%. Amberlite IR120H^+ resin at 0.6 g/mL dosage facilitated the removal of Al, Fe including trace elements from the P-rich leachate via ion exchange method. Recirculation of the P-rich solution free from metal ions for leaching purpose provides a greener route for struvite production by limiting use of fresh leaching reagents.

White-granulated and pure-crystalline struvites were obtained from pristine and recirculated leachates at Mg^{2+}:$NH_4{}^+$:$PO_4{}^{3-}$=1:1:1 and pH = 9.5. The recirculation of refined leachate for leaching purpose did not impose any threat to the morphology and spectral characteristics of the struvite precipitates. It should be noted that the fly ash is an extremely heterogeneous inorganic residue comprising of elements that potentially represent the entire periodic table with a low phosphorus concentration of 1.2 wt%. P content in the struvite precipitates obtained in this study was 12.5 wt%. The recovery treatment methods contribute a significant rise in P content by a factor of 10. Therefore, this study provides a sustainable way for the recovery of high-grade phosphorous as $AlPO_4$ and $MgNH_4PO_4 \cdot 6\,H_2O$ (struvite, a slow releasing fertilizer) from fly ash and ash residue alike and assists in the mitigation of challenges associated with phosphorus security and sustainability.

The extraction technologies developed in this study can be further improved, especially in the optimization of desilication treatments and removal of metal ions from leachate solution. Although the high molar concentration of acid assists silica polymerization and its removal, accumulation of the major and trace elements in the leachate may be seen as a disadvantage. On the other hand, it provides a prospect of recovery of the noble metals from such leachate solutions and adds value to the recovery process.

References

[1] F. H. Westheimer. "The Role of Phosphorus in Chemistry and Biochemistry". In: *Phosphorus Chemistry*. 1992. Chap. 1, pp. 1–17.

[2] F. Westheimer. "Why nature chose phosphates". In: *Science* 235.4793 (1987), pp. 1173–1178.

[3] K. Ruttenberg. "The Global Phosphorus Cycle". In: *Treatise on Geochemistry*. Ed. by H. D. Holland and K. K. Turekian. Oxford: Pergamon, 2003, pp. 585 –643.

[4] J. T. A. Verhoeven and M. B. Schmitz. "Control of plant growth by nitrogen and phosphorus in mesotrophic fens". In: *Biogeochemistry* 12.2 (1991), pp. 135–148.

[5] C. P. Vance, C. Uhde-Stone, and D. L. Allan. "Phosphorus acquisition and use: critical adaptations by plants for securing a nonrenewable resource". In: *New Phytologist* 157.3 (2003), pp. 423–447.

[6] G. M. Filippelli. "The Global Phosphorus Cycle: Past, Present, and Future". In: *Elements* 4.2 (2008), pp. 89–95.

[7] J. Köhler. "Detergent phosphates: an EU policy assessment". In: *Journal of business chemistry* 3.2 (2006), pp. 15–30.

[8] V. Smil. "PHOSPHORUS IN THE ENVIRONMENT: Natural Flows and Human Interferences". In: *Annual Review of Energy and the Environment* 25.1 (2000), pp. 53–88.

[9] D. Cordell, J.-O. Drangert, and S. White. "The story of phosphorus: Global food security and food for thought". In: *Global Environmental Change* 19.2 (2009). Traditional Peoples and Climate Change, pp. 292 –305.

[10] J. Lubczak and R. Lubczak. "Melamine Polyphosphate – the Reactive and Additive Flame Retardant for Polyurethane Foams". In: 63 (Mar. 2016), pp. 77–87.

[11] G. Filippelli and M. L. Delaney. "Similar phosphorus fluxes in ancient phosphorite deposits and a modern phosphogenic environment". In: 20 (Jan. 1992), pp. 709–712.

[12] I. Steen. "Phosphorus availability in the 21st Century: management of a non-renewable resource". In: *Phosphorus and Potassium* 217.Cl (1998), pp. 25–31.

[13] P. Cornel and C. Schaum. "Phosphorus recovery from wastewater: needs, technologies and costs". In: *Water Science & Technology* 59.6 (2009), p. 1069.

[14] B. E. Rittmann, B. Mayer, P. Westerhoff, and M. Edwards. "Capturing the lost phosphorus". In: *Chemosphere* 84.6 (2011). The Phosphorus Cycle, pp. 846 –853.

[15] Y. Liu, G. Villalba, R. U. Ayres, and H. Schroder. "Global Phosphorus Flows and Environmental Impacts from a Consumption Perspective". In: *Journal of Industrial Ecology* 12.2 (2008), pp. 229–247.

[16] K.F.Isherwood. *Mineral Fertilizer Use*. International Fertilizer Industry Association, 2000, p. 50.

[17] European Commission. *Renewable Energy Road Map. Renewable energies in the 21st century: building a more sustainable future*. COM(2006) 848 final. Available at: http://www.eu-oplysningen.dk/upload/application/pdf/52ee9584/20060846.pdf. 2007.

[18] *Finish Statistical yearbook of Forestry*. . Available from: http://www.metla.fi/metinfo/tilasto/julkaisut/vsk/2014/vsk14_wood_flows_in_Finland_2013.pdf. Accessed on: (10.09.2015). 2014, pp. 30–31.

[19] M. Salomón, T. Savola, A. Martin, C.-J. Fogelholm, and T. Fransson. "Small-scale biomass CHP plants in Sweden and Finland". In: *Renewable and Sustainable Energy Reviews* 15.9 (2011), pp. 4451 –4465.

[20] P. J. Mago and A. D. Smith. "Methodology to estimate the economic, emissions, and energy benefits from combined heat and power systems based on system component efficiencies". In: *International Journal of Energy Research* 38.11 (2014). ER-13-3889.R1, pp. 1457–1466.

[21] Suomen virallinen tilasto (Official Statistics of Finland). *Production of electricity and heat*. Available at: http://www.stat.fi/til/salatuo/2016/salatuo_2016_2017-11-02_en.pdf. Stastistic Finland, 2016.

[22] I. Obernberger, T. Brunner, and G. Bärnthaler. "Chemical properties of solid biofuels—significance and impact". In: *Biomass and Bioenergy* 30.11 (2006). Standarisation of Solid Biofuels in Europe, pp. 973 –982.

[23] S. Koppatz, C. Pfeifer, and H. Hofbauer. "Comparison of the performance behaviour of silica sand and olivine in a dual fluidised bed reactor system for steam gasification of biomass at pilot plant scale". In: *Chemical Engineering Journal* 175 (2011), pp. 468 –483.

[24] S. Emilsson. *International Handboook From Extraction of Forest Fuels to Ash Recycling*. Swedish Forest Agency, 2006, pp. 4–18.

[25] H. Nurmesniemi, M. Mäkelä, R. Pöykiö, K. Manskinen, and O. Dahl. "Comparison of the forest fertilizer properties of ash fractions from two power plants of pulp and paper mills incinerating biomass-based fuels". In: *Fuel Processing Technology* 104 (2012), pp. 1 –6.

[26] P. Thy, B. Jenkins, S. Grundvig, R. Shiraki, and C. Lesher. "High temperature elemental losses and mineralogical changes in common biomass ashes". In: *Fuel* 85.5 (2006), pp. 783 –795.

[27] P. Thy, C. Yu, B. M. Jenkins, and C. E. Lesher. "Inorganic Composition and Environmental Impact of Biomass Feedstock". In: *Energy & Fuels* 27.7 (2013), pp. 3969–3987.

[28] H. Nurmesniemi, K. Manskinen, R. Pöykiö, and O. Dahl. "Forest fertilizer properties of the bottom ash and fly ash from a large-sized (115 MW) industrial power plant incinerating wood-based biomass residues". In: *Journal of the University of Chemical Technology and Metallurgy* 47 (1 2012), pp. 43–52.

[29] J. Capablo, P. A. Jensen, K. H. Pedersen, K. Hjuler, L. Nikolaisen, R. Backman, and F. Frandsen. "Ash Properties of Alternative Biomass". In: *Energy & Fuels* 23.4 (2009), pp. 1965–1976.

[30] E. Levlin and K Stark. "Phosphorus recovery from sludge incineration ash and supercritical water oxidation residues with use of acids and bases". In: *Proceedings of a Polish-Swedish Seminar* 28 (Jan. 2004).

[31] K.-J. Hong, N. Tarutani, Y. Shinya, and T. Kajiuchi. “Study on the Recovery of Phosphorus from Waste-Activated Sludge Incinerator Ash”. In: *Journal of Environmental Science and Health, Part A* 40.3 (2005), pp. 617–631.

[32] B. K. Biswas, K. Inoue, H. Harada, K. Ohto, and H. Kawakita. “Leaching of phosphorus from incinerated sewage sludge ash by means of acid extraction followed by adsorption on orange waste gel”. In: *Journal of Environmental Sciences* 21.12 (2009), pp. 1753 –1760.

[33] S. Donatello, D. Tong, and C. Cheeseman. “Production of technical grade phosphoric acid from incinerator sewage sludge ash (ISSA)”. In: *Waste Management* 30.8 (2010), pp. 1634 –1642.

[34] C. Adam, B. Peplinski, M. Michaelis, G. Kley, and F.-G. Simon. “Thermochemical treatment of sewage sludge ashes for phosphorus recovery”. In: *Waste Management* 29.3 (2009), pp. 1122 –1128.

[35] G. Sturm, H. Weigand, C. Marb, W. Weiß, and B. Huwe. “Electrokinetic phosphorus recovery from packed beds of sewage sludge ash: yield and energy demand”. In: *Journal of Applied Electrochemistry* 40.6 (June 2010), pp. 1069–1078.

[36] J. Zimmermann and W. Dott. “Sequenced Bioleaching and Bioaccumulation of Phosphorus from Sludge Combustion – A New Way of Resource Reclaiming”. In: *Advanced Materials Research* 71-73 (2009), pp. 625–628.

[37] K Stendahl and S Jäfverström. “Recycling of sludge with the Aqua Reci process”. In: *Water science and technology* 49 (2004), pp. 233–240.

[38] E Levlin, M Löwén, and K Stark. “Phosphorus Recovery From Sludge Incineration Ash and Supercritical Water Oxidation Residues With Use of Acid and Base”. In: *Water Resources* (2007), pp. 19–28.

[39] Y. Kalmykova and K. K. Fedje. “Phosphorus recovery from municipal solid waste incineration fly ash”. In: *Waste Management* 33.6 (2013), pp. 1403 –1410.

[40] B. Gao, K. K. Fedje, and A.-M. Strömvall. “Phosphorus Recovery from Sorted Municipal Solid Waste Incineration Ash”. In: *The Journal of Solid Waste Technology and Management* 41.3 (2015).

[41] K. Kaikake, T. Sekito, and Y. Dote. “Phosphate recovery from phosphorus-rich solution obtained from chicken manure incineration ash”. In: *Waste Management* 29.3 (2009), pp. 1084 –1088.

[42] K. Kuligowski and T. G. Poulsen. “Phosphorus and zinc dissolution from thermally gasified piggery waste ash using sulphuric acid”. In: *Bioresource Technology* 101.14 (2010), pp. 5123 –5130.

[43] A. Korpilahti, M. Moilanen, and L. Finér. “Wood ash recycling and environmental impacts - state-of-the-art in Finland”. In: *Developing Systems for Integrating Bioenergy into Environmentally Sustainable Forestry* 211 (1999). Proceedings of the International Energy Agency Bioenergy Agreement Task 18 workshop incorporating a joint workshop session with Task 25, 7-11 September, 1998, Nokia, Finland / Ed. Lowe, A.T. & Smith, C.T.,New Zealand, pp. 82–89.

[44] R. Lauhanen, M. Moilanen, K. Silfverberg, H. Takamaa, and J. Issakainen. “The profitability of wood ash-fertilizing of drained peatland Scots pine stands [Puutuhkalannoituksen kannattavuus eräissä ojitusaluemänniköissä]”. In: *Suo* 48.3 (1997), pp. 71–82.

[45] K Väätäinen, T Tahvanainen, E Sirparanta, and S Lamminen. *Energy wood from early thinnings, 5EURES (EIE/04/086/S07.38582).* Tech. rep. Finnish Forest Research Institute, 2007, p. 30.

[46] N. Huotari, E. Tillman-Sutela, J. Pasanen, and E. Kubin. "Ash-fertilization improves germination and early establishment of birch (*Betula pubescens* Ehrh.) seed-lings on a cut-away peatland". In: *Forest Ecology and Management* 255.7 (2008), pp. 2870 –2875.

[47] E. Karltun, A. Saarsalmi, M. Ingerslev, M. Mandre, S. Andersson, T. Gaitnieks, R. Ozolinčius, and I. Varnagiryte-Kabasinskiene. "Wood Ash Recycling – Possibilities And Risks". In: *Sustainable Use of Forest Biomass for Energy: A Synthesis with Focus on the Baltic and Nordic Region.* Ed. by D. Röser, A. Asikainen, K. Raulund-Rasmussen, and I. Stupak. Dordrecht: Springer Netherlands, 2008, pp. 79–108.

[48] C. E. Housecroft and A. G. Sharpe. *Inorganic chemistry.* 4th ed. Pearson Education, 2012, pp. 490–515.

[49] B. D. Ellis and C. L. B. Macdonald. "Phosphorus (I) Iodide: A Versatile Metathesis Reagent for the Synthesis of Low Oxidation State Phosphorus Compounds". In: *Inorganic Chemistry* 45.17 (2006). PMID: 16903744, pp. 6864–6874.

[50] R. Gilmour. *Phosphoric Acid: Purification, Uses, Technology, and Economics.* Taylor & Francis, 2013.

[51] G. Emich. "Phosphate rock". In: *Ind. Miner. Rocks* 2 (1984), pp. 1017–1047.

[52] A. Abouzeid, I. El-Jallad, and M. Orphy. "Calcareous phosphate and their calcined products". In: *Minerals Science and Engineering* 12.2 (1980), pp. 73–83.

[53] P. v. Straten. *Rocks for crops, Agrominerals of sub-Saharan Africa.* ICRAF, 2004, p. 10.

[54] S. K. Kawatra. *Beneficiation of Phosphate Ore.* Vol. First edition. SME, 2014, pp. 9–11.

[55] A. A. C. Pereira and R. A.-s. M. Papini. "Processes for phosphorus removal from iron ore - a review". en. In: *Rem: Revista Escola de Minas* 68 (Sept. 2015), pp. 331 –335.

[56] R. Klee and T. Graedel. "Elemental cycles: A Status Report on Human or Natural Dominance". In: *Annual Review of Environment and Resources* 29.1 (2004), pp. 69–107.

[57] J. Schroder, D. Cordell, A. Smit, and A. Rosemarin. *Sustainable use of phosphorus.* EU tender ENV.B1/ETU/2009/0025, Report 357. 2010.

[58] S. Khoshjavan and B. Rezai. "Beneficiation of refractory rock phosphate by calcination and flotation." In: *Minerals & Metallurgical Processing* 28.4 (2011), pp. 187 –192.

[59] A.-Z. M. Abouzeid. "Physical and thermal treatment of phosphate ores — An overview". In: *International Journal of Mineral Processing* 85.4 (2008), pp. 59 –84.

[60] A. Silvia and P. Andery. "Mining and beneficiation of apatite rock at the Jacupiranga mine, Brazil". In: *Phosphorus Potassium* 57 (1972), pp. 37–40.

[61] H. Sis and S. Chander. "Reagents used in the flotation of phosphate ores: a critical review". In: *Minerals Engineering* 16.7 (2003), pp. 577 –585.

[62] A. Teague and M. Lollback. "The beneficiation of ultrafine phosphate". In: *Minerals Engineering* 27-28 (2012), pp. 52 –59.

[63] P. Zhang, Y. Yu, and M. Bogan. “Challenging the “Crago” double float process II. Amine-fatty acid flotation of siliceous phosphates”. In: *Minerals Engineering* 10.9 (1997), pp. 983 –994.

[64] M. Gharabaghi, M. Noaparast, and M. Irannajad. “Selective leaching kinetics of low-grade calcareous phosphate ore in acetic acid”. In: *Hydrometallurgy* 95.3 (2009), pp. 341 –345.

[65] M. Muhammed and Y. Zhang. “A hydrometallurgical process for the dephosphorization of iron ore”. In: *Hydrometallurgy* 21.3 (1989), pp. 277 –292.

[66] Y.-s. Jin, T. Jiang, Y.-b. Yang, Q. Li, G.-h. Li, and Y.-f. Guo. “Removal of phosphorus from iron ores by chemical leaching”. In: *Journal of Central South University of Technology* 13.6 (Dec. 2006), pp. 673–677.

[67] W. Sadeddin and S. Abu-Eishah. “Minimization of free calcium carbonate in hard and medium-hard phosphate rocks using dilute acetic acid solution”. In: *International Journal of Mineral Processing* 30.1-2 (1990), pp. 113–125.

[68] H. Sengul, A. Ozer, and M. Gulaboglu. “Beneficiation of Mardin-Mazidagi (Turkey) calcareous phosphate rock using dilute acetic acid solutions”. In: *Chemical Engineering Journal* 122.3 (2006), pp. 135–140.

[69] M. Gharabaghi, M. Noaparast, and S. Shafaei Tonkaboni. “Lar Mountain phosphate ore processing using flotation approach”. In: *Iranian Journal of Science and Technology, Transaction B: Engineering* 31.4 (2007), pp. 447–450.

[70] M. Ashraf, Z. I. Zafar, and T. M. Ansari. “Selective leaching kinetics and upgrading of low-grade calcareous phosphate rock in succinic acid”. In: *Hydrometallurgy* 80.4 (2005), pp. 286 –292.

[71] L. Fang, J. shan Li, M. Z. Guo, C. Cheeseman, D. C. Tsang, S. Donatello, and C. S. Poon. “Phosphorus recovery and leaching of trace elements from incinerated sewage sludge ash (ISSA)”. In: *Chemosphere* 193 (2018), pp. 278 –287.

[72] G. J A, F Blázquez, M L García, P. Delvasto, A. Ballester, J. Muñoz, F. González, M. L. Blázquez, and C. García-Balboa. “Exploring the possibilities of biological beneficiation of iron- ores: The phosphorus problem”. In: (2005). Proceedings of the 15th Steelmaking Conference, 5th Ironmaking Conference & 1st Environment and Recycling Symposium IAS (CD- ROM). Argentinean Steelmaking Institute (IAS). San Nicolás, Buenos Aires, Argentina, November 7–10, 2005, pp 71–82.

[73] P. Delvasto, A. Ballester, J. Muñoz, F. González, M. L. Blázquez, J. Igual, A. Valverde, and C. García-Balboa. “Mobilization of phosphorus from iron ore by the bacterium Burkholderia caribensis FeGL03”. In: *Minerals Engineering* 22 (1 2008), pp. 1–9.

[74] N. Pradhan, B Das, S Acharya, R. Kar, L. Sukla, and V. Misra. “Removal of phosphorus from LD slag using Heterotrophic bacteria”. In: *Minerals and Metallurgical Processing* 21 (2004), pp. 149–152.

[75] N. Marhual, N. Pradhan, N. Mohanta, L. Sukla, and B. Mishra. “Dephosphorization of LD slag by phosphorus solubilising bacteria”. In: *International Biodeterioration & Biodegradation* 65 (2011), pp. 404–409.

[76] W. Stumm and J. Morgan. *Aquatic chemistry: chemical equilibria and rates in natural waters*. Environmental science and technology. Wiley, 1996, pp. 404–409.

[77] E. Diamadopoulos, K. Megalou, M. Georgiou, and N. Gizgis. “Coagulation and Precipitation as Post-Treatment of Anaerobically Treated Primary Municipal Wastewater”. In: *Water Environment Research* 79.2 (2007), pp. 131–139.

[78] T. Clark, T. Stephenson, and P. Pearce. “Phosphorus removal by chemical precipitation in a biological aerated filter”. In: *Water Research* 31.10 (1997), pp. 2557 –2563.

[79] X. Wang, S. Xia, L. Chen, J. Zhao, N. Renault, and J. Chovelon. “Nutrients removal from municipal wastewater by chemical precipitation in a moving bed biofilm reactor”. In: *Process Biochemistry* 41.4 (2006), pp. 824 –828.

[80] Y. Yu, R. Wu, and M. Clark. “Phosphate removal by hydrothermally modified fumed silica and pulverized oyster shell”. In: *Journal of Colloid and Interface Science* 350.2 (2010), pp. 538 –543.

[81] J. Chen, Y. Cai, M. Clark, and Y. Yu. “Equilibrium and Kinetic Studies of Phosphate Removal from Solution onto a Hydrothermally Modified Oyster Shell Material”. In: *PLOS ONE* 8.4 (Apr. 2013), pp. 1–10.

[82] S. Lee, S. Weon, C. Lee, and B Koopman. “Removal of nitrogen and phosphate from wastewater by addition of bittern”. In: *Chemosphere* 51.4 (2003), pp. 265 –271.

[83] R. D. Schuiling and A. Andrade. “Recovery of Struvite from Calf Manure”. In: *Environmental Technology* 20.7 (1999), pp. 765–768.

[84] M. W. Zdybiewska and B. Kula. “Removal of Ammonia Nitrogen by the Precipitation Method, on the Example of Some Selected Waste Waters”. In: *Water Science and Technology* 24.7 (1991), pp. 229–234.

[85] O. Tünay, I. Kabdasli, D. Orhon, and S. Kolçak. “Ammonia removal by magnesium ammonium phosphate precipitation in industrial wastewaters”. In: *Water Science and Technology* 36.2-3 (1997), pp. 225–228.

[86] H. Chen, Z. Sun, X. Song, and J. Yu. “Efficient Extraction of Phosphoric Acid with a Trialkyl Amine-Based Solvent Mixture”. In: *Journal of Chemical & Engineering Data* 61.1 (2016), pp. 438–443.

[87] F. Ruiz, A. Marcilla, A. M. Ancheta, and J. A. Caro. “Purification of wet process phosphoric acid by solvent extraction with isoamyl alcohol. Part I. Liquid–liquid equilibrium of the water–phosphoric acid–isoamyl alcohol at 25^{o}C.” In: *Solvent Extraction and Ion Exchange* 3.3 (1985), pp. 331–343.

[88] A. Marcilla, F. Ruiz, J. Campus, and M. Asensio. “Purification of wet process phosphoric acid by solvent extraction with dibutyl ether. Part I. Liquid–liquid equilibrium of the system water–phosphoric acid–dibutyl ether at 25^{o}C.” In: *Solvent Extraction and Ion Exchange* 7.2 (1989), pp. 201–210.

[89] M. Feki, M. Fourati, M. M. Chaabouni, and H. F. Ayedi. “Purification of wet process phosphoric acid by solvent extraction liquid-liquid equilibrium at 25 and 40^{o}C of the system water - phosphoric acid - methylisobutylketone”. In: *The Canadian Journal of Chemical Engineering* 72.5 (1994), pp. 939–944.

[90] A. Hannachi, D. Habaili, C. Chtara, and A. Ratel. “Purification of wet process phosphoric acid by solvent extraction with TBP and MIBK mixtures”. In: *Separation and Purification Technology* 55.2 (2007), pp. 212 –216.

[91] Y. Zhang and M. Muhammed. “Extraction of phosphoric acid from nitrate solutions with isoamyl alcohol”. In: *Solvent Extraction and Ion Exchange* 6.6 (1988), pp. 973–992.

[92] A. G. Gilani, H. G. Gilani, and S. Ahmadifar. “Experimental and correlational study of phase equilibria in aqueous mixtures of phosphoric acid with aromatic hydrocarbons at various temperatures”. In: *The Journal of Chemical Thermodynamics* 91 (2015), pp. 121 –126.

[93] E. Levlin. “Recovery of Phosphate From Sewage Sludge and Separation of Metals By Ion Exchange”. In: (2001). Proceedings of a Polish-Swedish seminar. Wastewater, Sludge and Solid Waste Management Nowy Targ - Zakopane, Poland, October 24-26, 2001, Water Resources Engineering, KTH, TRITA-AMI REPORT 3088, pp. 81–90.

[94] L. Liberti, G. Boari, N. Limoni, C. Longobardi, and R. Passino. “The Rim-Nut Process for Recovery of N/P Fertilizer from Sewage. Start-Up of Bari’s Plant”. In: *Fundamentals and Applications of Ion Exchange*. Ed. by L. Liberti and J. R. Millar. Dordrecht: Springer Netherlands, 1985, pp. 134–143.

[95] Z. Tan and A. Lagerkvist. “Phosphorus recovery from the biomass ash: A review”. In: *Renewable and Sustainable Energy Reviews* 15.8 (2011), pp. 3588 –3602.

[96] J. Wan, X. Jiang, T. C. Zhang, J. Hu, D. Richter-Egger, X. Feng, A. Zhou, and T. Tao. “The activated iron system for phosphorus recovery in aqueous environments”. In: *Chemosphere* 196 (2018), pp. 153 –160.

[97] K. Haddad, S. Jellali, M. Jeguirim, A. B. H. Trabelsi, and L. Limousy. “Investigations on phosphorus recovery from aqueous solutions by biochars derived from magnesium-pretreated cypress sawdust”. In: *Journal of Environmental Management* (2017).

[98] T. Zhang, H. Xu, H. Li, X. He, Y. Shi, and A. Kruse. “Microwave digestion-assisted HFO/biochar adsorption to recover phosphorus from swine manure”. In: *Science of The Total Environment* (2017).

[99] C. Wan, S. Ding, C. Zhang, X. Tan, W. Zou, X. Liu, and X. Yang. “Simultaneous recovery of nitrogen and phosphorus from sludge fermentation liquid by zeolite adsorption: Mechanism and application”. In: *Separation and Purification Technology* 180 (2017), pp. 1 –12.

[100] O. Coskuner and E. A. A. Jarvis. “Coordination Studies of Al-EDTA in Aqueous Solution”. In: *The Journal of Physical Chemistry A* 112.12 (2008). PMID: 18293948, pp. 2628–2633.

[101] T. Zhang, K. E Bowers, J. H Harrison, and C. Shulin. “Releasing Phosphorus from Calcium for Struvite Fertilizer Production from Anaerobically Digested Dairy Effluent”. In: *Water environment research* 82 (Jan. 2010), pp. 34–42.

[102] I. S. S. Pinto, S. M. Sadeghi, and H. M. V. M. Soares. “Separation and recovery of nickel, as a salt, from an EDTA leachate of spent hydrodesulphurization catalyst using precipitation methods”. In: *Chemical Engineering Science* 122 (2015), pp. 130–137.

[103] P. Jadhao, G. Chauhan, K. Pant, and K. Nigam. “Greener approach for the extraction of copper metal from electronic waste”. In: *Waste Management* 57 (2016). WEEE: Booming for Sustainable Recycling, pp. 102 –112.

[104] L. Longquan, W. Cheng, and L. Yadong. “Separation of cobalt and nickel by emulsion liquid membrane with the use of EDTA as masking reagent”. In: *Journal of Membrane Science* 135.2 (1997), pp. 173 –177.

[105] S. J. Zarrouk, B. C. Woodhurst, and C. Morris. “Silica scaling in geothermal heat exchangers and its impact on pressure drop and performance: Wairakei binary plant, New Zealand”. In: *Geothermics* 51 (2014), pp. 445 –459.

[106] S. Bai, G. Naren, M. Nakano, Y. Okaue, and T. Yokoyama. “Effect of polysilicic acid on the precipitation of calcium carbonate”. In: *Colloids and Surfaces A: Physicochemical and Engineering Aspects* 445.Supplement C (2014), pp. 54 –58.

[107] L. G. Dyer, W. R. Richmond, and P. D. Fawell. “Simulation of iron oxide/silica precipitation in the paragoethite process for the removal of iron from acidic zinc leach solutions”. In: *Hydrometallurgy* 119.Supplement C (2012), pp. 47 –54.

[108] D. Hermosilla, R. Ordóñez, L. Blanco, E. de la Fuente, and . Blanco. “pH and Particle Structure Effects on Silica Removal by Coagulation”. In: *Chemical Engineering & Technology* 35.9 (2012), pp. 1632–1640.

[109] Y. Liu, M. Tourbin, S. Lachaize, and P. Guiraud. “Silica Nanoparticle Separation from Water by Aggregation with AlCl3”. In: *Industrial & Engineering Chemistry Research* 51.4 (2012), pp. 1853–1863.

[110] D. L. Gallup, F. Sugiaman, V. Capuno, and A. Manceau. “Laboratory investigation of silica removal from geothermal brines to control silica scaling and produce usable silicates”. In: *Applied Geochemistry* 18.10 (2003), pp. 1597 –1612.

[111] K. Sasan, P. V. Brady, J. L. Krumhansl, and T. M. Nenoff. “Exceptional selectivity for dissolved silicas in industrial waters using mixed oxides”. In: *Journal of Water Process Engineering* 20 (2017), pp. 187 –192.

[112] K. Sasan, P. V. Brady, J. L. Krumhansl, and T. M. Nenoff. “Removal of dissolved silica from industrial waters using inorganic ion exchangers”. In: *Journal of Water Process Engineering* 17 (2017), pp. 117 –123.

[113] N. A. Milne, T. O’Reilly, P. Sanciolo, E. Ostarcevic, M. Beighton, K. Taylor, M. Mullett, A. J. Tarquin, and S. R. Gray. “Chemistry of silica scale mitigation for RO desalination with particular reference to remote operations”. In: *Water Research* 65 (2014), pp. 107 –133.

[114] S. Chuang, T. Chang, C. Ouyang, and J. Leu. “Colloidal silica removal in coagulation processes for wastewater reuse in a high-tech industrial park”. In: *Water Science and Technology* 55.1-2 (2007), pp. 187–195.

[115] S. S. Cob, C. Yeme, B. Hofs, E. Cornelissen, D. Vries, F. G. Güner, and G. Witkamp. “Towards zero liquid discharge in the presence of silica: Stable 98% recovery in nanofiltration and reverse osmosis”. In: *Separation and Purification Technology* 140 (2015), pp. 23 –31.

[116] S. Wilhelm and M. Kind. “Influence of pH, temperature and sample size on natural and enforced syneresis of precipitated silica”. In: *Polymers* 7.12 (2015), pp. 2504–2521.

[117] M. A. Bezerra, R. E. Santelli, E. P. Oliveira, L. S. Villar, and L. A. Escaleira. “Response surface methodology (RSM) as a tool for optimization in analytical chemistry”. In: *Talanta* 76.5 (2008), pp. 965 –977.

[118] B. Dejaegher and Y. V. Heyden. “Experimental designs and their recent advances in set-up, data interpretation, and analytical applications”. In: *Journal of Pharmaceutical and Biomedical Analysis* 56.2 (2011), pp. 141 –158.

[119] J. Fox. “The R Commander: A Basic Statistics Graphical User Interface to R”. In: *Journal of Statistical Software* 14.9 (2005), pp. 1–42.

[120] U. Groemping. *RcmdrPlugin.DoE: R Commander Plugin for (industrial) Design of Experiments*. R package version 0.12-3. 2014.

[121] R Core Team. *R: A Language and Environment for Statistical Computing*. R Foundation for Statistical Computing. Vienna, Austria, 2017.

[122] D. R. Cox and N. Reid. *The theory of the design of experiments*. Chapman & Hall/CRC, 2000.

[123] E. Poussel, J. Mermet, and O. Samuel. "Simple experiments for the control, the evaluation and the diagnosis of inductively coupled plasma sequential systems". In: *Spectrochimica Acta Part B: Atomic Spectroscopy* 48.6 (1993), pp. 743 –755.

[124] I. Novotny, J. Farinas, W. Jia-liang, E. Poussel, and J.-M. Mermet. "Effect of power and carrier gas flow rate on the tolerance to water loading in inductively coupled plasma atomic emission spectrometry". In: *Spectrochimica Acta Part B: Atomic Spectroscopy* 51.12 (1996), pp. 1517 –1526.

[125] J. Mermet. "Use of magnesium as a test element for inductively coupled plasma atomic emission spectrometry diagnostics". In: *Analytica Chimica Acta* 250 (1991), pp. 85 –94.

[126] A. Ilander and A. Väisänen. "An ultrasound-assisted digestion method for the determination of toxic element concentrations in ash samples by inductively coupled plasma optical emission spectrometry". In: *Analytica Chimica Acta* 602.2 (2007), pp. 195 –201.

[127] I. Puigdomenech. "MEDUSA and HYDRA: Software for Chemical Equilibrium Calculations". In: *Dept. of Inorganic Chemistry, Royal Institute of Technology (KTH), Stockholm, Sweden.* (2015).

[128] G. Itskos, S. Itskos, and N. Koukouzas. "Size fraction characterization of highly-calcareous fly ash". In: *Fuel Processing Technology* 91.11 (2010), pp. 1558 –1563.

[129] C. Lanzerstorfer. "Cyclone fly ash from a grate-fired biomass combustion plant: Dependence of the concentration of various components on the particle size". In: *Fuel Processing Technology* 131 (2015), pp. 382 –388.

[130] O. Dahl, H. Nurmesniemi, R. Pöykiö, and G. Watkins. "Heavy metal concentrations in bottom ash and fly ash fractions from a large-sized (246 MW) fluidized bed boiler with respect to their Finnish forest fertilizer limit values". In: *Fuel Processing Technology* 91.11 (2010), pp. 1634 –1639.

[131] C. Lanzerstorfer. "Model based prediction of required cut size diameter for fractionation of fly ash from a grate-fired wood chip incineration plant". In: *Fuel Processing Technology* 92.5 (2011), pp. 1095 –1100.

[132] K. Väätäinen, L. Sikanen, and A. Asikainen. *Rakeistetun puutuhkan metsäänpalautuksen logistiikka (Logistics of recycling granulated wood ash back to forest)*. Tech. rep. Research Notes 116 (In Finnish). Joensuu: University of Joensuu, Faculty of Forest, 2000.

[133] P. Vesterinen. *Wood Ash Recycling State of the Art in Finland and Sweden*. Tech. rep. VTT Processes, 2003, pp. 52–53.

[134] J. Bałdyga, M. Jasińska, K. Jodko, and P. Petelski. "Precipitation of amorphous colloidal silica from aqueous solutions—Aggregation problem". In: *Chemical Engineering Science* 77.Supplement C (2012). 18th International Symposium on Industrial Crystallization, pp. 207 –216.

[135] E. A. Gorrepati, P. Wongthahan, S. Raha, and H. S. Fogler. "Silica precipitation in acidic solutions: Mechanism, pH effect, and salt effect". In: *Langmuir* 26.13 (2010), pp. 10467–10474.

[136] V. Lenher and H. B. Merrill. "The solubility of silica". In: *Journal of the American Chemical Society* 39.12 (1917), pp. 2630–2638.

[137] T. H. ELMER and M. E. NORDBERG. "Solubility of Silica in Nitric Acid Solutions". In: *Journal of the American Ceramic Society* 41.12 (1958), pp. 517–520.

[138] R. K. Iler. "Isolation and characterization of particle nuclei during the polymerization of silicic acid to colloidal silica". In: *Journal of Colloid And Interface Science* 75.1 (1980), pp. 138–148.

[139] O. Weres, A. Yee, and L. Tsao. "Kinetics of silica polymerization". In: *Journal of Colloid And Interface Science* 84.2 (1981), pp. 379–402.

[140] H. Rothbaum and A. Rohde. "Kinetics of silica polymerization and deposition from dilute solutions between 5 and 180^{o}C". In: *Journal of Colloid and Interface Science* 71.3 (1979), pp. 533 –559.

[141] A. C. Makrides, M. Turner, and J. Slaughter. "Condensation of silica from supersaturated silicic acid solutions". In: *Journal of Colloid and Interface Science* 73.2 (1980), pp. 345 –367.

[142] K. Quarch and M. Kind. "Inorganic Precipitated Silica Gel. Part 1: Gelation Kinetics and Gel Properties". In: *Chemical Engineering & Technology* 33.6 (2010), pp. 1034–1039.

[143] A. D. Bishop and J. L. Bear. "The thermodynamics and kinetics of the polymerization of silicic acid in dilute aqueous solution". In: *Thermochimica Acta* 3.5 (1972), pp. 399 –409.

[144] C. Brinker. "Hydrolysis and condensation of silicates: Effects on structure". In: *Journal of Non-Crystalline Solids* 100.1 (1988). Glasses and Glass Ceramics from Gels, pp. 31 –50.

[145] C. B. Hurd and R. W. Barclay. "Studies on Silicic Acid Gels. X. The Time of Set of Gel Mixtures Containing High Concentrations of Mineral Acids". In: *The Journal of Physical Chemistry* 44.7 (1940), pp. 847–851.

[146] J. Beck and S. Unterberger. "The behaviour of phosphorus in the flue gas during the combustion of high-phosphate fuels". In: *Fuel* 85.10 (2006), pp. 1541 –1549.

[147] A. Pettersson, M. Zevenhoven, B.-M. Steenari, and L.-E. Åmand. "Application of chemical fractionation methods for characterisation of biofuels, waste derived fuels and CFB co-combustion fly ashes". In: *Fuel* 87.15 (2008), pp. 3183 –3193.

[148] M. Lee and D.-J. Kim. "Identification of phosphorus forms in sewage sludge ash during acid pre-treatment for phosphorus recovery by chemical fractionation and spectroscopy". In: *Journal of Industrial and Engineering Chemistry* 51.Supplement C (2017), pp. 64 –70.

[149] H. Xiong, Y. Liao, and L. Zhou. "Influence of Chloride and Sulfate on Formation of Akaganéite and Schwertmannite through Ferrous Biooxidation by Acidithiobacillus Ferrooxidans Cells". In: *Environmental Science & Technology* 42.23 (2008). PMID: 19192781, pp. 8681–8686.

[150] E. Asenath-Smith and L. A. Estroff. “Role of Akaganeite ($\beta-FeOOH$) in the Growth of Hematite ($\alpha-Fe_2O_3$) in an Inorganic Silica Hydrogel”. In: *Crystal Growth & Design* 15.7 (2015), pp. 3388–3398.

[151] P. Persson, N. Nilsson, and S. Sjöberg. “Structure and Bonding of Orthophosphate Ions at the Iron Oxide–Aqueous Interface”. In: *Journal of Colloid and Interface Science* 177.1 (1996), pp. 263 –275.

[152] L. S. Burrell, C. T. Johnston, D. Schulze, J. Klein, J. L. White, and S. L. Hem. “Aluminium phosphate adjuvants prepared by precipitation at constant pH. Part I: composition and structure”. In: *Vaccine* 19.2 (2000), pp. 275 –281.

[153] X. H. Zhao, Y. Q. Zhao, and P. Kearney. “Phosphorus recovery as AlPO 4 from beneficially reused aluminium sludge arising from water treatment”. In: *Environmental Technology* 34.2 (2013). PMID: 23530339, pp. 263–268.

[154] T. Roncal-Herrero, J. D. Rodríguez-Blanco, L. G. Benning, and E. H. Oelkers. “Precipitation of Iron and Aluminum Phosphates Directly from Aqueous Solution as a Function of Temperature from 50 to 200 ^{o}C”. In: *Crystal Growth & Design* 9.12 (2009), pp. 5197–5205.

[155] M. Takahashi, S. Kato, H. Shima, E. Sarai, T. Ichioka, S. Hatyakawa, and H. Miyajiri. “Technology for recovering phosphorus from incinerated wastewater treatment sludge”. In: *Chemosphere* 44.1 (2001). ICUPCT, pp. 23 –29.

[156] H. Huang, J. Liu, and Y. Jiang. “Crystallization and precipitation of phosphate from swine wastewater by magnesium metal corrosion”. In: *Scientific Reports* (), pp. 1–13.

[157] M. T. Munir, B. Li, I. Boiarkina, S. Baroutian, W. Yu, and B. R. Young. “Phosphate recovery from hydrothermally treated sewage sludge using struvite precipitation”. In: *Bioresource Technology* (), pp. 171–179.

[158] G. Jia, H. Zhang, J. Krampe, T. Muster, B. Gao, N. Zhu, and B. Jin. “Applying a chemical equilibrium model for optimizing struvite precipitation for ammonium recovery from anaerobic digester effluent”. In: *Journal of Cleaner Production* (), pp. 297–305.

[159] M. S. Rahaman, N. Ellis, and D. S. Mavinic. “Effects of various process parameters on struvite precipitation kinetics and subsequent determination of rate constants”. In: 57.5 (2008), pp. 647–654.

[160] N. Y. Acelas, E. Flórez, and D. López. “Phosphorus recovery through struvite precipitation from wastewater: effect of the competitive ions”. In: *Desalination and Water Treatment* 9 (), pp. 2468–2479.

[161] Y. J. Shih, R. R. M. Abarca, M. D. G. de Luna, Y. H. Huang, and M. C. Lu. “Recovery of phosphorus from synthetic wastewaters by struvite crystallization in a fluidized-bed reactor: Effects of pH, phosphate concentration and coexisting ions”. In: *Chemosphere* (), pp. 466–473.

[162] C. Tang, Y. Qiu, Y. Wang, X. Wang, Z. Zhang, and L. Yang. “Kinetic studies on Al³⁺removal from phosphoric acid by cation exchange resin”. In: *Canadian Journal of Chemical Engineering* 9999 (2017), pp. 1–11.

[163] M. E. Goher, A. M. Hassan, I. A. Abdel-moniem, A. H. Fahmy, M. H. Abdo, and S. M. El-sayed. “Removal of aluminum , iron and manganese ions from industrial wastes using granular activated carbon and Amberlite IR-120H”. In: *The Egyptian Journal of Aquatic Research* 2 (), pp. 155–164.

[164] P. Meshram, S. K. Sahu, B. D. Pandey, V. Kumar, and T. R. Mankhand. "Removal of Chromium(III) from the Waste Solution of an Indian Tannery by Amberlite IR 120 Resin". In: *International Journal of Nonferrous Metallurgy* October (), pp. 32–41.

[165] P. Dr. Waleed Mohammad Salih, H. Gzar, and N. Falah Hassan. "Sorption of Lead, Zinc and Copper from Simulated Wastewater by Amberlite IR-120 Resin". In: *Journal of Engineering* 18 (Sept. 2012), pp. 1042–1054.

[166] P. E. Franco, M. T. Veit, C. E. Borba, G. da Cunha Gonçalves, M. R. Fagundes-Klen, R. Bergamasco, E. A. da Silva, and P. Y. R. Suzaki. "Nickel(II) and Zinc(II) removal using Amberlite IR-120 resin: Ion exchange equilibrium and kinetics". In: *Chemical Engineering Journal* 221 (2013), pp. 426 –435.

[167] K. R. Hall, L. C. Eagleton, A. Acrivos, and T. Vermeulen. "Pore- and Solid-Diffusion Kinetics in Fixed-Bed Adsorption under Constant-Pattern Conditions". In: *Industrial & Engineering Chemistry Fundamentals* 5.2 (1966), pp. 212–223.

[168] K. Kadirvelu and C. Namasivayam. "Agricutural By-Product as Metal Adsorbent: Sorption of Lead(II) from Aqueous Solution onto Coirpith Carbon". In: *Environmental Technology* 21.10 (2000), pp. 1091–1097.

[169] A. A. Rouff. "Sorption of chromium with struvite during phosphorus recovery". In: *Environmental Science and Technology* 46.22 (2012), pp. 12493–12501.

[170] C. C. Su, R. R. M. Abarca, M. D. G. de Luna, and M. C. Lu. "Phosphate recovery from fluidized-bed wastewater by struvite crystallization technology". In: *Journal of the Taiwan Institute of Chemical Engineers* 5 (), pp. 2395–2402.

[171] Z. Ye, Y. Shen, X. Ye, Z. Zhang, S. Chen, and J. Shi. "Phosphorus recovery from wastewater by struvite crystallization: Property of aggregates". In: *Journal of Environmental Sciences (China)* 26.5 (2014), pp. 991–1000.

Paper I

PARTICLE SIZE BASED RECOVERY OF PHOSPHORUS FROM COMBINED PEAT AND WOOD FLY ASH FOR FOREST FERTILIZATION

by
Roshan Budhathoki
Ari Väisänen

Fuel Processing Technology
146 (2016)
85-89

Fuel Processing Technology 146 (2016) 85–89

Contents lists available at ScienceDirect

Fuel Processing Technology

journal homepage: www.elsevier.com/locate/fuproc

Research article

Particle size based recovery of phosphorus from combined peat and wood fly ash for forest fertilization

Roshan Budhathoki *, Ari Väisänen

Department of Chemistry, Renewable Natural Resources and Chemistry of Living Environment, University of Jyväskylä, P.O. Box 35, FI-40014 Jyväskylä, Finland

ARTICLE INFO

Article history:
Received 9 November 2015
Received in revised form 10 February 2016
Accepted 11 February 2016
Available online 24 February 2016

Keywords:
Phosphorus recycle
Forest fertilizer
Fly ash utilization

ABSTRACT

Correlations between the concentrations of P, K, and As with particle size in fly ash from power plants were examined with a viewpoint to obtain fractions suitable for forest fertilization. Fly ash samples from several CHP plants were fractionated by using four sieves and the five fractions were analyzed by ICP-OES; it was found that both P and K are concentrated in smallest size (<45 μm) fractions. Some fly ash samples were found to contain As in excess of the legal limit of 40 mg/kg, but even in these cases it was possible to obtain size fractions that pass the legal limit while containing useful amounts of P and K. Fractionating fly ash into different sizes is identified as a viable phosphorus recovery method for obtaining legally acceptable fractions for forest fertilization.

1. Introduction

Utilization of forest resources has increased in Finland in recent decades. The total volume of the growing stock for extraction amounts to 2357 million m^3 over bark and 16 million m^3 are utilized annually for energy production [1]. In addition, 9.3 million ha of land area are covered by peatlands and 0.6% of this, 60,000 ha, are used for peat production [2]. Such harvesting removes nutrients from the forest and peatlands and may lead to the acidification of growing sites, affecting tree growth and the chemistry of runoff water [3]. Studies of ash utilization, such as Ref. [4,5], have indicated a deficiency of mineralized phosphorus in Scots pine growing on drained thick-peated mires. It is thus very essential to return the nutrients to these sites to sustain the mineral cycle and tree growth. Combined heat and power plants in Finland produce over 150,000 t of wood ash and 450,000 t of peat ash annually. 30% of their fly ash and 70% of bottom ash are generally utilized in some way. Most of the wood fly ash are being used as forest fertilizer which replaces the nutrients removed in biomass harvesting, counteracts soil acidification and improves tree growth. For example, 27,000 t of wood ash were used as forest fertilizer in 2004 [3]. Experimental studies have reported 3.1–12.1 $m^3 ha^{-1}$ a^{-1} of growth increase, and 44–56 years of fertilizer influence when 5000–16,000 kg ha^{-1} were utilized [6]. Thus, refining of wood ash for forest and ground vegetation fertilization has been developed at an industrial scale in Finland during recent years [7].

Typical mineral elements in wood and peat fly ash are silicon (Si), calcium (Ca), potassium (K), phosphorus (P), magnesium (Mg), manganese (Mn), iron (Fe), sodium (Na), aluminum (Al), boron (B) and titanium (Ti). The fertilizing effect of ash depends mainly on its phosphorus and potassium content, while calcium and magnesium exhibit a liming effect [8]. However, it lacks nitrogen, which is lost as flue gas during combustion. According to Väätäinen et al., the fertilizing effect of wood ash lasts for 30–40 years. On the contrary, fertilizing effect for chemical fertilizers with similar phosphorus and potassium concentration has been estimated to last for 15–25 years [5]. The reason for this difference is the different leaching rates of phosphorus between wood ash and chemical fertilizers. The slow leaching rates of phosphorus in wood ash have been attributed to the adsorption of P by Al and Fe [9]. In addition, wood and peat ash contain various heavy metals which are classified as harmful and toxic. Thus, the forest use of ash is regulated by a new Decree on fertilizer products, imposed by the Finnish legislature in 2011. According to the new Decree on fertilizer products the minimum recommended sum of phosphorus and potassium concentrations should be 2% d.w. (20 g/kg) and for calcium 6% by weight or 60 g/kg. Furthermore, the new Decree on fertilizer products imposes no limit values for pH, moisture, dry matter content, neutralizing value or the concentration of chloride [10]. Meanwhile, the same Decree also sets maximum limit values for heavy metals as shown in Table 1.

Fly ash is, in general, an extremely inhomogeneous material. However, its elemental composition seems to be a function of its particle size distribution. A limited number of studies [11,12] have focused upon the correlation of ash mineralogy with its particle size distribution, while Dahl et al., and Lanzerstorfer [13,14] considered heavy metals and found that metals such as As, Cd, Cr, Cu, Ni, Pb and Zn are more concentrated in smaller particle size (<75 μm) fractions than in the larger ones. However, discrete studies on effect of size fractionation of fly ash on the elements with fertilizing qualities like P and K have not yet been conducted. Therefore, this study aims to investigate the dependence of fly ash chemistry on its particle size and the effect of fractionation on the

* Corresponding author.
E-mail address: roshan.budhathoki@jyu.fi (R. Budhathoki).

http://dx.doi.org/10.1016/j.fuproc.2016.02.016
0378-3820/

Table 1
Physical and chemical properties of fly ash originated from various mixtures of peat (P) and wood based biomass (B) as fuel (subscripts indicate the fuel composition used for combustion).

Parameters	Fly ash samples							Limit value [10] (max.)
	P_{100}	$P_{80}B_{20}$	$P_{70}B_{30}$	$P_{65}B_{35}$	$P_{50}B_{50}$	$P_{30}P_{70}$	B_{100}	
(a) Particle size distribution profile (μm)								
D_{10}	7.1	11.2	13.6	15.2	7	13.9	12	
D_{50}	21.3	72.1	102.9	119.9	46.4	116.7	196.3	
D_{90}	81.2	168.3	230	236.5	148.1	176.4	494.1	
AMD	22	52	70	78	37	71	114	
(b) Weight fraction of sieved samples (wt.%)								
<45 μm	61.3	48.9	28.6	32.2	53.2	29.4	22	
45–63 μm	9.2	14.2	18.3	13.6	16.7	13.7	20.8	
63–125 μm	22.8	24.7	28	23.7	19.4	27	16.1	
125–250 μm	6.8	12.3	20.6	23.9	7.4	25.3	16.6	
>250 μm	0	0	4.4	6.5	3.2	4.6	24.5	
(c) Elements/mineral composition (10^3 mg/kg)								
C	10.8	2.6	8.2	6.8	22.1	20.8	13.6	
H	2.9	–	–	–	1.6	1.1	2	
N	–	–	–	–	–	0.4	–	
Al	79.3	91.4	99.9	86.1	60.1	47.7	33.8	
Ca	304.3	92.2	81.7	86.4	131.1	47.5	154	
Fe	107.3	142.8	106.7	80.3	60.4	31.7	20	
K	14.4	19.8	22.4	19.1	21.7	14.3	31	
Mg	23.5	16.5	13.5	12.6	16.9	8.5	21.6	
Mn	1.3	3.3	2.6	3	6.6	2	8.7	
Na	10.3	11	14.5	11	7.3	6.5	9	
P	10.1	13.3	9	9.5	17.2	4.9	12.1	
Si	145.6	189.1	207.4	190	187.8	296.4	173.1	
Ti	2.1	3.3	3.4	3	2	1.6	1.5	
d) Heavy metal composition (mg/kg)								
As	33.4	78.9	34.5	33.1	61.6	24.3	6.7	40
Cd	1.1	2.7	1.1	2.2	7.4	4	8.6	25
Cr	36.2	67.6	53.7	35.3	57.8	34.7	45.1	300
Cu	84.2	100	93.5	130.4	125.7	112.6	89.6	700
Ni	29	31.8	23.2	28	37.5	26.5	24.6	150
Pb	40.4	82.4	39.6	43.9	69.9	38.2	26.3	150
Zn	114.9	274.7	188.5	224.4	675.7	239.2	1704	4500

AMD = arithmetic mean diameter, (–) = below detection limit.

total phosphorus and potassium concentration of the fractions as an aid in the selection of suitable fraction for potential forest use.

2. Material and methods

Seven samples of fly ash were received from three different combined heat and power (CHP) plants of Finland. The seven fly ash samples originated from different combinations of peat and wood based biomass as a fuel for combustion in the power plants. A large number of ash samples allow us to generalize the correlation between element distribution and particle size of fly ash originating from various fuel mixtures. The fuel composition varies from 100% peat to 100% wood based fuel. The fly ash samples are labeled on the basis of their fuel composition, and are indicated as P_{100}, $P_{80}B_{20}$, $P_{70}B_{30}$, $P_{65}B_{35}$, $P_{50}B_{50}$, $P_{30}B_{70}$ and B_{100}, where P and B indicate the fuel type and refer to peat and woody biomass. In addition, the subscripts indicate the fuel composition percentage by weight. P_{100} is received from Keljonlahti CHP, while $P_{80}B_{20}$, $P_{70}B_{30}$, $P_{65}B_{35}$, $P_{50}B_{50}$ and $P_{30}B_{70}$ are from Rauhalahti CHP, and B_{100} is from Alholmens Kraft CHP.

The particle size distribution profiles (PSDPs) for all seven samples were evaluated with a Fritsch Analysetter 22 Economy particle size analyzer using a wet dispersion method in a saturated sodium chloride solution. The use of saturated solution is presumed to mitigate the problems associated with the dissolution of fly ash particles in water. RETSCH sieve shaker (AS200 basic) was employed for dry sieving with a screening time of 30 min. Samples of 20 g of each fly ash were taken for screening. Then the sieved fractions were collected and weighed. The following five fractions were obtained: [(0–45), (45–63), (63–125), (125–250), (>250)] μm. In the present study, mechanical sieving method has been employed solely for quantitative analysis of element distribution. Sieving may not be an appealing separation method in industrial scale, however methods such as air classification could be feasible.

The elemental composition of the fly ash samples was determined with an Elementar vario EL(III) and an ICP-OES PerkinElmer Optima 8300 instrument. All reagents used were of analytical grade. 0.25 g samples of primary fly ash and fractioned fly ash samples were dissolved in 3 ml of aqua-regia with 3–4 drops of hydrofluoric acid. The digestion was further assisted by ultrasound for 18 min with sonication procedure divided into six equal steps (3 min). All samples were shaken in between and the evolved gas was released. The samples were diluted to 100 ml in plastic volumetric flasks with high purity water produced by a Maxima water purification system provided by Elga. The sample matrices were analyzed with ICP-OES for heavy metals. The same samples were further diluted by a factor of 10 for mineral elements analysis in order to get suitable element concentrations for analysis by ICP-OES. A similar digestion method was employed for a standard reference material, SRM1633c [15], certified by NIST and recovery percentages of >98% for all heavy metals and phosphorus and 82–92% for most mineral elements were achieved, except for Si for which about 80% was obtained. Three replicate analyses were performed resulting in RSDs of about 5–10%. Due to the greater precision in the determination of heavy metals and mineral elements like phosphorus and potassium, this digestion method was adopted in this study. Relative composition of phosphorus and potassium on respective weight fraction (F_1–F_5) is estimated as;

$$M_{F_i} = C_{F_i}^{M} \cdot F_i^{\text{wt.\%}} \text{ and } M_{F_i}\% = \frac{M_{F_i}}{\sum_{i=1}^{5} M_{F_i}}$$

where M_{F_i} is the relative concentration of element in F_i weight fraction, $C_{F_i}^{M}$ is the concentration of element in F_i determined with ICP-OES and $F_i^{\text{wt.\%}}$ is the weight proportion of the F_i fraction.

3. Results and discussion

3.1. Physical and chemical properties of fly ash and its fractions

Seven fly ash samples originated from different fuel mixtures from three power plants of Finland were compared in terms of particle size distribution. Fig. 1 shows the significant variation in their particle size distribution, and the results of their diameter range is listed in Table 1a. According to Dahl et al. [13], the quality of fly ash including PSDPs is also affected by power plant processing conditions and collection system. The sieving of all fly ash samples indicates that a large proportion of the particles belongs to the smallest size range, 0–45 μm. This trend is valid for all seven fly ash samples in Table 1b.

A comprehensive elemental analysis of seven fly ash samples reveal significant variation in the distribution of elements in fly ash originating from different fuel mixtures and the results are listed in Table 1c. The phosphorus composition varies from 4.9 to 17.2 g/kg of ash while the potassium varies from 14.4 to 31 g/kg of ash. Such quantity of P and K in fly ash makes it adequate for forest fertilization. However, the composition of heavy metals in fly ash solely regulates its use as forest fertilizer, according to the Decree on fertilizer products. The heavy metal analysis of seven fly ash samples reveals the unsuitability of $P_{80}B_{20}$ and $P_{50}B_{50}$ for forest use because their arsenic (As) concentration exceeds its limit value of 40 mg/kg. Meanwhile, P_{100}, $P_{70}B_{30}$, $P_{65}B_{35}$, $P_{30}B_{70}$ and B_{100} can be utilized in fulfilling the requirements of the Decree on fertilizer products.

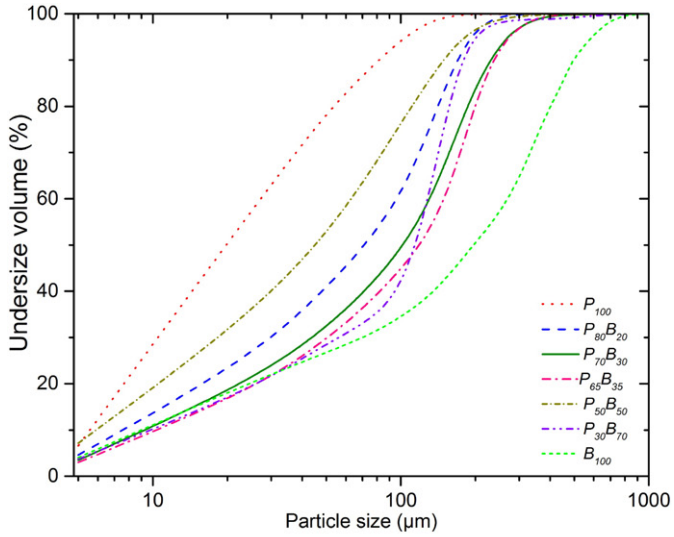

(a) Undersize volume distribution

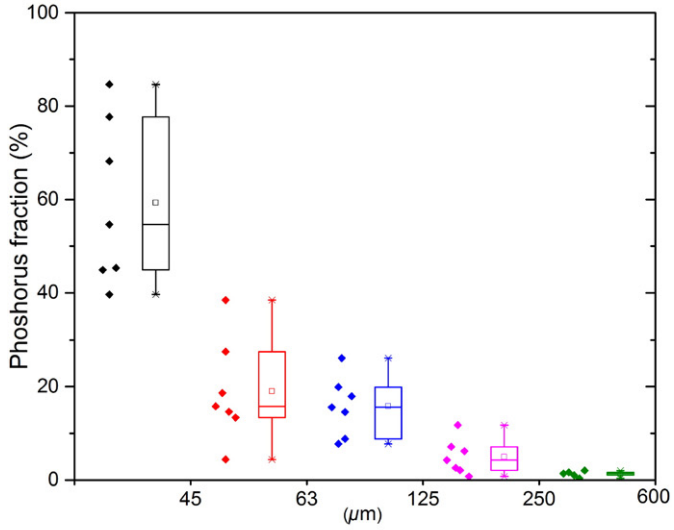

(b) Phosphorus distribution

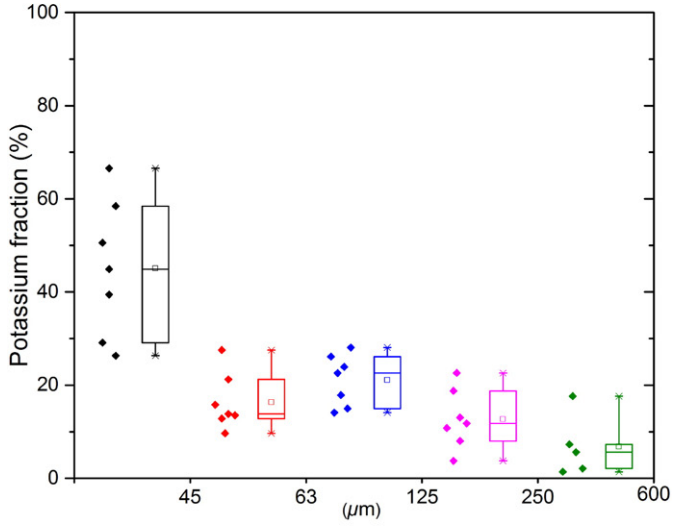

(c) Potassium distribution

3.2. Distribution of P and K in fly ash particle size

It has been mentioned earlier that phosphorus and potassium are the key elements having fertilizing characteristics, while alkaline earth metals such as Ca and Mg have a liming effect [8]. Therefore, the distribution of phosphorus and potassium in different particle sizes has been emphasized in this study.

The ranges of P and K concentration in seven fly ash samples are illustrated in Fig. 1b & c, where the data points represent the M_{F_i} percentages and the box chart shows the ranges of mineral element contents in the F_i fractions. The analysis implies that P is more concentrated in the F_1 fraction with a mean value of about 59%, while F_2 and F_3 fractions have average values of 19% and 16% respectively. Likewise, the F_1 fraction contains 45% of the total K while F_2 and F_3 have 16% and 21%. Therefore, fractions having smaller particle size (<125 μm) are more appropriate for fertilization use. Even so, the use of such fractions could be restricted due to limitation imposed by their heavy metal content; this will be evaluated in the next section.

3.3. Heavy metal content and potential use of ash fractions

In Section 3.1, P_{100}, $P_{70}B_{30}$, $P_{65}B_{35}$, $P_{30}B_{70}$ and B_{100} are identified as suitable for use as forest fertilizer, while the use of $P_{80}B_{20}$ and $P_{50}B_{50}$ is restricted as per Finnish legislation. The distribution profile indicates higher heavy metal concentrations in smaller particle sizes, these findings are consistent with the results in Ref. [13]. Since the utilization of an ash fraction is determined by its heavy metal content, the effect of fractionation into different fractions on total mineral element and heavy metal concentration has been assessed on B_{100} and $P_{70}B_{80}$ (classified as non-restricted ash) and on $P_{50}B_{50}$ and $P_{80}P_{20}$ (classified as restricted ash) samples, the evaluation is presented in Table 2.

In Table 2, all fractions (F_1–F_5) of B_{100} are suitable for forest fertilization. The concentration of P in F_1 and F_2 is twice that of primary ash samples (B_{100}), while the K concentration is almost 1.6 times higher. The F_3 fraction has a similar P and K composition, and F_4 and F_5 have less of P and K than the primary B_{100} ash. Heavy metal concentrations for all fractions are also lower than the maximum allowed value. In addition, the weight fractions of F_1 and F_2 are 22% and 20.8%, respectively. Thus, the utilization of F_1 or F_2 fractions of B_{100} offers a substantial benefit over the use of primary B_{100} or the F_4 and F_5 fractions, because F_1 and F_2 fractions can recycle the mineral elements almost two times more effectively than the primary ash. Likewise, F_2 of $P_{70}B_{30}$, which represents 18.3 wt.%, is the most befitting fraction in comparison to other fractions because its P and K concentrations are higher by a factor of 1.3. The use of the F_1 fraction of $P_{70}B_{30}$ is restricted due to its elevated concentration of As.

The results from B_{100} and $P_{70}B_{30}$ suggest that the fractionation has caused the ash chemistry to differ significantly between the fractionated fractions and the primary ash samples. This interpretation is also validated by evaluating the chemistry of the fractionated fly ash. Data listed in Table 2 show the results from the fractionation of fly ash $P_{50}B_{50}$ and $P_{80}B_{20}$. Though F_1 of $P_{50}B_{50}$ and F_1, and F_2 of $P_{80}B_{20}$ are not suitable for forest use, the F_2 and F_3 of $P_{50}B_{50}$, and F_3 and F_4 of $P_{80}B_{20}$, possess minimum recommended values of P and K. These fractions are thus allowed for forest use, but there is less phosphorus and potassium in them due to the selection of fractions belonging to the large particle size group. Such results imply that a proportion of restricted ash can be recovered using

Fig. 1. (a) The undersize volume distribution of seven fly ash samples originating from different mixtures of peat and wood based biomass as fuel. (b, c) Relative distribution of phosphorus and potassium in (F_1–F_5) particle size fraction of seven fly ash samples; where the individual data point represents the relative proportion of P and K in respective fractions and the box plot is based on population size (n) of seven fly ash samples.

Table 2
Elemental composition of five sieved fractions of fly ash classified as restricted (concentration of at least one heavy metal exceeding the legal limit value) and non-restricted (none of the heavy metals exceeding the legal limit value concentration).

	B_{100}					$P_{70}B_{30}$				
	F_1	F_2	F_3	F_4	F_5	F_1	F_2	F_3	F_4	F_5
(A) Element composition of non-restricted fly ash (mg/kg)										
P	25.3	26	13.6	3.6	1.1	12.6	12.3	9.8	8.2	7.9
K	51.3	51.5	26.2	25.2	28	22.7	25.1	25	24.5	24.7
Ca	398	317	131	37.3	30.5	110	110	90.5	77.6	75.5
Mg	45	44.1	24.1	9.3	7.3	15.1	15.8	14.1	12.6	12.4
As	6.8	8	3.8	3	1.2	65.5[a]	38.5	10.7	2.8	3.9
Cd	13.5	13.6	5.1	1.9	1.2	4.5	3.6	2.4	1.7	1.7
Cr	58.8	66.3	64.7	36.6	21	76.5	64.2	46.9	25.7	23.9
Cu	137	149	99.6	52.5	52.6	180	162	180	137	251
Ni	37.3	41.1	34.1	19	9.7	35.6	30.3	21.5	10.4	9.2
Pb	51.3	48.8	25	14.6	10.7	59.3	40	15	9.2	8.7
Zn	3411	3385	1125	539	727	250	146	66.3	60	94
(B) Element composition of restricted fly ash (mg/kg)										
P	20.3	11.1	5.5	1.5	1.6	16.5	15.5	13.2	11.8	
K	51.7	33.4	30	20.9	26.9	19	18.7	18.1	18.3	
Ca	266	130	72.5	26.9	28.8	114	107	92.1	84.1	
Mg	39	23.6	16.9	7.6	9.1	17.4	16.7	15.3	14.6	
As	44.3[a]	28.6	6.5	4.9	4.6	113[a]	47.4[a]	25.1	6.5	
Cd	3.9	3.2	2	1.6	1.6	6.3	4.1	3	1.9	
Cr	49	47.6	35	18.2	15.4	83.7	74	55.7	33.8	
Cu	292	423	166	133	51.4	112	158	110	78.1	
Ni	42.8	41.1	27.6	9.7	7.2	42.8	34	24	12.2	
Pb	90.2	51.4	18.3	8.6	4.2	119	54.4	29.8	13.5	
Zn	508	303	117	87.4	158	298	192	82.8	82	

F_1 = (0–45) μm, F_2 = (45–63) μm, F_3 = (63–125) μm, F_4 = (125–250) μm, F_5 = (>250) μm.
Concentration of P, K, Ca and Mg is in order of 10^3 (mg/kg).
[a] Concentration exceeding the limit value (40 mg/kg for Arsenic).

size separation. Characteristics such as pH, moisture, dry matter content, neutralizing value, chloride concentration and proportion of total water-soluble P or K of fly ash and respective fractions are not evaluated, as the Decree on fertilizer products does not impose any limits on these parameters.

4. Conclusion

Five fly ashes out of seven have been identified as potential fertilizer material. The utilization of two fly ashes is restricted because their concentrations of As exceed the limit value of 40 mg/kg. Particle sizes lower than 45 μm have the highest proportion of phosphorus and potassium with average values (with n = 7) of 59% and 45%, respectively. Nevertheless, it is the heavy metal content that regulates the utilization of ash as fertilizer, not the mineral element concentration. Heavy metal concentrations are also elevated in lower particle sizes. Hence, ash fractions of lower size ranges such as F_1 and F_2 are not always good choices, if concentrations of any of the heavy metals are higher than the limit values, as is the case in $P_{50}B_{50}$ and $P_{80}B_{20}$. Fractionation of restricted fly ash also results in the recovery of fractions that are suitable for forest fertilization. On the other hand, sieving of non-restricted fly ash leads to increases in P and K concentrations by 1.3–2 and 1.3–1.6 percentage units, respectively, in the small size fraction. This indicates that fractionation of fly ash has potential to improve the fertilizing properties, and can be suggested as a potential tool for manipulating fly ash chemistry. Meanwhile, selection of the suitable fly ash fractions should to be based on their P and K content, while their heavy metal concentration remains a criterion for their acceptance. The higher P and K content of the accepted fractions helps to recycle lost nutrients back to nature. Recovered ash fractions with increased concentrations of P and K may possess different fertilizing properties such as fertilizer influence time, pH and leachability. Therefore, further investigation of such properties is needed in order to assess the full effect of the utilization of fractionated fly ash as forest fertilizer.

Acknowledgments

The author wishes to thank the Keljonlahti heat and power plant, the Rauhalahti heat and power plant and Alholmens Kraft Oy for providing fly ash samples.

References

[1] Finnish statistical yearbook of forestry (2014) 30–31Available from http://www.metla.fi/metinfo/tilasto/julkaisut/vsk/2014/vsk14_wood_flows_in_Finland_2013.pdf (Accessed on: 10.09.2015) 2016.
[2] Finnish Peat Industry In a Nutshell, Turveteollisuusliitto (Association of Finnish Peat Industries), Available from: http://www.turveteollisuusliitto.fi/index.php?id=223. Accessed on: 10.09.2015.
[3] S. Emilsson, International Handboook from Extraction of Forest Fuels to Ash Recycling, Swedish Forest Agency, 2006.
[4] K. Karsisto, On the duration of fertilization influence in peatland forests with special reference to the results obtained from experiments with different phosphorus fertilizers, Proceedings of International Symposium of Forest Drainage 2–6 September 1974 Jyväskyla-Oulu, Finland, pp. 309–327.
[5] K. Väätäinen, L. Sikanen, A. Asikainen, Rakeistetun puutuhkan metsäänpalautuksen logistiikka (logistics of recycling granulated wood ash back to forest), Tech. rep., University of Joensuu, Faculty of Forest, Joensuu, 2000 (Research Notes 116 (In Finnish)).
[6] R. Lauhanen, M. Moilanen, K. Silfverberg, H. Takamaa, J. Issakainen, The profitability of wood ash-fertilizing of drained peatland scots pine stands [puutuhkalannoituksen kannattavuus eräissä ojitusaluemänniköisä], Suo 48 (3) (1997) 71–82.
[7] K. Väätäinen, T. Tahvanainen, E. Sirparanta, S. Lamminen, Energy wood from early thinnings, 5EURES (EIE/04/086/S07.38582), Tech. rep. Finnish Forest Research Institute, 2007.
[8] P. Vesterinen, Wood Ash Recycling State of the Art in Finland and Sweden, Tech. rep., VTT Processes, 2003.
[9] J. Larsen, G. Warren, R. Langston, Effect of iron, aluminum and humic acid on phosphorus fixation by organic soils, Soil Sci. Soc. Am. J. 23 (6) (1959) 438–440.
[10] H. Nurmesniemi, M. Mäkelä, R. Pöykiö, K. Manskinen, O. Dahl, Comparison of the forest fertilizer properties of ash fractions from two power plants of pulp and paper mills incinerating biomass-based fuels, Fuel Process. Technol. 104 (2012) 1–6.
[11] G. Itskos, S. Itskos, N. Koukouzas, Size fraction characterization of highly-calcareous fly ash, Fuel Process. Technol. 91 (11) (2010) 1558–1563.
[12] C. Lanzerstorfer, Cyclone fly ash from a grate-fired biomass combustion plant: dependence of the concentration of various components on the particle size, Fuel Process. Technol. 131 (2015) 382–388.

[13] O. Dahl, H. Nurmesniemi, R. Pyki, G. Watkins, Heavy metal concentrations in bottom ash and fly ash fractions from a large-sized (246 MW) fluidized bed boiler with respect to their Finnish forest fertilizer limit values, Fuel Process. Technol. 91 (11) (2010) 1634–1639.
[14] C. Lanzerstorfer, Model based prediction of required cut size diameter for fractionation of fly ash from a grate-fired wood chip incineration plant, Fuel Process. Technol. 92 (5) (2011) 1095–1100.
[15] Certificate of analysis: Standard reference material 1633b, Tech. rep., National Institute of Standards and Technology, certificate Issue Date:, 2004 Info: https://www-s.nist.gov/srmors/certificates/archive/1633b.pdf.

Paper II

REMOVAL OF SILICON FROM CFB-DERIVED FLY ASH LEACHATE IN THE CONTEXT OF PHOSPHORUS RECOVERY

by
Roshan Budhathoki
Ari Väisänen

Hydrometallurgy
179 (2018)
215-221

Hydrometallurgy 179 (2018) 215–221

Contents lists available at ScienceDirect

Hydrometallurgy

journal homepage: www.elsevier.com/locate/hydromet

Technical note

Removal of silicon from CFB-derived fly ash leachate in the context of phosphorus recovery

Roshan Budhathoki*, Ari Väisänen

Department of Chemistry, Renewable Natural Resources and Chemistry of Living Environment, University of Jyväskylä, P.O. Box 35, FI-40014 Jyväskylä, Finland

ARTICLE INFO

Keywords:
Phosphorus recycle
Silica removal
Silica polymerization
Fly ash utilization

ABSTRACT

High concentrations of dissolved silica in the acid leachate impose two major challenges on precipitation based recovery of phosphorus (P). Firstly, co-precipitation of colloidal silica in the acidic regimes decreases the purity and value of precipitated P-products. In addition, silica scaling on internal surfaces of equipment is also a problematic issue in industrial operations. Therefore, removal of dissolved silica prior to P-recovery process minimizes the risks of Si-contamination in P-products and Si-scaling. In the present study, silica removal was achieved by accelerated silica polymerization with higher acidity and ionic strength of mineral acid, which also assisted the leaching of CFB-derived fly ash, by aging of the leachate solution. The effects of acid concentration, temperature, and stirring on silica removal rate in acid leachate were also investigated. Higher concentrations of H^+ and Cl^- and higher temperature significantly reduce the silica removal time. HCl was more suitable for improving leachability of phosphorous and precipitating silica in comparison with HNO_3. The silica removal method discussed in this work has been shown to be capable of removing > 98% of dissolved silica from the acid leachate solution.

1. Introduction

Phosphorus, being a limited and depleting element, has a large anthropogenic footprint. Production of phosphorus-containing products highly depends on apatite minerals as raw materials (Pettersson et al., 2008). As an alternative to natural resources, phosphorous can be recycled from waste-to-energy products, such as municipal solid waste incineration fly ash (Kalmykova and Fedje, 2013), chicken manure incineration ash (Kaikake et al., 2009), sewage sludge ash (Lee and Kim, 2017), etc. using hydrometallurgical methods (acid leaching). Depending on temperature and combustion technology, the residual inorganic ash is composed of silicates, oxides, carbonates, phosphates, sulphates, hydroxides, and halides of mineral elements that potentially represent the entire periodic table (Thy et al., 2006; Thy et al., 2013). In recent years, circulating fluidized bed (CFB) boilers have attracted attention in combustion technology due to their high efficiency, fuel flexibility and low pollutant emission (Xiao et al., 2005; Skrifvars et al., 1997). Due to the usage of silica sand in the CFB combustion of biomass as fuel, silicon (Si) can be retained in the fly ash (Valmari et al., 1999) up to 20*w%* (Johansson et al., 2008; Budhathoki and Väisänen, 2016). Phosphorus recovery from ash residues involves chemical leaching which extracts phosphorus from solid to aqueous phase along with various impurities, including silicon as a major contaminant.

Silica scaling is one of the most problematic issues in many industrial operations. It occurs when Si concentration increases above the saturation level at a given temperature and pH in the presence of other metal ions and is extremely difficult and costly to remove (Zarrouk et al., 2014). Whilst the effect of silica on phosphorus precipitation in acidic solutions has not yet been investigated, the inhibiting effect of silicic acid on the precipitation of $CaCO_3$ and co-precipitation of silica with iron during Zn recovery have been reported (Dyer et al., 2012; Bai et al., 2014). Silica precipitation as amorphous or colloidal silica in both acidic and basic solutions via polymerization, agglomeration and aggregation possesses a great threat to the purity of any product being recovered. Therefore, the removal of silica from the feed solution improves the product quality and the economy of the overall operation. Soluble and colloidal silica have been successfully removed from industrial feeds by a number of different methods including coagulation, nano-filtration (NF), reverse osmosis (RO), precipitation of Si particles, precipitation with polyvalent metal hydroxides, lime-soda softening, seeding or inorganic ion-exchange (Hermosilla et al., 2012; Liu et al., 2012; Gallup et al., 2003; Sasan et al., 2017a, 2017b). A major limitation of coagulation is that it mostly occurs at high pH and requires high dosages of the coagulants and flocculants (Hermosilla et al., 2012; Chuang et al., 2007). Drawbacks of NF and RO processes are associated with fouling problems and high energy consumption (Cob et al., 2015).

* Corresponding author.
E-mail address: roshan.budhathoki@jyu.fi (R. Budhathoki).

https://doi.org/10.1016/j.hydromet.2018.06.007
Received 16 November 2017; Received in revised form 3 May 2018; Accepted 14 June 2018
Available online 20 June 2018
0304-386X/

Numerous studies have reported the precipitation of Si particles in acidic solutions in the context of Si-gel formation and its characterization (Dyer et al., 2012; Gorrepati et al., 2010; Bałdyga et al., 2012; Wilhelm and Kind, 2015a). These studies also emphasize that Si-gel precipitation is accelerated by H^+ ions (as indicated by pH), salt ($AlCl_3$, $CaCl_2$, NaCl) concentration, ionic strength of the solution and temperature.

In an effort to develop simple, low-cost and efficient silica removal methods from highly acidic CFB-derived fly ash leachate solution, this study mainly explores the effect of acid concentration and temperature on the feasibility and rate of silica removal prior to phosphorus recovery via precipitation. One of the primary objectives in this study was to avoid contamination and complexity during phosphorus recovery. Hence, the addition of coagulants or other antiscalant products, which promote coagulation and aggregation of silica, were not considered due to the high quantities of coagulants demanded by high Si concentration in leachate solutions. The efficiency of silica removal coupled with efficient phosphorus leaching in minerals acids, mainly HCl and HNO_3, is explored. The kinetics and mechanism of silica precipitation is also discussed.

2. Experimental section

2.1. Materials

Fly ash (FA) samples originated from wood-based biomass fuel in a circulatory fluidized bed reactor were collected from Alholmens Kraft Oy. A RETSCH sieve shaker (AS200 basic) was employed for dry sieving with sieve size of 125 μm for 30 min. 100 g of FA was taken for screening. Then the fractionated FA (FFA) containing particle size lower than 125 μm (59 g) was used for acid leaching, since these fractions contain the major proportion of the phosphorus and less silica than the pristine fly ash (Budhathoki and Väisänen, 2016). Hydrochloric acid (≥37%) from Honeywell-Fluka and nitric acid (≥65%) from Sigma-Aldrich were used in the leaching experiments.

2.2. Leaching experiments

A high molar acid concentration with lower leaching time is adopted in this study, since the former facilitates Si precipitation, while a prolonged leaching in low acid concentration would complicate dephosphorization because of phosphorus reprecipitation with other metal ion released during the leaching (Jin et al., 2006). 2 M, 5 M and 8 M solutions of HCl and HNO_3 were prepared for leaching tests of fly ash. Preliminary investigation indicated an optimal liquid to solid (LS) ratio of 12 for a leaching time of 15–20 min. Therefore, 20 g of fractionated fly ash was added to 240 mL of mineral acid. The leaching process was assisted with mechanical stirring (rate of 500 rpm) and ultra-sound digestion (37 kHz, at room temperature) for 20 min. The undissolved residues were separated with centrifugation.

2.3. Silica precipitation experiment

pH, temperature and ionic strength of the solution are the key parameters that affect the precipitation of Si-gel particles in acidic media (Gorrepati et al., 2010; Bałdyga et al., 2012; Wilhelm and Kind, 2015a). Wilhelm and Kind employed an unstirred setup for investigating the influence of these parameters on the formation of the solid and the resulting gel network to avoid an adiabatic temperature rise due to stirring. Moreover, stirring also causes destruction of the gel network allowing its shrinkage, hinders growth of silica gel polymers and yields smaller Si particles (Wilhelm and Kind, 2015a, 2015b). Therefore, this study adopts unstirred batch precipitation to study the effect of acid concentration and temperature on the formation of Si-gel particles in the context of their removal from the solution. A separate investigation was also carried out to study the effect of stirring on silica removal.

In this study, 10 mL of each leachate solution obtained after centrifugation were transferred to a 15 mL centrifuge tube and left for aging of silica gel at room temperature and also at 40 and 60 °C (with an accuracy of ± 3 °C) in order to examine the influence of temperature. Magnetic stirring was employed for the stirring experiments. Each sample was centrifuged after a certain time interval (0–75 h) to separate the silica gel. Centrifugation was used to shrink the volume of polymeric silicic acid gel-network, as the applied" enforced syneresis" in mechanical or external form contribute to shorter shrinkage time (Quarch et al., 2010).

2.4. Analytical methods

2.4.1. Sample characterization

The elemental composition of fly ash samples was determined with an ICP-OES PerkinElmer Optima 8300 instrument. 0.25 g of FA and FFA were dissolved in 3 mL of aqua regia with 3–4 drops of hydrofluoric acid. The digestion was further assisted by ultrasound for 18 min at 60 °C. The samples were shaken in between the digestion to release the evolved gas.

The silica gels were dried and characterized with Zeiss EVO-50XVP Scanning Electron Microscope (SEM) and Bruker Quantax 400 EDS for visual and elemental analysis.

2.4.2. Measurement of soluble and precipitated silica

1 mL of supernatant was extracted after separation of Si-gel via centrifugation and diluted to 100 mL to quench further polymerization of Si and precipitation. The concentration of dissolved or soluble silica and other analytes was determined from the quenched fraction with ICP-OES as a function of time. The concentration of precipitated Si-gel at given times was determined by subtraction from the known initial soluble silica concentration in the solution.

3. Results and discussion

3.1. Silica removal during fractionation

The elemental composition of the pristine FA and FFA determined with ICP-OES is presented in Table 1. The advantage of fly ash fractionation was studied and presented in our earlier study (Budhathoki and Väisänen, 2016); it summarizes that sieving of fly ash can remove up to 73% of silicon by discarding 41w% of fly ash. This fractionation increased the phosphorus content by a factor of 1.38 and the concentration of other matrix elements and heavy metals also increased, as shown in Table 1.

Table 1
Major element and heavy metal contents of FA and FFA determined by ultrasound acid digestion followed by ICP-OES measurement.

Element	Major element (g/kg)						Heavy metal (mg/kg)						
	P	Al	Fe	Si	Mg	Ca	Zn	Cu	Cr	Pb	Ni	As	Cd
FA	12.1	33.8	20	173	21.6	154	1704	89.6	45.1	26.3	24.6	6.7	8.6
FFA	16.7	31	20.3	45.4	28.3	217.5	2595	99.7	50.4	35.2	33.7	11.7	11.5

Table 2
Concentration of P, Si, Fe, Al Mg and Ca in the leachate solution obtained after leaching and the approximated H^+ remaining in the leachate.

Acid (M)		Concentration (mg/L)						$H^+_{leachate}$ (M)
		P	Si	Fe	Al	Mg	Ca	
HCl	2	1407	2403	760	1346	2162	18,831	0.72
		(100.9)[a]	(63.6)	(44.8)	(52.1)	(91.7)	(103.9)	
	5	1388	2135	911	1319	2097	17,410	3.82
		(99.5)	(56.5)	(53.7)	(51.1)	(88.9)	(96)	
	8	1425	1947	1154	1380	2181	17,324	6.84
		(102.2)	(51.5)	(68.0)	(53.4)	(92.4)	(95.6)	
HNO_3	2	1298	2472	673	1343	2123	18,301	0.74
		(93.1)	(65.4)	(39.7)	(52)	(90)	(101)	
	5	1355	2179	767	1347	2100	18,098	3.78
		(97.2)	(57.6)	(45.2)	(52.1)	(89)	(99.8)	
	8	1288	1811	760	1234	1950	16,701	6.89
		(92.3)	(47.9)	(44.8)	(47.8)	(82.6)	(92.1)	

[a] Values in () indicates leaching recovery %.

3.2. Leaching behavior of P, Si and other matrices in HCl and HNO_3

The mineral acid used and its concentration are the major factors that affect the leaching behavior of phosphorus and other elements (Pettersson et al., 2008; Kalmykova and Fedje, 2013). Details of the leaching experiments are summarized in Table 2. Phosphorus leaching was more efficient with HCl than with HNO_3, while varying the acid concentration between 2 M and 8 M had only a small effect on the P leachability. On the other hand, lower concentrations of acid showed the highest Si leachability, the order of leaching feasibility being 2 M > 5 M > 8 M for both HCl and HNO_3. A similar behavior of Si leaching from zeolite analcime and sodium metasilicate nonahydrate (SMN) with HCl was also reported by Fogler et al. (Gorrepati et al., 2010). The low dissolution of silicon in concentrated acid may be attributed to the low availability of OH^- groups that assist the formation and stabilization of orthosilicic acid ($Si(OH)_4$) in the leachate solution and simultaneous precipitation of silica gel particles.

This study uses acid concentrations higher than the stoichiometric concentration required to dissolve the phosphates from ash residues. In order to attribute the effect of H^+ ions on Si removal, the remaining H^+ ion concentration was estimated by Eq. (1).

$$H^+_{leachate} = H^+_{added} - 1.1 \times (2 \times [Ca] + 2 \times [Mg] + 2 \times [Si]) + 3 \times [P] \quad (1)$$

where $H_{added}{}^+$ is the molar concentration of acids used during leaching and [Ca], [Mg], [Si] and [P] are the concentrations (mol/L) of Ca, Mg, Si and P in the leachate solution. Factors multiplying the analyte concentration term are the fractions of H^+ consumed per mole of the analytes during dissolution of the model solid as shown in Eqs. (2)–(5). Ca, Mg and Si are the major matrix elements in the leachate solution that consume most of the H^+ ions during dissolution of the CaO, MgO and $NaAlSi_2O_6$ (analcite) as model compounds. It is also assumed that an additional 10% of H^+ is consumed by other compounds. Similar strategy was employed to determine the stoichiometric concentration of H_2SO_4 required to leach phosphorus from sewage sludge ash (SSA) (Donatello et al., 2010; Franz, 2008). The remaining H^+ in the leachate solutions is also presented in Table 2.

$$H_3PO_4 -> 3H^+ + PO_4^{3-} \quad ([H^+]/[P]) = 3 \quad (2)$$

$$CaO + 2HCl -> CaCl_2 + H_2O \quad ([H^+]/[Ca]) = 2 \quad (3)$$

$$MgO + 2HCl -> MgCl_2 + H_2O \quad ([H^+]/[Mg]) = 2 \quad (4)$$

$$NaAlSi_2O_6 + 4HCl + 2H_2O -> 2Si(OH)_4 + AlCl_3 + NaCl \quad ([H^+]/[Si]) = 2 \quad (5)$$

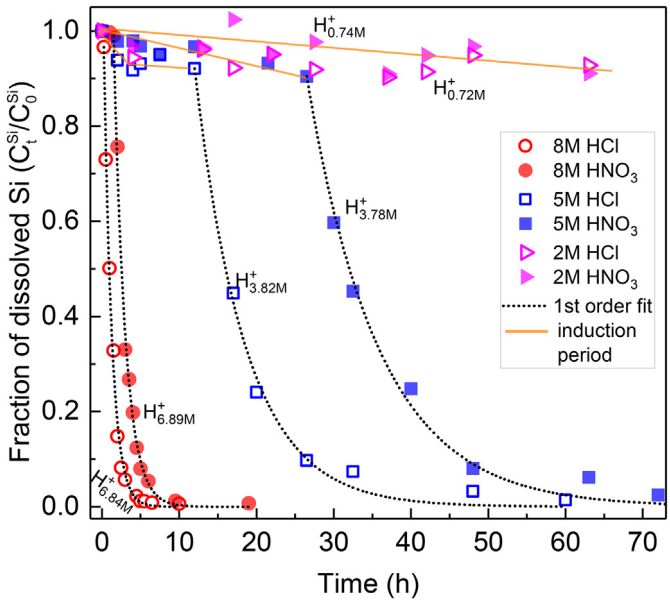

Fig. 1. Disappearance of dissolved silica concentration (C_t^{Si}) as a function of time showing the measured data and best fitted modeled data for Si-gelation in acid leached solutions. C_0^{Si} is the total dissolved silica at $t = 0$ h and respective concentration are shown in Table 2.

3.3. Effects of acid matrix on silica removal

The disappearance of dissolved silica was followed as a function of time (Fig. 1). The consumption of soluble silica, especially in leachate obtained with 5 M acid, exhibits two kinetic regimes; (i) first regime with slow consumption until silica conversion reaches ≈10% and (ii) second regime with rapid depletion of soluble silica. The earlier phase is referred to as induction time/period, while the later is called polymerization or aggregation zone (Iler, 1980; Weres et al., 1981; Rothbaum and Rohde, 1979). Noguera et al. interpreted induction time as the period until the first particles are detected (Noguera et al., 2015). The length of induction period is dependent on pH, temperature and silicic acid concentration. Higher supersaturation and acidity are also linked with shorter induction times (Chan, 1989). An inverse relation between the solubility of silica and acid concentration was reported in HCl and HNO_3 matrices (Lenher and Merrill, 1917; Elmer and Nordberg, 1958). A decrease in solubility of silica is associated with an increase in the supersaturation and thereby promotes the silica precipitation. In addition, the polymerization reaction controlling the particle formation and adhesion to initiate gel growth is also charge-catalyzed. Si polymerization below isoelectric point, pH 2 for silicic acid, is catalyzed by H^+-ions, while above isoelectric point it is OH^- catalyzed (Makrides et al., 1980; Quarch and Kind, 2010). In this study, shorter induction times and higher Si precipitation rates were observed for leachate solution obtained with high molar concentration of acids. This is attributed to reduced solubility of silica at high concentration of acid and promotion of silica polymerization by H^+-ions.

The polymerization process is in a good agreement with a first order kinetic model with respect to the disappearance of dissolved silica. Using the Akaike (AIC) and the Bayesian (BIC) information criteria (Table 3) it was found that the first order had a better fit to the measured data than the second order kinetic models. However, both first order (Iler, 1980; Potapov et al., 2007) and second order (Gorrepati et al., 2010) consumption of monosilicic acid has been reported in acidic solution.

There is also a clear discrepancy between the leachates obtained with 5 M concentration of HCl and HNO_3. The approximate H^+ ion concentrations in these leachates are similar, with respective values of 3.82 and 3.78 M. However, these leachates evidently differ in their

Table 3
Comparison between 1st and 2nd order kinetic models with respect to the consumption of dissolved silica from the solution.

Acid	(M)	Kinetic model							
		1st order				2nd order			
		-K	R^2	AIC	BIC	-K	R^2	AIC	BIC
HCl	5	0.155	0.991	34.70	31.59	0.0014	0.982	40.22	37.11
	8	0.960	0.995	44.25	43.89	0.0089	0.942	74.57	74.20
HNO3	5	0.107	0.992	33.95	30.84	0.0008	0.968	44.29	41.18
	8	0.667	0.996	35.42	34.31	0.0063	0.945	61.68	60.57

anion (Cl^- and NO_3^-) concentrations. Previous studies have reported the catalyzing nature of F^- ions in silica polymerization (Wilhelm and Kind, 2015a; Brinker, 1988). In general, anions of single charge, small size, or low polarizability promote the coordination number of silicon (IV) from four to six (Bishop and Bear, 1972) and reduce the electron density on unsaturated tetravalent Si making it more susceptible to nucleophilic attack from another coordinatively unsaturated Si (Brinker, 1988). This linkage of two monomeric Si species forming a siloxane bond (Si–O–Si) is very critical for increasing silica polymer length and particle growth. Cl^- ions, sharing the same group in periodic table, possess similar characteristics as F^- ions. Therefore, catalysis by Cl^-, in the present context, is a possible explanation to the discrepancy between 5 M HCl and HNO_3 acid matrices.

A separate investigation is carried out to examine the catalytic effect of Cl^- ions in the leachate solution obtained from 5 M HCl acid by addition of 1 M of NaCl as source of Cl^-. In order to differentiate the extent of Cl^- catalysis from the influence of increased ionic strength, 1 M of $NaNO_3$ was added in another batch since 1 M of both salts induce equal increases in the ionic strength. In this case, the solution was stirred (magnetic stirring at 400–600 rpm) for only 5 min to assist dissolution of salts. Fig. 2 shows that addition of 1 M Cl^- ions accelerates the consumption of dissolved silica from the leachate solution by two orders of magnitude. The increment in the instantaneous reaction rate

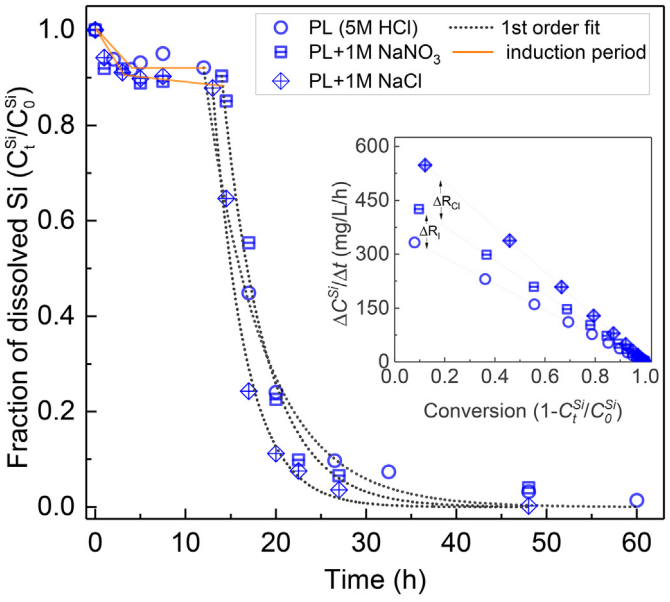

Fig. 2. Normalized conversion of dissolved silica vs. time showing increment on silica disappearance rate due to added Cl in 5 M HCl pristine leachate (PL) solution, and comparison of instantaneous reaction rate ($\Delta C^{Si}/\Delta t$) against the conversion of dissolved silica for PL, and leachate with added 1 M of $NaNO_3$ and NaCl. ΔR_I indicates the increased Si consumption rate due to increase in ionic strength and ΔR_{Cl} denotes the increment due to added Cl. (C_t^{Si} = Si concentration at time, t; C_0^{Si} = initial dissolved Si concentration).

with 1 M $NaNO_3$ is attributed to the increase in ionic strength. Higher salinities (Cl^- concentration) at pH 4.5 and 95 °C were found to relate with a higher polymerization rate and shorter induction period (Makrides et al., 1980). This clearly provides evidence for the results herein. However, a relation between Cl^- concentration and the length of induction period was not observed in this study for 1 M of added Cl^- ions.

Mechanism of H^+ and Cl^- catalysis for the formation of silica particles and silica gel is presented in Fig. 3. It commences with formation of H^+ and Cl^- catalyzed siloxane bond where monomeric and dimeric silicic acid polymerizes to yield long oligomers or polymers of silicic acid. These polymeric silica units grow by addition of monomeric silicic acid to yield primary particles (~20–50 nm) that aggregate to form particulates of silica followed by gel formation and precipitation (Wilhelm and Kind, 2015a). Since gelation is a bonding phenomenon between the aggregates forming particulate network, it is affected by process parameters such as pH, supersaturation, temperature and ions in the solution. Therefore, the removal of silica occurs by formation of Si-gels and precipitation of gel particles by further aggregation.

The total times required to remove 98% of silicon from the HCl and HNO_3 leachate solutions, were 5 and 10 h for 8 M concentration, and 48 and 73 h for 5 M, respectively. Higher H^+ and Cl^- ion concentrations are in a strong relation with shorter induction period and higher Si precipitation rate. Therefore, a high concentration of HCl acid is identified as suitable reagent in terms of better phosphorus leachability and faster removal of silica from the leachate solution.

3.4. Effect of temperature on Si precipitation

The temperature dependence of silica precipitation is examined on leachate obtained with 5 M HCl solution due to the presence of two kinetic regimes. Fig. 4 shows the disappearance of dissolved silica against time at 20, 40 and 60 °C. Increase in temperature significantly reduces the induction time and also increases the silica removal rate. Temperature influences the polymerization of silica by increasing the solubility of monomeric silicic acid and thus affecting its supersaturation (Wilhelm and Kind, 2015a). A strong acceleration of silica gelation is in correlation with increasing temperature in the case of acid-catalyzed polymerization (Wilhelm and Kind, 2015a; Hurd, 1935). In addition, the activation energy estimated for silica polymerization in this study for highly acidic leachate solution with H^+ molar concentration of 3.82 M, is ca. 39.25 kJ/mol. This is also in agreement with the reported activation energy of 37.6 kJ/mol for highly acidic gel prepared in 1.65 M of hydrochloric acid (Hurd and Barclay, 1940).

3.5. Effect of stirring on Si removal

Stirring or mixing the solution is one of the important parameters in the kinetics of silica polymerization and precipitation (Quarch et al., 2010). In silica polymerization assisted with coagulants or preparation of silica gel from various silica sources, stirring is employed to improve the dissolution and diffusion of the added reagents. Stirring of the solution increases the dissipation energy during gel formation and results in smaller gel fragments (Wilhelm and Kind, 2015a). In addition, effect of stirring on the morphology and particle size distribution of the precipitated silica is also reported (Meoto et al., 2017). However, this study examines the effects of stirring on H^+ and Cl^- catalyzed silica polymerization emphasizing the removal of dissolved silica from the pristine leachate solution.

Fig. 5 indicates a small reduction in the induction time due to stirring, while a significant deviation in consumption of dissolved silica and reaction kinetics is observed. Second order consumption of dissolved silica in the stirred case shows better agreement with the measured data in contrast to first order consumption under unstirred conditions. In addition, stirring prolongs the silica removal with minimum 40 h required to remove 90% of the dissolved silica, while only 27 h

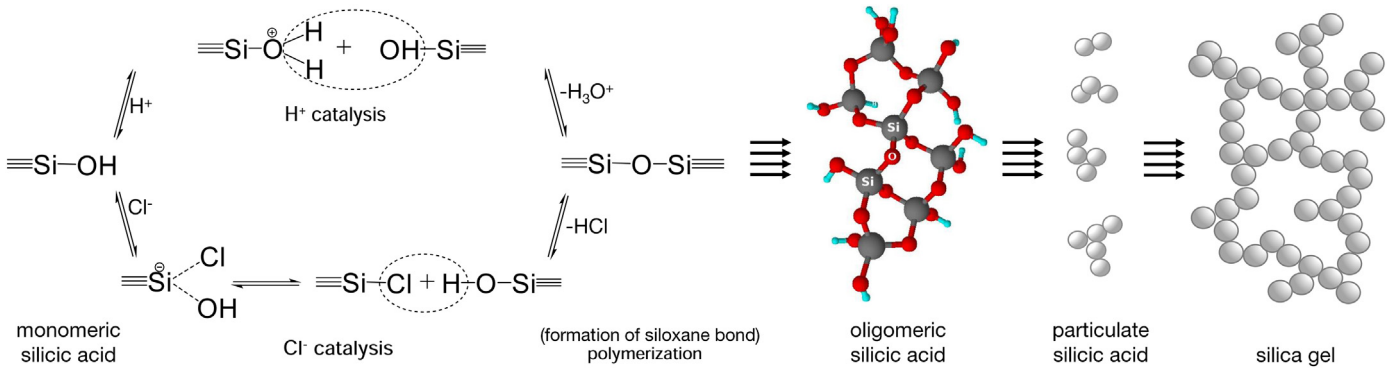

Fig. 3. Mechanism of H^+ and Cl^- catalyzed polymerization of monosilicic acid forming silica gel (based on Matthias (Wilhelm and Kind, 2015a) and Brinker (Brinker, 1988)).

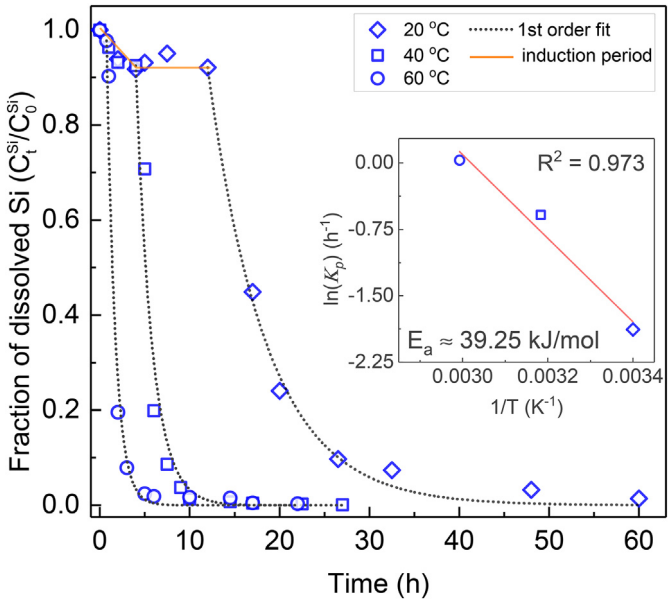

Fig. 4. Fraction of dissolved silica in leachate solution as a function of time at various temperatures showing Arrhenius relationship ($K_p = Ae^{-E_a/RT}$) between the temperature (T) and the first order polymerization reaction constant (K_p) with an activation energy (E_a) of 39.25 kJ/mol.

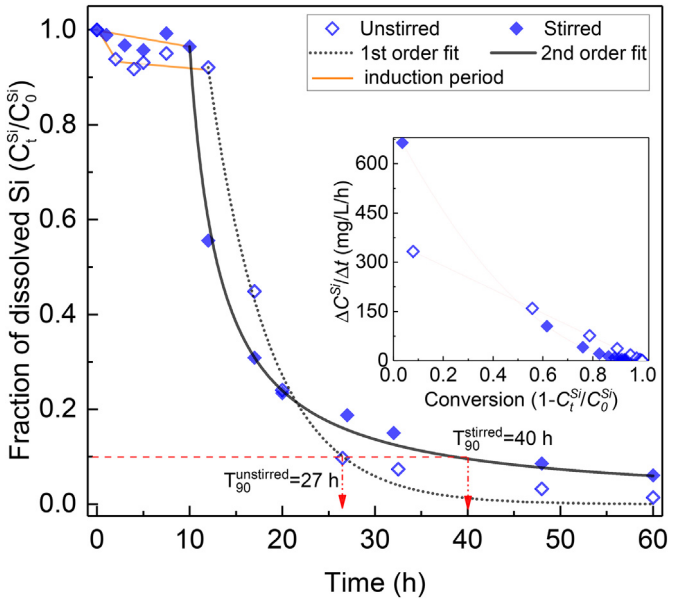

Fig. 5. Disappearance of dissolved silica with first and second order consumption in unstirred and stirred batch precipitation showing adverse effect of stirring on polymerization rate ($\Delta C^{Si}/\Delta t$) after reaching 50% of conversion and resulting in longer removal time. Time to remove 90% of silica (T_{90}) from the leachate solutions were 27 and 40 h for unstirred and stirred case respectively.

was required in case of unstirred solution. This effect is attributed to either fragmentation of silica gel or hindrance in particle growth due to continuous stirring. In this study, unstirred conditions assist in quick removal of silica from the solution in comparison to the stirred case. However, further investigation is required on the impacts of continuous stirring and stirring only in initial kinetic regimes in the context of silica removal at various mixing rates in highly acidic conditions.

3.6. Comparison of silica removal rate induced by operational parameters

A brief comparison of instantaneous silica polymerization rates induced by H^+, Cl^- and temperature is shown in Fig. 6. In this study, using one variable at a time (OVAT) method, high concentration of HCl matrix and high temperature are established as important factors that promote silica removal via Si-gelation and precipitation. This study shows that 8 M HCl leachates at 20 °C and 5 M HCl leachates at 60 °C prompt 99% of silica removal in 5 h; concentrations of their analytes before and after Si-removal are listed in Table 4.

Based on the volume of leachate recovered after Si-gelation, the fraction of analytes retained in the gel is estimated with equation;

$$(\%) = (1 - v_f(C_f/C_i)) \times 100 \quad (6)$$

where C_i, C_f are initial and final concentrations of analytes and v_f is the fraction of leachate volume recovered after Si-gel separation. The major difference appears in terms of recovered leachate volume; 75 and 87% of leachate volume were recovered for leachate obtained with 5 M HCl aged at 60 °C and 8 M HCl aged at 20 °C. This difference in the recovered volume is linked with a larger gel volume at higher temperature. The large gel volume is due to a stiffer, stronger gel network (Quarch and Kind, 2010) and lower tendency of gel shrinkage at higher temperatures for acid-catalyzed polymerization (Wilhelm and Kind, 2015a). In addition, macroscopic silica particles were not visible in gel at the higher temperature. Due to larger gel volume, more analytes are retained in the gel.

3.7. Morphology of silica gels

The formation of particulate silica gel in an 8 M HCl matrix over time is shown in Fig. 7(a-b). The development of macroscopic silica particulates can also be noticed in an HCl leachate solution, as depicted in Fig. 7(c). On the contrary, under similar conditions macroscopic silica particles were not observed in HNO_3 leachate solutions. An SEM analysis of oven-dried silica gel reveals various structures of primary

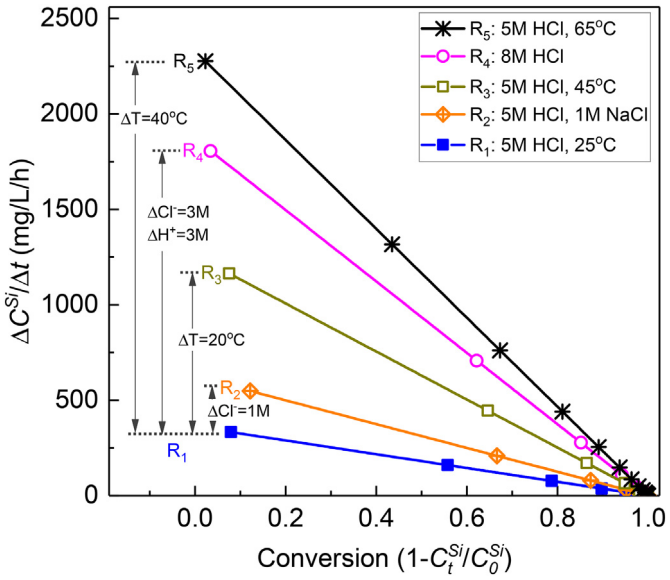

Fig. 6. Comparison of H^+, Cl^- and temperature induced silica removal rate ($\Delta C^{Si}/\Delta t$) as a function of normalized silica conversion.

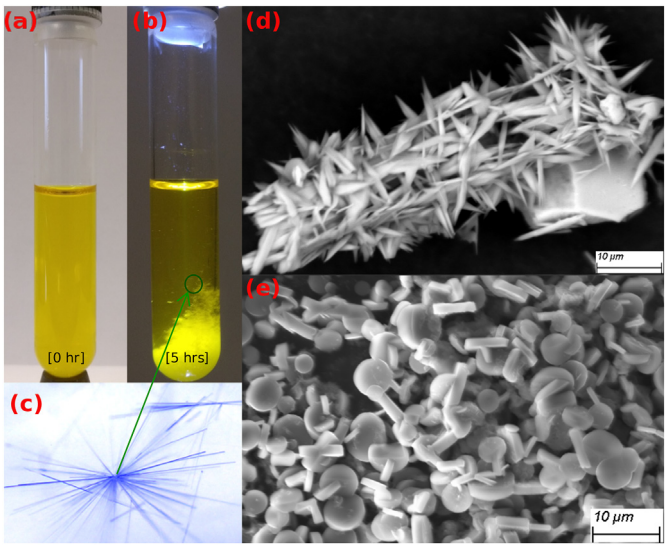

Fig. 7. Course of silica gel formation in HCl leachate solution at 0 h (a), 5 h (b), macro image of silica hydrogel (c) and SEM images of dry silica gel particles formed in HCl matrix (d), and HNO_3 matrix (e).

Table 4
Initial and final (after 5 h of aging) concentration of major and trace elements for 8 M HCl leachate at 20 °C and 5 M HCl leachate at 60 °C.

Element	8 M HCl leachate, 20 °C			5 M HCl leachate, 60 °C		
	Initial (t = 0)	Final (t = 5 h)	Retained in Si-gel	Initial (t = 0)	Final (t = 5 h)	Retained in Si-gel
	(mg/L)		(%)⊗	(mg/L)		(%)
P	1450	1490	10.6	1522	1509	25.6
Si	1950	21	99.1	2435	8	99.8
Al	1320	1340	11.7	1355	1377	23.8
Fe	1095	1110	11.8	1038	1058	23.5
Mg	2150	2180	11.8	2453	2482	24.1
Ca	17,700	17,400	14.5	16,191	16,188	25.0
Zn	227	226	13.4	195	198	23.8
Cu	7.6	7.4	15.3	7.1	7	26.1
Cr	3.4	3.3	15.6	2.9	2.95	23.7
Pb	3.1	3.2	10.2	2.6	2.8	19.2
Ni	2.5	2.3	20.0	2.3	2.4	21.7
As	1.1	0.7	44.6	1	0.8	40.0
Cd	1	1	13.0	0.9	1	16.7

silica particles that seems to be dependent on acid matrix. Gels derived from HCl leachate exhibit pointed rod-shaped particulates (Fig. 7(d)) that consist of 3.2–5.77 w_{dry}% of Si (determined with ICP-OES and Bruker Quantax 400 EDS) and Cl up to 21% (determined with Bruker Quantax 400 EDS). On the other hand, gels from HNO_3 leachate solution show both spherical and rod-shaped particulates (Fig. 7(e)) up to 10 µm size and Si concentration of 2–3.8 w_{dry}%. Minor amounts of Ca, Mg, K, and S were also present. In depth characterization of Si-gels were not performed, since the primary scope of this study was to remove silica from the solution. However, purification, characterization and utilization of silica gels and particles obtained is scheduled for future investigation.

4. Conclusion

The aim of this work was to remove silica from CFB-derived fly ash leachate solution with lower chemical and energy demand. This is achieved from a higher molar concentration of acid during leaching process followed by aging of leachate solution. HCl was more suitable due to its higher phosphorus leaching and silica removal efficiency in comparison with HNO_3. The kinetics date demonstrate that the silica removal rate in acid leachate is dependent on the acid concentration and temperature. The reaction rate increases significantly as acid concentration increases from 2 M to 8 M. Aging of 8 M HCl leachate for 5 h reduced the dissolved silica concentration by > 98%. Moreover, an increase in temperature from 20 to 60 °C in 5 M HCl leachate solution decreased the aging time from 48 to 5 h and also facilitated the removal of 98% of dissolved silica.

Risks imposed by silica scaling on operational equipment and co-precipitation of colloidal silica during phosphorus precipitation are minimized in silicon-free leachate solutions. Future work will be focused on the selective precipitation of phosphorus from Si-free leachate solution.

5. Acknowledgements

The author wishes to thank the Alholmens Kraft heat and power plant for providing fly ash samples.

References

Bai, S., Naren, G., Nakano, M., Okaue, Y., Yokoyama, T., 2014. Effect of polysilicic acid on the precipitation of calcium carbonate. Colloids Surf. A 445 (Supplement C), 54–58.
Bałdyga, J., Jasińska, M., Jodko, K., Petelski, P., 2012. Precipitation of amorphous colloidal silica from aqueous solutions—aggregation problem. Chem. Eng. Sci. 77 (Supplement C), 207–216.
Bishop, A.D., Bear, J.L., 1972. The thermodynamics and kinetics of the polymerization of silicic acid in dilute aqueous solution. Thermochim. Acta 3 (5), 399–409.
Brinker, C., 1988. Hydrolysis and condensation of silicates: Effects on structure. J. Non-Cryst. Solids 100 (1), 31–50.
Budhathoki, R., Väisänen, A., 2016. Particle size based recovery of phosphorus from combined peat and wood fly ash for forest fertilization. Fuel Process. Technol. 146, 85–89. http://dx.doi.org/10.1016/j. fuproc.2016.02.016.
Chan, S., 1989. A review on solubility and polymerization of silica. Geothermics 18 (1), 49–56.
Chuang, S., Chang, T., Ouyang, C., Leu, J., 2007. Colloidal silica removal in coagulation processes for wastewater reuse in a high-tech industrial park. Water Sci. Technol. 55 (1–2), 187–195.
Cob, S.S., Yeme, C., Hofs, B., Cornelissen, E., Vries, D., Güner, F.G., Witkamp, G., 2015. Towards zero liquid discharge in the presence of silica: Stable 98 nanofiltration and reverse osmosis. Sep. Purif. Technol. 140, 23–31.
Donatello, S., Tong, D., Cheeseman, C., 2010. Production of technical grade phosphoric acid from incinerator sewage sludge ash (issa). Waste Manag. 30 (8), 1634–1642.
Dyer, L.G., Richmond, W.R., Fawell, P.D., 2012. Simulation of iron oxide/silica precipitation in the paragoethite process for the removal of iron from acidic zinc leach solutions. Hydrometallurgy 119 (Supplement C), 47–54. http://dx.doi.org/10.1016/j.hydromet.2012.02.017.
Elmer, T.H., Nordberg, M.E., 1958. Solubility of silica in nitric acid solutions. J. Am.

Ceram. Soc. 41 (12), 517–520.
Franz, M., 2008. Phosphate fertilizer from sewage sludge ash (ssa). Waste Manag. 28 (10), 1809–1818.
Gallup, D.L., Sugiaman, F., Capuno, V., Manceau, A., 2003. Laboratory investigation of silica removal from geothermal brines to control silica scaling and produce usable silicates. Appl. Geochem. 18 (10), 1597–1612.
Gorrepati, E.A., Wongthahan, P., Raha, S., Fogler, H.S., 2010. Silica precipitation in acidic solutions: mechanism, pH effect, and salt effect. Langmuir 26 (13), 10467–10474. http://dx.doi.org/10.1021/la904685x.
Hermosilla, D., Ordóñez, R., Blanco, L., de la Fuente, E., 2012. Blanco, ph and particle structure effects on silica removal by coagulation. Chem. Eng. Technol. 35 (9), 1632–1640. http://dx.doi.org/10.1002/ceat. 201100527. URL. https://doi.org/10.1002/ceat.201100527.
Hurd, C.B., 1935. Studies on silicic acid gels. VI. Influence of temperature and acid upon the time of set. J. Phys. Chem. 40 (1), 21–26.
Hurd, C.B., Barclay, R.W., 1940. Studies on silicic acid gels. X. The time of set of gel mixtures containing high concentrations of mineral acids. J. Phys. Chem. 44 (7), 847–851.
Iler, R.K., 1980. Isolation and characterization of particle nuclei during the polymerization of silicic acid to colloidal silica. J. Colloid Interface Sci. 75 (1), 138–148. http://dx.doi.org/10.1016/0021-9797(80) 90357-4.
Jin, Y.-s., Jiang, T., Yang, Y.-b., Li, Q., Li, G.-h., Guo, Y.-f., 2006. Removal of phosphorus from iron ores by chemical leaching. J. Cent. S. Univ. Technol. 13 (6), 673–677.
Johansson, L.S., Leckner, B., Tullin, C., Åmand, L.E., Davidsson, K., 2008. Properties of particles in the fly ash of a biofuel-fired circulating fluidized bed (CFB) boiler. Energy Fuels 22 (5), 3005–3015. http://dx.doi.org/10.1021/ef800266c.
Kaikake, K., Sekito, T., Dote, Y., 2009. Phosphate recovery from phosphorus-rich solution obtained from chicken manure incineration ash. Waste Manag. 29 (3), 1084–1088. http://dx.doi.org/10.1016/ j.wasman.2008.09.008.
Kalmykova, Y., Fedje, K.K., 2013. Phosphorus recovery from municipal solid waste incineration fly ash. Waste Manag. 33 (6), 1403–1410. http://dx.doi.org/10.1016/j.wasman.2013.01.040.
Lee, M., Kim, D.-J., 2017. Identification of phosphorus forms in sewage sludge ash during acid pre-treatment for phosphorus recovery by chemical fractionation and spectroscopy. J. Ind. Eng. Chem. 51 (Suppl. C), 64–70.
Lenher, V., Merrill, H.B., 1917. The solubility of silica. J. Am. Chem. Soc. 39 (12), 2630–2638.
Liu, Y., Tourbin, M., Lachaize, S., Guiraud, P., 2012. Silica nanoparticle separation from water by aggregation with alcl3. Ind. Eng. Chem. Res. 51 (4), 1853–1863.
Makrides, A.C., Turner, M., Slaughter, J., 1980. Condensation of silica from supersaturated silicic acid solutions. J. Colloid Interf. Sci. 73 (2), 345–367.
Meoto, S., Kent, N., Nigra, M.M., Coppens, M.-O., 2017. Effect of stirring rate on the morphology of fdu-12 mesoporous silica particles. Microporous Mesoporous Mater. 249, 61–66.
Noguera, C., Fritz, B., Clément, A., 2015. Precipitation mechanism of amorphous silica nanoparticles: A simulation approach. J. Colloid Interf. Sci. 448, 553–563.
Pettersson, A., Åmand, L.-E., Steenari, B.-M., 2008. Leaching of ashes from co-combustion of sewage sludge and wood—part i: Recovery of phosphorus. Biomass Bioenergy 32 (3), 224–235. http://dx.doi.org/10.1016/j.biombioe.2007.09.016.
Potapov, V.V., Serdan, A.A., Kashpura, V.N., Gorbach, V.A., 2007. Polycondensation kinetics of orthosilicic acid in a hydrothermal solution. Russ. J. Phys. Chem. A 81 (10), 1698–1702. http://dx.doi.org/10.1134/S0036024407100287.
Quarch, K., Kind, M., 2010. Inorganic precipitated silica gel. Part 1: Gelation kinetics and gel properties. Chem. Eng. Technol. 33 (6), 1034–1039.
Quarch, K., Durand, E., Kind, M., 2010. Inorganic precipitated silica gel. Part 2: Fragmentation by mechanical energy. Chem. Eng. Technol. 33 (7), 1208–1212.
Rothbaum, H., Rohde, A., 1979. Kinetics of silica polymerization and deposition from dilute solutions between 5 and 180°c. J. Colloid Interface Sci. 71 (3), 533–559. http://dx.doi.org/10.1016/0021-9797(79)90328-X.
Sasan, K., Brady, P.V., Krumhansl, J.L., Nenoff, T.M., 2017a. Exceptional selectivity for dissolved silicas in industrial waters using mixed oxides. J. Water Process Eng. 20, 187–192.
Sasan, K., Brady, P.V., Krumhansl, J.L., Nenoff, T.M., 2017b. Removal of dissolved silica from industrial waters using inorganic ion exchangers. J. Water Process Eng. 17, 117–123.
Skrifvars, B.-J., Sfiris, G., Backman, R., Widegren-Dafgård, K., Hupa, M., 1997. Ash behavior in a CFB boiler during combustion of Salix. Energy Fuels 11 (4), 843–848. http://dx.doi.org/10.1021/ef960208z.
Thy, P., Jenkins, B., Grundvig, S., Shiraki, R., Lesher, C., 2006. High temperature elemental losses and mineralogical changes in common biomass ashes. Fuel 85 (5), 783–795.
Thy, P., Yu, C., Jenkins, B.M., Lesher, C.E., 2013. Inorganic composition and environmental impact of biomass feedstock. Energy Fuel 27 (7), 3969–3987.
Valmari, T., Lind, T.M., Kauppinen, E.I., Sfiris, G., Nilsson, K., Maenhaut, W., 1999. Field study on ash behavior during circulating fluidized-bed combustion of biomass. 1. Ash formation. Energy Fuels 13 (2), 379–389. http://dx.doi.org/10.1021/ef980085d.
Weres, O., Yee, A., Tsao, L., 1981. Kinetics of silica polymerization. J. Colloid Interface Sci. 84 (2), 379–402. http://dx.doi.org/10.1016/ 0021-9797(81)90230-7.
Wilhelm, S., Kind, M., 2015a. Influence of pH, temperature and sample size on natural and enforced syneresis of precipitated silica. Polymers 7 (12), 2504–2521. http://dx.doi.org/10.3390/polym7121528.
Wilhelm, S., Kind, M., 2015b. Gelation, Fragmentation and Reorganization of Precipitated Silica. Springer International Publishing, pp. 175–204.
Xiao, X., Yang, H., Zhang, H., Lu, J., Yue, G., 2005. Research on carbon content in fly ash from circulating fluidized bed boilers. Energy Fuel 19 (4), 1520–1525. http://dx.doi.org/10.1021/ef049678g.
Zarrouk, S.J., Woodhurst, B.C., Morris, C., 2014. Silica Scaling in Geothermal Heat Exchangers and Its Impact on Pressure Drop and Performance: Wairakei Binary Plant. vol. 51. pp. 445–459. http://dx.doi.org/10.1016/j.geothermics.2014.03.005. (New zealand, Geothermics). http://www.sciencedirect.com/science/article/pii/S0375650514000297.

Paper III

SELECTIVE RECOVERY OF PHOSPHORUS AS $AlPO_4$ FROM SILICON-FREE CFB-DERIVED FLY ASH LEACHATE

by
Roshan Budhathoki
Ari Väisänen
Manu Lahtinen

Hydrometallurgy
178 (2018)
30-36

Hydrometallurgy 178 (2018) 30–36

Contents lists available at ScienceDirect

Hydrometallurgy

journal homepage: www.elsevier.com/locate/hydromet

Selective recovery of phosphorus as $AlPO_4$ from silicon-free CFB-derived fly ash leachate

Roshan Budhathoki*, Ari Väisänen, Manu Lahtinen

Department of Chemistry, Renewable Natural Resources and Chemistry of Living Environment, University of Jyväskylä, P.O. Box 35, FI-40014 Jyväskylä, Finland

ARTICLE INFO

Keywords:
Phosphorus recovery
Fly ash utilization
$AlPO_4$ precipitation
Fe-EDTA chelation

ABSTRACT

The prospect of phosphorus (P) recovery from siliceous fly ash was investigated. The phosphorus content in the pristine fly ash was 1.21%. Obtaining pure phosphorus products from fly ash is very challenging because of high concentration of other elements, silicon (Si) at 17.3% being the major contaminant. The fly ash was fractionated with sieve size of 125 μm to concentrate the phosphorus in the small-size fraction, which also facilitated the removal of 78% of silica (Si) in the solid phase. The fractionated fly ash was treated with 8 M HCl in order to remove 98% of Si by aging (5 h) of leachate until precipitation of Si-gel, and a phosphorus-rich solution is obtained. Iron (Fe) is also considered an impurity in the recovered P-product and its co-precipitation is prevented by the use of EDTA as Fe-masking reagent at [EDTA]/[Fe] ratio of 1. About 70% of Fe is retained in the solution during recovery of phosphorus with aluminum at pH 4. Amorphous white solid was recovered containing 18.08% P, this is 15 times high than that in the pristine fly ash used as raw material in this recovery process.

1. Introduction

Phosphorus (P) is an irreplaceable essential element for crop growth and food production. Modern agricultural practice requires a steady supply of chemical fertilizer containing phosphorus. Apatite mineral is the main raw material used in manufacturing P-fertilizer, this is depleting and about 100 years of economical mining is estimated to remain (Steen, 1998; Pettersson et al., 2008a). As a sustainable supply of affordable phosphorus is at risk, immediate measures are required to reduce our use of non-renewable phosphate rock by being more efficient in the use of phosphorus and recycling of P-rich wastes (Cooper et al., 2011; Mayer et al., 2016). Inorganic ash residues from the combustion of various fuels are being considered as resources for phosphorus recycling. P recovery using chemical extraction from sewage sludge ash (Levlin and Stark, 2004; Hong et al., 2005; Biswas et al., 2009; Donatello et al., 2010; Adam et al., 2009; Sturm et al., 2010; Zimmermann and Dott, 2009), municipal solid-waste incineration fly ash (Kalmykova and Fedje, 2013), chicken manure incineration ash (Kaikake et al., 2009), and fractionation from biomass fly ash (Budhathoki and Väisänen, 2016) show great potential towards mitigating the threat of a phosphorus-supply crisis.

In recent years, recovery methods for phosphorus from solid ash materials have been extensively studied. Some methods involve release of P to liquid phase by various means, such as supercritical water oxidation (Levlin et al., 2007) and acid extraction followed by precipitation (Levlin and Stark, 2004; Kalmykova and Fedje, 2013; Kaikake et al., 2009), liquid-liquid/solvent extraction (Hong et al., 2005; Donatello et al., 2010) and adsorption (Biswas et al., 2009) based recovery, while other methods include P-recovery via thermo-chemical (Adam et al., 2009), electro-kinetic (Sturm et al., 2010), and bio-leaching and accumulation (Zimmermann and Dott, 2009). Feasibility of the extraction procedures and the purity of P-products greatly depend on concentration of phosphorus and other major elements, such as iron (Fe), aluminum (Al), calcium (Ca), and silicon (Si) in the leachate solution (Kalmykova and Fedje, 2013; Tan and Lagerkvist, 2011). Previous precipitation-based attempts of P recovery from fly ash leachate solutions were focused on precipitation of phosphorus with calcium due to the higher solubility of Ca—P solids in water than that of Al/Fe-P solids, and their potential usability as chemical fertilizers. In addition, these studies demonstrated a two step precipitation method involving removal of Fe impurities at pH 3, and recovery of P at pH 4; and a loss of phosphorus of up to 27% has been reported (Levlin and Stark, 2004; Kalmykova and Fedje, 2013; Kaikake et al., 2009). The fraction of P in the precipitate is highly affected by the pH and stoichiometric concentrations of Fe, Al, Ca, and Si, because phosphorus could potentially precipitate as $FePO_4$ at pH 1–3 (Al-Sogair et al., 2002), $AlPO_4$ at pH 3–5 (Zhao et al., 2013), and $Ca_5(PO_4)_3OH$ at pH > 4 (Kaikake et al., 2009). Due to lack of commercial value as a raw material for the phosphate industry and its low solubility, iron phosphate is less favoured for P recovery from secondary resources

* Corresponding author.
E-mail address: roshan.budhathoki@jyu.fi (R. Budhathoki).

https://doi.org/10.1016/j.hydromet.2018.03.025
Received 2 January 2018; Received in revised form 19 March 2018; Accepted 31 March 2018
Available online 06 April 2018
0304-386X/

(Levlin et al., 2007). Besides precipitation based removal of iron from the solution at lower pH; which is associated with a significant loss of P, Fe can be retained in the solution above pH 3 by adding certain chelating agents which react with Fe to form stable iron chelates (Harris, 1964), thus allowing precipitation of P with either Al or Ca.

This paper describes the procedure and results of P recovery in single precipitation step by retaining Fe in solution via EDTA chelation from the Si-free leachate solution obtained in our previous study (Budhathoki and Väisänen, 2018). pH values for precipitation and EDTA concentration have been optimized, and the obtained phosphorus products have been characterized and their usability is discussed.

2. Experimental

2.1. Materials

A fly ash (FA) sample originated from wood based biomass as fuel for combustion process was provided by Alholmens Kraft Oy. A RETSCH sieve shaker (AS200 basic) was employed for dry sieving with sieve size of 125 μm for 30 min. 100 g of FA was taken for screening. Then the fractionated FA (FFA) of particle size lower than 125 μm was used for acid leaching, while the other fraction was discarded. 0.25 g of each solid ash sample was dissolved in 3 mL of aqua regia with 3–4 drops of hydrofluoric acid. The digestion was further assisted by ultrasound for 18 min at 60 °C. Elmasonic P (70H) from Elma Schmidbauer GmbH was employed as ultrasonic source. The samples were shaken in between to release the evolved gas. This acid-digested solution was further diluted to 100 mL for element composition determination. Hydrochloric acid (≥37% HCl) from Honeywell-Fluka, nitric acid (≥65% HNO_3) and disodium ethylenediaminetetraacetic acid (EDTA) from Sigma-Aldrich, and sodium hydroxide (NaOH) from VWR chemicals, all of analytical grade, were used in the experiments.

2.2. Preparation of Si-free leachate solution

20 g of FFA was leached in 240 mL (LS ratio of 12) of 8 M hydrochloric acid solution. The leaching experiment was assisted with mechanical stirring and ultrasonic digestion for 20 min. The leachate solution was transferred to centrifuge tube and centrifuged (at 3500 rpm) for 15 min to separate the solid residue. Then the leachate solution was left for 5 h to precipitate the silicon as silica-gel which was removed from the leachate solution by centrifugation. Details of Si-gel formation mechanism and kinetics are presented in our previous study (Budhathoki and Väisänen, 2018).

2.3. Identification of P recovery parameters

The composition of fly ash is important in the development of phosphorus extraction. The wet chemical extraction of P-products is based on the solubility of its salts as a function of pH (Stumm and Morgan, 1996). Hence, only pH and the ratio of EDTA concentration to iron and aluminum concentration (ER = [EDTA]/[Fe + Al]) are selected as important parameters for P recovery in this study. The precipitation-based recovery of P was conducted at room temperature.

2.4. Experimental method

Response surface method (RSM), a combination of mathematical and statistical techniques (Leardi, 2009), was used to study the effects of pH and ER. Orthogonal central composite design (CCD) consisting of total 12 runs including 4 repeats on the center points was created and analyzed using RcmdrPlugin.DoE plug-in (version 0.12-3) (Fox, 2005; Groemping, 2014) in an R software environment (R Core Team, 2017). 10 mL of Si-free leachate solution was taken and the required weight of EDTA was added to maintain the ER value with an accuracy of ± 0.01. These solutions were titrated with freshly prepared 3 M NaOH to achieve the targeted pH with an accuracy of ± 0.1. The analyte concentration was determined only from the supernatant. Table S1 shows the operating parameters for the experimental runs. Using least-square regression from the software, optimum conditions for total recovery of phosphorus were then identified.

2.5. Recovery experiment

An additional study was conducted to analyze the effect of pH on the purity of precipitated P-products at optimal ER values. For this study, 20 mL of Si-free leachate solution was titrated with 3 M NaOH to adjust the pH between 3 and 5; three replicates were used in the experiment. The titrated solutions were left to stand for several hours. The solution was then filtered (with Whatman No. 41 filter paper) and washed 5 times with ultrapure water. The precipitant was oven dried at 60 °C and samples were recovered directly from filter paper for characterization.

2.6. Analysis of leachate solution

Speciation of the solution phase was done with the Medusa & Hydra program (Puigdomenech, 2009). The components considered were aluminum, iron, calcium, phosphorus as $H_nPO_4^{(3-n)-}$, EDTA and chlorine. Concentrations of analytes similar to the leachate solution were used in the equilibrium calculation; the dilution effect due to NaOH addition during titration was also considered. The ionic strength of the solution is set at 1, unless otherwise stated. All the soluble and solid complexes available in the database were allowed.

2.7. Analytical methods

The concentration of analytes in the solution was determined by an inductively coupled plasma optical emission spectrometry (ICP-OES PerkinElmer Optima 8300). Titration of acid leachate solution with 3 M NaOH was conducted with TitroLine easy unit (SCHOTT Instruments GmbH). Bruker Quantax400 EDS coupled with Zeiss EVO-50XVP and Bruker Alpha Platinum-ATR were employed respectively for elemental and infrared analysis of precipitant obtained at pH 3–4.6. 250 mg of final P-product (precipitant obtained at optimal pH and ER value) was dissolved in 3 mL of aqua regia and diluted to 50 mL for determination of trace elements by ICP-OES. The aliquot was further diluted by a factor of 10 for determination of P and other elements. An X–ray powder diffraction analysis of final P-product was done with a PANalytical X'Pert Pro alpha 1 diffractometer using Johansson monochromatized Cu $K_{\alpha 1}$ radiation (λ = 1.5406; tube settings: 45 kV, 40 mA). The data were recorded from a spinning sample by X'Celerator detector in the 2θ-range of 6–80° with a step size of 0.017° and counting times of 120 s per step. The diffraction data were handled by X'Pert HighScore Plus v. 4.5 program.

3. Results and discussion

3.1. Fly ash and acid leachate characterization

The elemental composition of the pristine fly ash (FA), recovered fly ash with particle size lower than 125 μm (FFA) and discarded fraction containing particles > 125 μm are listed in Table 1. In this study, FFA is used in the context of phosphorus recovery. Most of undesired elements, including Si, Ca, Fe, Al, etc. can be removed by sieving fractionation of fly ash (Budhathoki and Väisänen, 2016). Properties of fly ash and acid leachate solutions are briefly presented and discussed in our earlier study (Budhathoki and Väisänen, 2018), which summarizes that P concentration increases by a factor of 1.38 and Si decreases by a factor of 3.8 during the fly ash fractionation at sieve size of 125 μm. In addition, leaching of fly ash with 8 M HCl acid removes of 98% of silica as silica gel in 5 h. The obtained Si-free leachate solution is used in this

Table 1
Elemental composition and heavy metal content of FA (pristine fly ash), FFA (recovered fly ash with particle size lower than 125 μm) and DFA (discarded fraction of FA containing particles > 125 μm) measured by ICP-OES after extracting with aqua regia and 3–4 drops of HF.

Element	Major elements (%)						Trace elements (mg/kg)						
	P	Al	Fe	Si	Mg	Ca	Zn	Cu	Cr	Pb	Ni	As	Cd
FA	1.21	3.38	2.01	17.3	2.16	15.4	1704	89.6	45.1	26.3	24.6	6.7	8.6
FFA (< 125 μm)	1.67	3.11	2.03	4.54	2.83	21.7	2595	99.7	50.4	35.2	33.7	11.7	11.5
DFA (> 125 μm)	0.47	4.16	2.15	30.3	1.03	5.4	475	82.5	44.8	12.8	12.4	< LOQ	< LOQ

study for phosphorus recovery.

3.2. Phosphorus chemistry in leachate solution

Solid-ash residue may consist of phosphorus as P-oxide and phosphate of Ca, Al, Fe, and Mg metals (Beck and Unterberger, 2006; Pettersson et al., 2008b; Lee and Kim, 2017). $H_nPO_4^{(3-n)-}$ derivates of phosphate are generally assumed to predominate in the solution phase when metal phosphates and P-oxides react with acid or base (Gilmour, 2013). Furthermore, the fraction of $H_nPO_4^{(3-n)-}$ derivates is a function of pH and various salts of such phosphate derivatives may precipitate at different pH (Kalmykova and Fedje, 2013; Kaikake et al., 2009; Stumm and Morgan, 1996). Analysis of various phosphate species in acidic media with Medusa/Hydra program reveals predominance of $FePO_4$ below pH 2.5, $AlPO_4$ between pH 3–5, and $Fe_3(PO_4)_2$ and $Ca_5(PO_4)_3OH$ above pH 5 (Fig. 1). This strongly implies the possibility of P-recovery as $FePO_4$, $AlPO_4$ and $Ca_5(PO_4)_3OH$ at pH's where they predominate.

Stoichiometric concentrations of Fe, Al, and Ca and the reduction potential of the solution also play an important role in the efficient recovery of phosphorus. $Fe/P_{(mol)} \geq 1$ ($Fe/P_{(mass)} \geq 1.8$) and solutions with high reduction potential i.e., strong oxidizing conditions, are required for $FePO_4$ precipitation. However, recovery of phosphorus with iron is challenging because of akaganéite ($Fe(OH)_{1-x}Cl_x$) co-precipitation, this is a predominant species in chloride media and its solubility equilibria allows its precipitation at pH < 2 (Xiong et al., 2008; Asenath-Smith and Estroff, 2015). Fe speciation with Medusa/Hydra program in 2 M Cl^- solution also indicates the precipitation of akaganéite alongside $FePO_4$, which is shown in Fig. S1 (cf. supporting information). Furthermore, chloride concentration and reduction potential of the solution seem to have an adverse effect on $FePO_4$ formation as seen in Fig. S2. In the context of phosphorus recovery, $Fe/P_{(mol)}$ of 115 in first precipitant at pH 3 was observed by Kaikake et al., which indicates that iron phosphate was a minor component in the precipitate (Kaikake et al., 2009). Due to lack of commercial value of iron phosphate, lower value of Fe/P molar ratio (0.42 in the leachate solution) and tendency of akaganéite co-precipitation, phosphorus recovery with iron is not explored in this study. Instead, the prevention of the precipitation of iron from the solution with Fe-EDTA chelation and recovery of phosphorus with either aluminum or calcium is studied. Use of such a masking reagent is beneficial and economical in comparison to a two-step precipitation, since the earlier method avoids the use of a separate reactor during the recovery process.

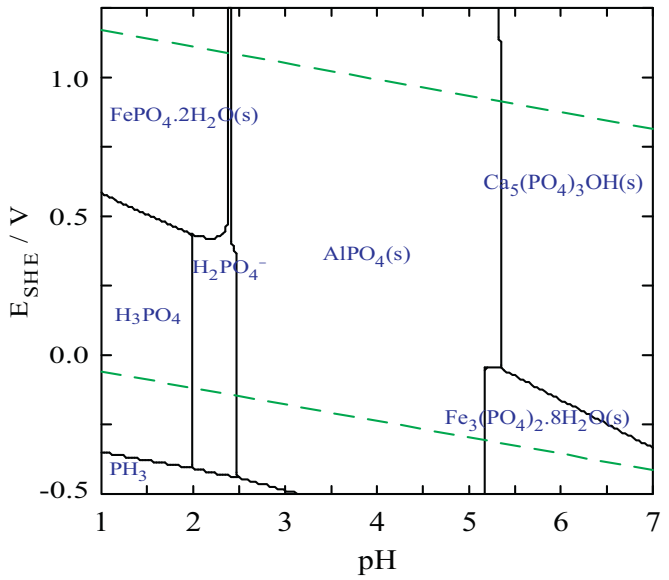

Fig. 1. Eh-pH diagram representing predominant phosphorus species in solution phase. Equilibrium calculations with 24 mM of [PO_4] and PO_4:Fe:Al:Ca = 1:1:1:10 (molar fraction) were made using the Medusa/Hydra program. Area between the dashed green line (- - -) represents the stability region of water.

3.3. Effect of pH and EDTA on phosphorus recovery

The interference of unwanted metals in the solution can be masked by ethylenediaminetetraacetic acid (EDTA). EDTA as a chelating agent in recovery processes has been used in struvite precipitation by Ca-masking (Zhang et al., 2010) and Ni recovery by Fe-masking (Pinto et al., 2015). Thus, excessive contamination of the recovered P-products is prevented by a careful control of EDTA concentration and pH of the solution. The dependence of phosphorus recovery on pH and efficacy of Fe chelation with EDTA were tested using response surface methodology. A central composite design consisting of 12 runs was created and the experiments were run on the sequential order as provided by the program (RcmdrPlugin.DoE plug-in in R environment). The operational value and experimental recovery values of P, Al, Fe, and Ca are presented in Table S2. A pH domain between 3.8 and 5.2 was evaluated to identify the optimum range for efficient phosphorus recovery. Meanwhile, the ratio of EDTA and sum of Fe and Al concentrations (ER = [EDTA]/[Fe + Al]) was varied between 0.29 and 1.71 to test the feasibility of phosphorus precipitation with aluminum or calcium. The concentration of EDTA is equal to that of Fe (i.e. [EDTA] = [Fe]) at an ER value of 0.29. Therefore, ER value of 0.29 is selected as minimum operating value for this study where complete chelation of Fe by EDTA is assumed, based on stoichiometric equilibria. An [EDTA]/[Fe] value of 1 was also used in the recovery of Ni by chelation of Fe with EDTA (Pinto et al., 2015). Higher ER values were also investigated in order to explore the feasibility of phosphorus precipitation with calcium because there is stoichiometric equilibrium between EDTA and the sum of Fe and Al concentration at an ER value of 1, which suggests chelation of both Fe and Al.

The predicted response surfaces for the recovery of phosphorus, aluminum and iron are presented in Fig. 2, while the predicted coefficients values for the quadratic model are summarized in Table S3. Multiple R^2 values of 0.966, 0.981, and 0.866 were obtained respectively for P, Al, and Fe response models and the fit based on the summary of least-square regression is depicted in Table S4. In addition, Fig. S3 also suggest lack of outliers within the experiment domain. Therefore, the reliability of predicted response surface within the experiment domain is validated with the help of regression parameters and the error in model prediction increases in the order of Al < P < Fe model. A lower ER value of 0.3 and pH range of 4–5 yield the highest

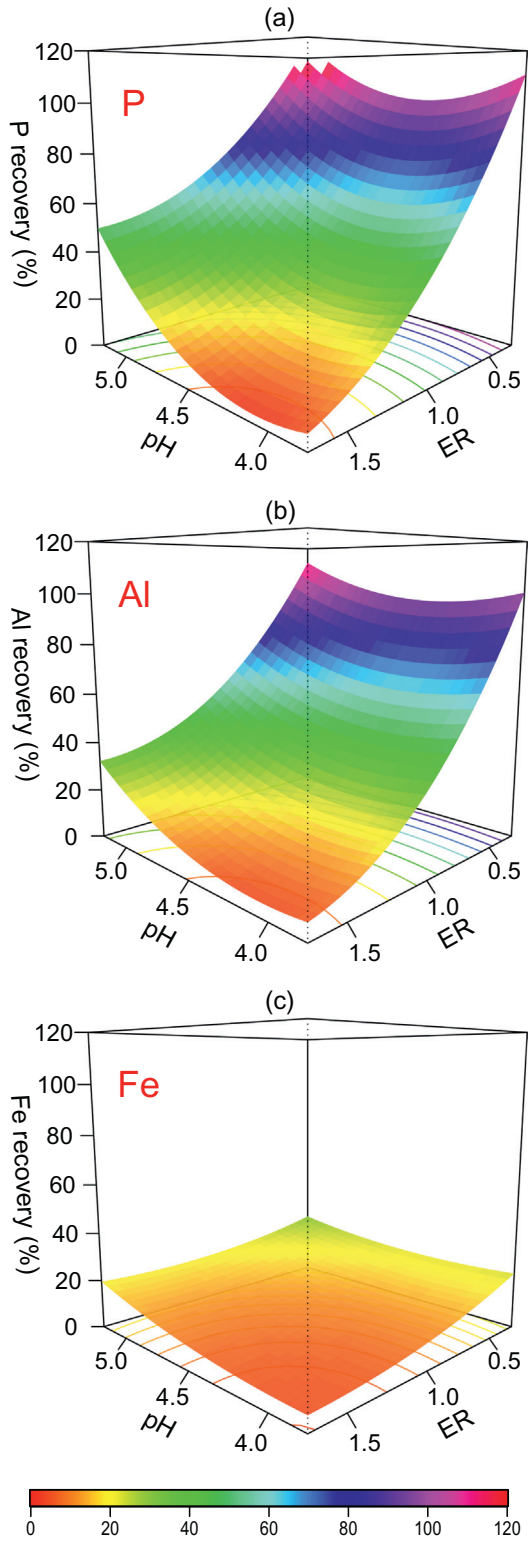

Fig. 2. Response surface for the recovery of phosphorus (a), aluminum (b), and iron (c) as a function of pH and ER (= [EDTA]/[Fe + Al]) based on central composite design (CCD). ER of 0.29 indicates stoichiometric equilibrium between EDTA and Fe i.e. [EDTA]/[Fe] = 1.

phosphorus recovery, the patterns of P and Al recoveries were similar which is expected due to $AlPO_4$ precipitation. When pH is increased from 3.8 to 5.2, more iron is precipitated from the solution; the amount decreases when the ER value is increased due to the formation of stable Fe-EDTA complexes. The progression of P, Al, and Fe precipitation from the solution is also supported with equilibrium model made in Medusa/Hydra program as portrayed in Fig. 3, which shows that the selectivity of EDTA in the experiment domain decreases in the order of Fe > Al > Ca. This indicates that higher EDTA concentrations also form stable EDTA chelates with Al and Ca, thus reducing the phosphorus precipitation, as seen in Fig. 2a. These calculations also point to the predominance of $AlPO_4$ solid in precipitation, which is highest near pH 4 and decreases with increasing EDTA concentration. Therefore, the effect of pH on the purity of recovered $AlPO_4$ product was further studied at an [EDTA]/[Fe] value of 1.

3.4. The purity of phosphorus product

The concentrations of selective analytes, P, Al, Fe and Ca, were measured at various pH's and the fractions remaining in the solution are shown in Fig. 4a. This shows that phosphorus and aluminum recoveries are near 100% at pH 4, while the efficiency of Fe chelation by EDTA is 70–75% which are similar to the results obtained with the RSM model. The elemental composition of dry precipitated products reveals that solids with higher P content (> 20%) are obtained between pH 3.5 and 4, as shown in Fig. 4b. The maximum theoretical phosphorus fraction in pure dry $AlPO_4$ is 25.4%. Infrared spectra of these precipitants were compared with those of synthetic $AlPO_4$ precipitated by the titration of solution containing 0.1 M of $Al(NO_3)_3$ and H_3PO_4 with 1 M NaOH at pH 4 (Fig. 4c). The recovered products exhibit characteristic P—O stretching peaks at 1050 cm^{-1} compared to those of synthetic $AlPO_4$ at 1065 cm^{-1}. As the pH increases, shifts of the ν(P—O) bands to lower energy, in terms of cm^{-1}, are also observed, which is due to a significant decrease in the force constant for the P-O and P-OH bands with decreasing protonation (Persson et al., 1996; Burrell et al., 2000). The difference between ν(P—O) bands of precipitated and synthetic $AlPO_4$ obtained at pH 4 is due to impurities in the precipitate which weaken the P—O bonds. Based on these observations, pH value of 4 and [EDTA]/[Fe] ratio of 1 are identified as the optimal conditions for the recovery of P-products with low level of impurities.

3.5. Efficacy of proposed phosphorus recovery method

The concentration of major (P, Al, Fe, Si, & Ca) and trace (Zn, Cu, Cr, Pb, Ni, As, & Cd) elements at each step during the recovery method is summarized in Table 2. Leaching efficiency of over 100% is accounted for some analytes, which is attributed to inhomogeneity of the fly ash and errors in analytical precision. This method includes the following steps; a) fractionation of fly ash with sieve size of 125 μm, b) 8 M HCl acid leaching, c) silica removal by aging of silica gel until precipitation, and d) phosphorus recovery with aluminum by masking Fe with EDTA. This method allows efficient removal of Si as gel prior to selective precipitation of phosphorus with aluminum by masking of iron with EDTA. Fig. S4 shows the advantage of Si removal on the composition of final product, where precipitation of the leachate obtained with 2 M HCl at pH 3.5 yields a phosphorus product containing 7.9, 9.1, 6.9, and 13.1%$_{(wt.)}$ of P, Al, Fe, and Si, respectively. This signifies the importance of Si removal prior to the phosphorus recovery via precipitation.

3.6. Characterization and usage of phosphorus product

Table 3 contains the element composition of the final P-product obtained at pH of 4 and [EDTA]/[Fe] ratio of 1. The pure precipitate consists of 16.31 and 18.08% of aluminum and phosphorus, giving an Al/P ratio of 0.90, which is close to the theoretical ratio of 0.87 in synthetic $AlPO_4$. The diffuse peaks near 28–29° 2θ in the XRD pattern (Fig. 5) indicate the formation of amorphous aluminum phosphates. Similar XRD patterns were observed for the aluminum phosphate precipitated from aluminum sludge (Zhao et al., 2013) and aqueous solution of 50–100 °C (Roncal-Herrero et al., 2009). In addition, the

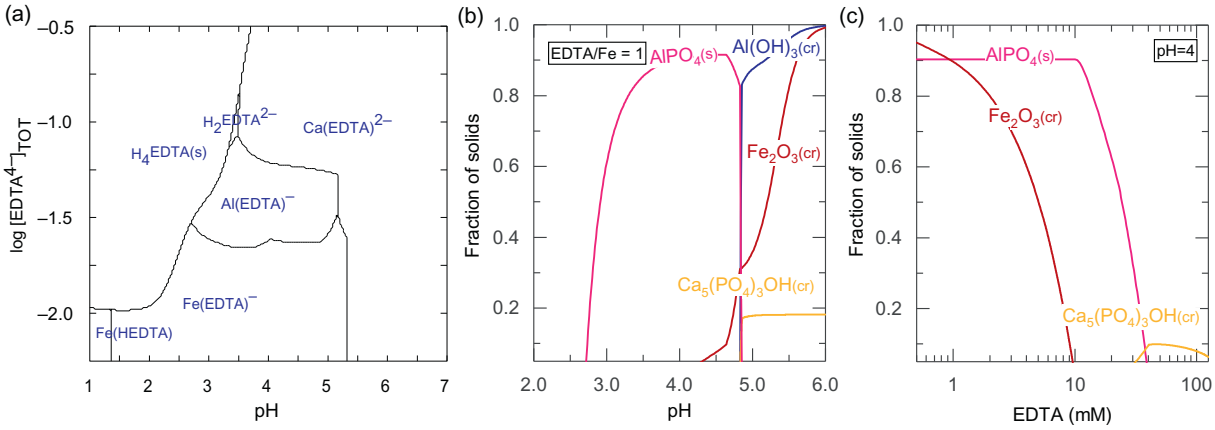

Fig. 3. Speciation of EDTA complexes as a function of pH and EDTA concentration (a), and solid species as a function of pH (b) and EDTA concentration (c) in the leachate solution using Medusa and Hydra program.

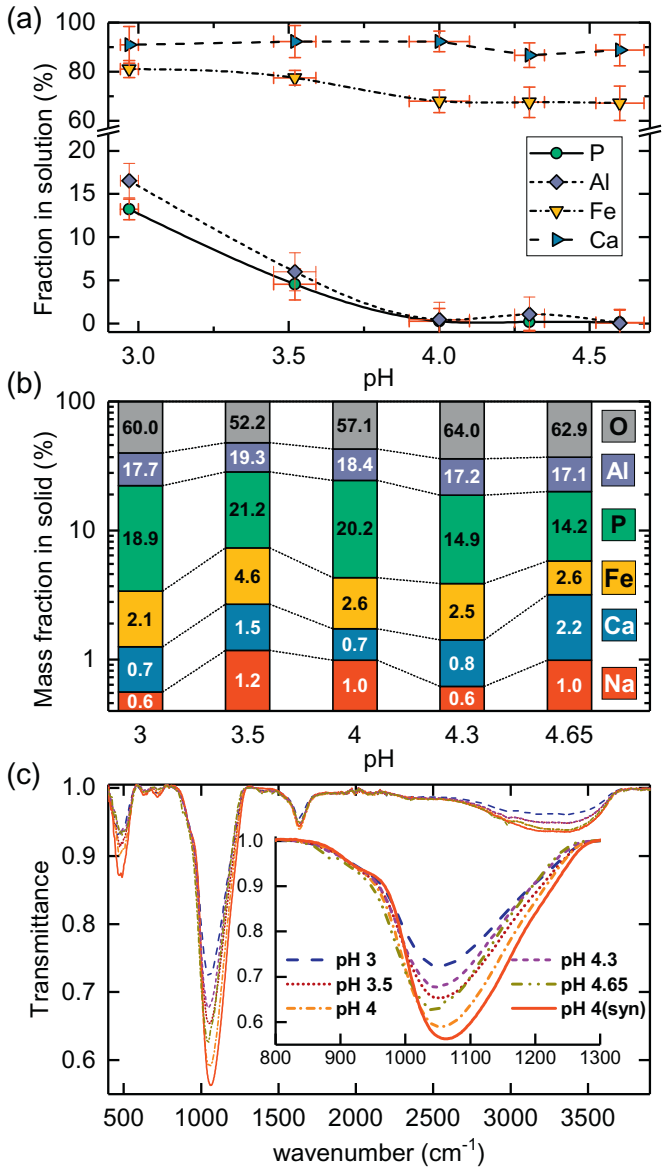

Fig. 4. Effect of pH on (a) recovery of phosphorus and other major analytes from solution, (b) fraction of P in solid precipitant, and (c) positioning of ν (P—O) bands of solids as compared to the synthetic $AlPO_4$ in IR spectrum.

infrared spectra of precipitated compounds resemble to that of synthetic aluminum phosphate (Fig. 4c). The recovered $AlPO_4$ also contains some EDTA fraction in the solid as shown by CHN values in Table 3. The major impurity in the recovered product is Fe at 2.18%, while that of other elements is < 1%. The trace metal concentrations were also determined with ICP-OES; their concentrations are lower than the maximum limit values for use as fertilizer (Nurmesniemi et al., 2012). Despite the low solubility of aluminum phosphate in water, these P-products can be used as slow P-releasing fertilizers. However, aluminum toxicity in plants may prohibit its use as fertilizer, especially in acidic soils (Roy et al., 1988). The industrial use of aluminum phosphate recovered from ash material is very limited. Therefore, either new uses of recycled aluminum phosphate and/or conversion of aluminum phosphate to more usable phosphorous compounds such as calcium and/or sodium phosphate need to be developed (Takahashi et al., 2001).

4. Conclusion

The recovery of P from highly siliceous fly ash originating from CFB-boilers with acid leaching followed by removal of Si by gelation was investigated in this study. The fly ash was treated with higher molar (8 M) concentration of hydrochloric acid to obtain a phosphorus-rich solution, despite the possibility of economical leaching with lower molar (2 M) HCl. Our previous study revealed that fly ash leaching with higher acid concentration facilitates the formation of Si-gel in a shorter time, thus allowing the removal of 98% of silica in only 5 h. The removal of silica from the solution is critical for the purity of the recovered P-product, as Si not only co-precipitates with phosphorus but also promotes co-precipitation of other metals. After removing Si from the solution, iron co-precipitation was prevented by EDTA chelation, which further increased the purity of recovered P-products. A pH value of 4 and [EDTA]/[Fe] ratio of 1 were identified as optimal conditions for phosphorus precipitation with aluminum. Besides 16.31% of Al and 18.08% of P, the recovered P-product contains of only 2.18% of Fe and 0.63% of Ca. In addition, the trace elements with hazardous character are present at low levels of concentration. The prevention of iron inclusion into the P-product by use of Fe-masking EDTA is recommended, instead of Fe removal via a two-step precipitation, since the earlier method significantly lowers the cost of recovery by eliminating the need of additional reactor and utilities.

In conclusion, the phosphorus content was significantly increased from 1.21% in pristine fly ash to 18.08% in the final product. The proposed recovery method provides a way for the recovery of high-grade phosphorous material; it may contribute to meet future phosphorus demand and sustain a continuous supply of phosphorus.

Table 2
Concentration of major and trace elements during fractionation of fly ash (FFA), acid leaching, silicon removal by Si-gel precipitation, and recovery of phosphorus via precipitation at pH 4.

Element	FFA	8 M HCl leaching (LS = 12)		Aging of Si-gel (5 h)		P-precipitation (pH = 4, [EDTA]/[Fe] = 1)		
	(< 125 μm)	Leachate	Dissolved	Supernatant	Retained in Si-gel	Filtrate		Recovery
	(mg/kg)	(mg/L)	(%)[a]	(mg/L)	(%)[b]	(mg(L)	SD	(%)
P	16,737	1452	104.1	1491	10.7	3.91	0.52	99.92
Al	31,002	1319	51.1	1337	11.8	6.07	0.66	98.52
Fe	20,365	1095	64.5	1106	12.1	230.5	11.4	31.93
Si	45,359	1950	32.3	20.95	98.5	–	–	–
Mg	28,314	2151	91.2	2176	12.0	574.7	21.9	13.71
Ca	217,524	17,720	97.8	17,370	14.7	4358	204	18.03
Zn	2595.47	226.62	104.8	225.50	13.4	50.59	0.88	26.72
Cu	99.73	7.57	91.1	7.36	15.4	1.95	0.03	13.48
Cr	50.36	3.37	80.2	3.34	13.8	0.27	0.02	73.32
Pb	35.21	3.07	104.8	3.15	10.9	0.37	0.03	61.88
Ni	33.66	2.43	86.5	2.34	16.0	0.52	0.01	27.64
As	11.71	1.06	108.7	0.74	39.1	0.17	0.03	23.98
Cd	11.54	0.99	103.1	0.98	13.6	0.25	0.01	18.00

[a] Recovery (%) = $(C^{leachate}_{mg/L}/C^{FFA}_{mg/kg}) \times LS \times 100$; where C = analytes concentration.
[b] Retained in Si-gel (%) = $(1 - v_f(C/C_0)) \times 100$; where $v_f = 0.87$ (volume fraction recovered after Si-gel removal) C_0, C are concentration before and after Si removal.

Table 3
Concentration of major and trace elements in the precipitate obtained at pH = 4 and [EDTA]/[Fe] = 1.

Major element	P	Al	Fe	Ca	Mg	C	H	N
(wt%)	18.08	16.31	2.18	0.63	0.12	1.26	3.13	0.15
Trace element	Zn	Cu	Cr	Pb	Ni	As	Cd	
(mg/kg)	1323	19.4	258	104	8.14	37.9	1.19	
	(4500)[a]	(700)	(300)	(150)	(150)	(40)	(25)	

[a] Values in () are limit values for fertilizer use (Nurmesniemi et al., 2012).

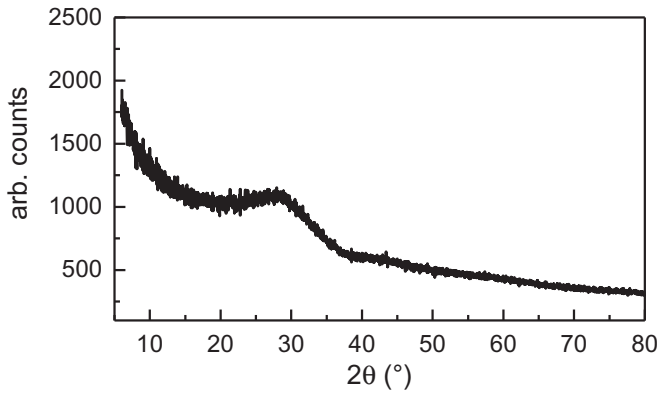

Fig. 5. X-ray diffraction pattern showing the amorphous nature of the P-product obtained at pH 4.

Acknowledgements

The author wishes to thank the Alholmens Kraft heat and power plant for providing fly ash samples.

Appendix A. Supplementary data

Supplementary data to this article can be found online at https://doi.org/10.1016/j.hydromet.2018.03.025.

References

Adam, C., Peplinski, B., Michaelis, M., Kley, G., Simon, F.-G., 2009. Thermochemical treatment of sewage sludge ashes for phosphorus recovery. Waste Manag. 29 (3), 1122–1128. http://dx.doi.org/10.1016/j.wasman.2008.09.011.

Al-Sogair, F., Marafie, H.M., Shuaib, N.M., Youngo, H.B., El-Ezaby, M.S., 2002. Interaction of phosphate with iron(iii) in acidic medium, equilibrium and kinetic studies. J. Coord. Chem. 55 (9), 1097–1109. http://dx.doi.org/10.1080/0095897021000010053.

Asenath-Smith, E., Estroff, L.A., 2015. Role of Akaganeite ($\beta-$FeOOH) in the growth of hematite ($\alpha-Fe_2O_3$) in an inorganic silica hydrogel. Cryst. Growth Des. 15 (7), 3388–3398. http://dx.doi.org/10.1021/acs.cgd.5b00475.

Beck, J., Unterberger, S., 2006. The behaviour of phosphorus in the flue gas during the combustion of high-phosphate fuels. Fuel 85 (10), 1541–1549. http://dx.doi.org/10.1016/j.fuel.2006.01.005.

Biswas, B.K., Inoue, K., Harada, H., Ohto, K., Kawakita, H., 2009. Leaching of phosphorus from incinerated sewage sludge ash by means of acid extraction followed by adsorption on orange waste gel. J. Environ. Sci. 21 (12), 1753–1760. http://dx.doi.org/10.1016/S10010742(08)62484-5.

Budhathoki, R., Väisänen, A., 2016. Particle size based recovery of phosphorus from combined peat and wood fly ash for forest fertilization. Fuel Process. Technol. 146, 85–89. http://dx.doi.org/10.1016/j.fuproc.2016.02.016.

Budhathoki, R., Väisänen, A., 2018. Removal of silicon from CFB-derived fly ash leachate in the context of phosphorus recovery. Hydrometallurgy (Under review).

Burrell, L.S., Johnston, C.T., Schulze, D., Klein, J., White, J.L., Hem, S.L., 2000. Aluminium phosphate adjuvants prepared by precipitation at constant ph. Part i: composition and structure. Vaccine 19 (2), 275–281. http://dx.doi.org/10.1016/S0264-410X(00)00160-2.

Cooper, J., Lombardi, R., Boardman, D., Carliell-Marquet, C., 2011. The future distribution and production of global phosphate rock reserves. Resour. Conserv. Recycl. 57 (Supplement C), 78–86. http://dx.doi.org/10.1016/j.resconrec.2011.09.009.

Donatello, S., Tong, D., Cheeseman, C., 2010. Production of technical grade phosphoric acid from incinerator sewage sludge ash (issa). Waste Manag. 30 (8), 1634–1642. http://dx.doi.org/10.1016/j.wasman.2010.04.009.

Fox, J., 2005. The R commander: a basic statistics graphical user interface to R. J. Stat. Softw. 14 (9), 1–42.

Gilmour, R., 2013. Phosphoric Acid: Purification, Uses, Technology, and Economics. Taylor & Francis.

Groemping, U., 2014. Rcmdrplugin.Doe: R Commander Plugin For (Industrial) Design Of Experiments, R Package Version 0.12-3.

H. Harris, Method of preventing precipitation of iron compounds from an aqueous solution, US Patent 3,150,081 (Sep. 22 1964). URL https://www.google.com/patents/US3150081.

Hong, K.-J., Tarutani, N., Shinya, Y., Kajiuchi, T., 2005. Study on the recovery of phosphorus from waste-activated sludge incinerator ash. J. Environ. Sci. Health A 40 (3), 617–631. http://dx.doi.org/10.1081/ESE-200046614.

Kaikake, K., Sekito, T., Dote, Y., 2009. Phosphate recovery from phosphorus-rich solution obtained from chicken manure incineration ash. Waste Manag. 29 (3), 1084–1088. http://dx.doi.org/10.1016/j.wasman.2008.09.008.

Kalmykova, Y., Fedje, K.K., 2013. Phosphorus recovery from municipal solid waste incineration fly ash. Waste Manag. 33 (6), 1403–1410. http://dx.doi.org/10.1016/j.wasman.2013.01.040.

Leardi, R., 2009. Experimental design in chemistry: A tutorial. Anal. Chim. Acta 652 (1), 161–172. fundamental and Applied Analytical Science. A Special Issue In Honour of Alan Townshend. https://doi.org/10.1016/j.aca.2009.06.015.

Lee, M., Kim, D.-J., 2017. Identification of phosphorus forms in sewage sludge ash during acid pre-treatment for phosphorus recovery by chemical fractionation and

spectroscopy. J. Ind. Eng. Chem. 51 (Supplement C), 64–70. http://dx.doi.org/10.1016/j.jiec.2017.02.013.
Levlin, E., Stark, K., 2004. Phosphorus recovery from sludge incineration ash and supercritical water oxidation residues with use of acids and bases. In: Proceedings of a Polish-Swedish Seminar, pp. 28.
Levlin, E., Löwén, M., Stark, K., 2007. Phosphorus recovery from sludge incineration ash and supercritical water oxidation residues with use of acid and base. Water Res. 19–28.
Mayer, B.K., Baker, L.A., Boyer, T.H., Drechsel, P., Gifford, M., Hanjra, M.A., Parameswaran, P., Stoltzfus, J., Westerhoff, P., Rittmann, B.E., 2016. Total value of phosphorus recovery. Environ. Sci. Technol. 50 (13), 6606–6620. http://dx.doi.org/10.1021/acs.est.6b01239. (pMID: 27214029).
Nurmesniemi, H., Mäkelä, M., Pöykiö, R., Manskinen, K., Dahl, O., 2012. Comparison of the forest fertilizer properties of ash fractions from two power plants of pulp and paper mills incinerating biomass-based fuels. Fuel Process. Technol. 104, 1–6.
Persson, P., Nilsson, N., Sjöberg, S., 1996. Structure and bonding of orthophosphate ions at the iron oxide–aqueous interface. J. Colloid Interface Sci. 177 (1), 263–275. http://dx.doi.org/10.1006/jcis.1996.0030.
Pettersson, A., Åmand, L.-E., Steenari, B.-M., 2008a. Leaching of ashes from co-combustion of sewage sludge and wood—part i: recovery of phosphorus. Biomass Bioenergy 32 (3), 224–235. http://dx.doi.org/10.1016/j.biombioe.2007.09.016.
Pettersson, A., Zevenhoven, M., Steenari, B.-M., Åmand, L.-E., 2008b. Application of chemical fractionation methods for characterisation of biofuels, waste derived fuels and CFB co-combustion fly ashes. Fuel 87 (15), 3183–3193. http://dx.doi.org/10.1016/j.fuel.2008.05.030.
Pinto, I.S.S., Sadeghi, S.M., Soares, H.M.V.M., 2015. Separation and recovery of nickel, as a salt, from an EDTA leachate of spent hydrodesulphurization catalyst using precipitation methods. Chem. Eng. Sci. 122, 130–137. http://dx.doi.org/10.1016/j.ces.2014.09.012.
Puigdomenech, I., 2009. MEDUSA and HYDRA: Software For Chemical Equilibrium Calculations. Dept. of Inorganic Chemistry, Royal Institute of Technology (KTH), Stockholm, Sweden.
R Core Team R, 2017. A Language and Environment for Statistical Computing. R Foundation for Statistical Computing, Vienna, Austria. https://www.R-project.org.
Roncal-Herrero, T., Rodríguez-Blanco, J.D., Benning, L.G., Oelkers, E.H., 2009. Precipitation of iron and aluminum phosphates directly from aqueous solution as a function of temperature from 50 to 200 °C. Cryst. Growth Des. 9 (12), 5197–5205. http://dx.doi.org/10.1021/cg900654m. (arXiv URL).
Roy, A.K., Sharma, A., Talukder, G., 1988. Some aspects of aluminum toxicity in plants. Bot. Rev. 54 (2), 145–178. http://dx.doi.org/10.1007/BF02858527.
Steen, I., 1998. Phosphorus availability in the 21st century: management of a non- renewable resource. Phosphorus Potassium 217, 25–31 Cl.
Stumm, W., Morgan, J., 1996. Aquatic chemistry: chemical equilibria and rates in natural waters. In: Environmental Science and Technology. Wiley.
Sturm, G., Weigand, H., Marb, C., Weiß, W., Huwe, B., 2010. Electrokinetic phosphorus recovery from packed beds of sewage sludge ash: yield and energy demand. J. Appl. Electrochem. 40 (6), 1069–1078. http://dx.doi.org/10.1007/s10800-009-0061-6.
Takahashi, M., Kato, S., Shima, H., Sarai, E., Ichioka, T., Hatyakawa, S., Miyajiri, H., 2001. Technology for recovering phosphorus from incinerated wastewater treatment sludge. Chemosphere 44 (1), 23–29. http://dx.doi.org/10.1016/S0045-6535(00)00380-5.
Tan, Z., Lagerkvist, A., 2011. Phosphorus recovery from the biomass ash: a review. Renew. Sust. Energ. Rev. 15 (8), 3588–3602. http://dx.doi.org/10.1016/j.rser.2011.05.016.
Xiong, H., Liao, Y., Zhou, L., 2008. Influence of chloride and sulfate on formation of akaganéite and schwertmannite through ferrous biooxidation by acidithiobacillus ferrooxidans cells. Environ. Sci. Technol. 42 (23), 8681–8686. http://dx.doi.org/10.1021/es801646j. (pMID: 19192781).
Zhang, T., Bowers, K.E., Harrison, J.H., Shulin, C., 2010. Releasing phosphorus from calcium for struvite fertilizer production from anaerobically digested dairy effluent. 82, 34–42.
Zhao, X.H., Zhao, Y.Q., Kearney, P., 2013. Phosphorus recovery as alpo 4 from beneficially reused aluminium sludge arising from water treatment. Environ. Technol. 34 (2), 263–268. http://dx.doi.org/10.1080/09593330.2012.692714. (pMID: 23530339).
Zimmermann, J., Dott, W., 2009. Sequenced bioleaching and bioaccumulation of phosphorus from sludge combustion – a new way of resource reclaiming. Adv. Mater. Res. 71-73, 625–628. http://dx.doi.org/10.4028/www.scientific.net/AMR.71-73.625.

Supporting Information

Selective recovery of phosphorus as $AlPO_4$ from silicon-free CFB-derived fly ash leachate

Roshan Budhathoki[a,*], Ari Väisänen[a], Manu Lahtinen[a]

[a]Department of Chemistry, University of Jyväskylä, P.O. Box 35 FI-40014 Jyväskylä, Finland, email: roshan.budhathoki@jyu.fi

Chemical speciation in leachate solution:

Speciation of iron in chloride media was made with Medusa/Hydra[1] program. Iron concentration of 24 mM and Fe:Al:PO_4:Ca ratio of 1:1:1:10 were used. All the soluble and solid complexes available in the database were included. The Eh-pH diagram (Fig. S1) indicates predominance of akaganeite even under very acidic conditions, while Fig. S2 shows the effect of chlorine concentration and reduction potential of solution on formation of akaganeite.

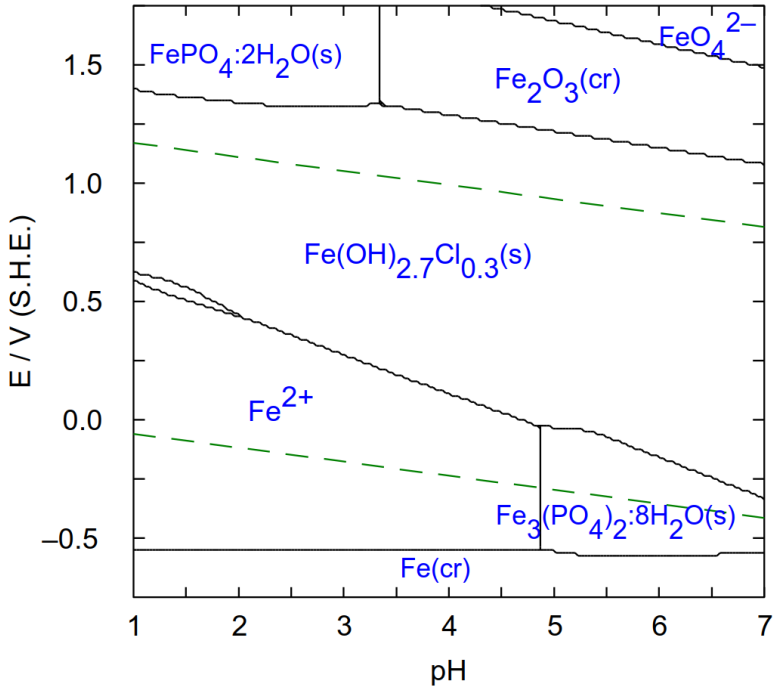

Figure S1. Predominance of iron species in leachate solution

(a)

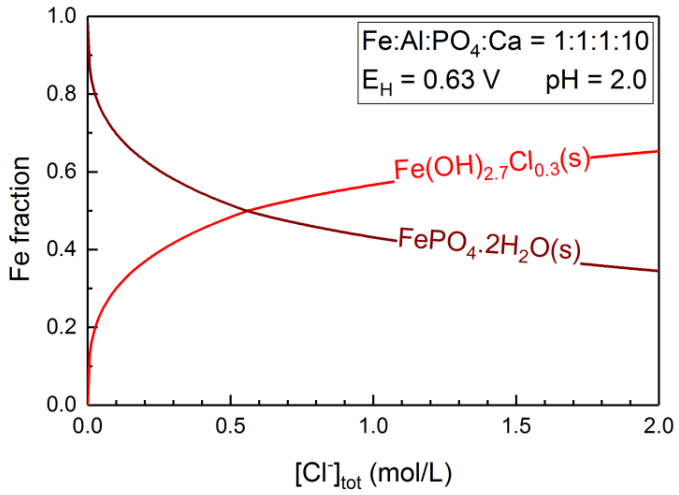

(b)

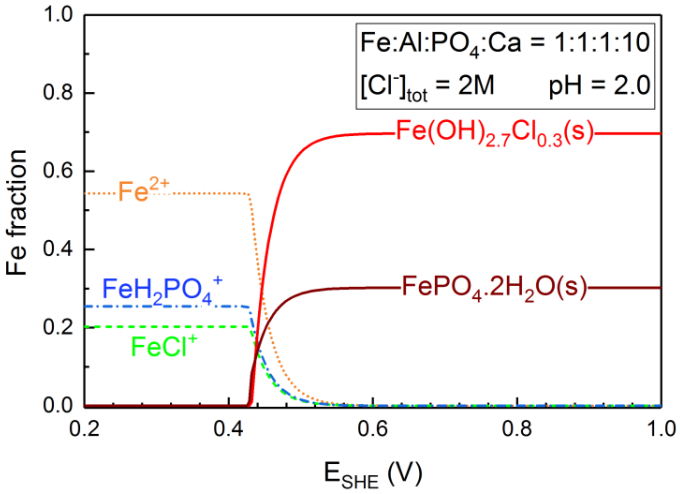

Figure S2. Effect of chlorine concentration (a) and standard electrode potential (b) in the leachate solution on iron speciation (I=1 is used in the speciation calculation).

Design of Experiments base on Response surface methodology (RSM)

Table S1 shows the experimental points that were designed based on the central composite design[2]. The selected variables were pH and ER ([EDTA]/[Fe+Al]. The experiment consisting of 12 runs was performed in the given order and the measured responses in the given set of tests are summarized in Table S2. Recoveries of P, Al, Fe and Ca were selected as responses of interest.

Table S1. Variable and designed experimental points based on central composite design.

Variables	Experimental point				
	-α	-1	0	1	+α
pH	3.8	4	4.5	5	5.2
ER ($[EDTA]/[Fe+Al]$)	0.29	0.5	1	1.5	1.71

Table S2. Experimental run order based on the response surface methodology and the selected response of interest

SID	variable		Recovery (%)			
	ER	pH	P	Al	Fe	Ca
C1.5	1	4.5	43.1	35.4	14.7	12.8
C1.4	1.5	5	29.9	21.8	14.7	10.2
C1.1	0.5	4	84.8	74.8	17.5	10.9
C1.2	0.5	5	92.3	79.1	20.4	10.2
C1.3	1.5	4	8.7	10.9	7.4	8.7
C1.6	1	4.5	33.0	27.6	9.4	6.6
S2.2	1	5.21	77.8	59.5	21.6	10.8
S2.3	0.29	4.5	99.7	99.6	23.7	9.9
S2.6	1	4.5	45.9	34.6	15.2	9.2
S2.4	1.71	4.5	14.9	10.7	9.1	7.7
S2.5	1	4.5	29.6	38.6	8.8	5.3
S2.1	1	3.79	37.7	32.1	10.2	5.4

Least-square regressions were calculated for individual sets of response. Table S3 shows the estimated modelled coefficients (b_{0-5}) of the quadratic RSM equation (1):

$$\text{Response} = b_0 + b_1 \times pH + b_2 \times ER + b_3 \times pH \times ER + b_4 \times pH^2 + b_5 \times ER^2 \quad (1)$$

Table S3. Predicted model parameters for recovery of P, Al, and Fe.

Response (recovery)	Model coefficient					
	b_0	b_1	b_2	b_3	b_4	b_5
	Intercept	pH	ER	pH*ER	pH^2	ER^2
P	835.16	-317.55	-196.814	13.73	36.12	35.21
Al	500	-169.76	-167.55	6.48	16.64	38.34
Fe	152.45	-57.37	-43.27	4.23	6.64	7.58

Table S4 gives the summary of regressions, which indicates the good agreement between the measured and predicted data. The higher R-square values for P and Al responses indicate lower errors associated with those models. However, the Fe-model has higher errors but are in the acceptable region. The P-values are higher than the significance level (α) of 0.05, which indicates that there is no significant evidence at α|=|0.05| level for lack of fit in the regression model.

Table S4. Summary of least-square regression of model with P, Al, and Fe as responses.

Parameters		Response Surface Model		
		P	Al	Fe
R-squared	Multiple	0.966	0.981	0.866
	Adjusted	0.938	0.966	0.755
F-statistic on regression	Value	34.530	62.790	7.778
	on DF	5 & 6	5 & 6	5 & 6
	p-value	$2.39E^{-04}$	$4.24E^{-05}$	0.0134
Lack of fit	DF	3	3	3
	Sum Sq.	168.1	101.3	9.912
	Mean Sq.	56.00	33.80	3.304
	F value	0.911	1.589	0.284
	Pr(>F)	0.530	0.356	0.836

Fig. S3(a-c) presents normal probability plots of the residuals with the theoretical percentiles of the normal distribution and shows an almost linear relation between them. Thus, the normal probability plot of the residuals suggest that the error terms of the model are indeed normally distributed. Furthermore, Fig. S3(d-f) shows the Cook distance for the respective model. The Cook distance signifies the leverage of the experimental points on the model. Cook distances higher that 1 are considered as influential in this study. For phosphorus recovery model the Cook distances are less than 0.5 for 10 experiment points, while the other two points had the Cook distance value between 0.5 and 0.7. Therefore, it was concluded that there are no possible outliers in the experiment domain.

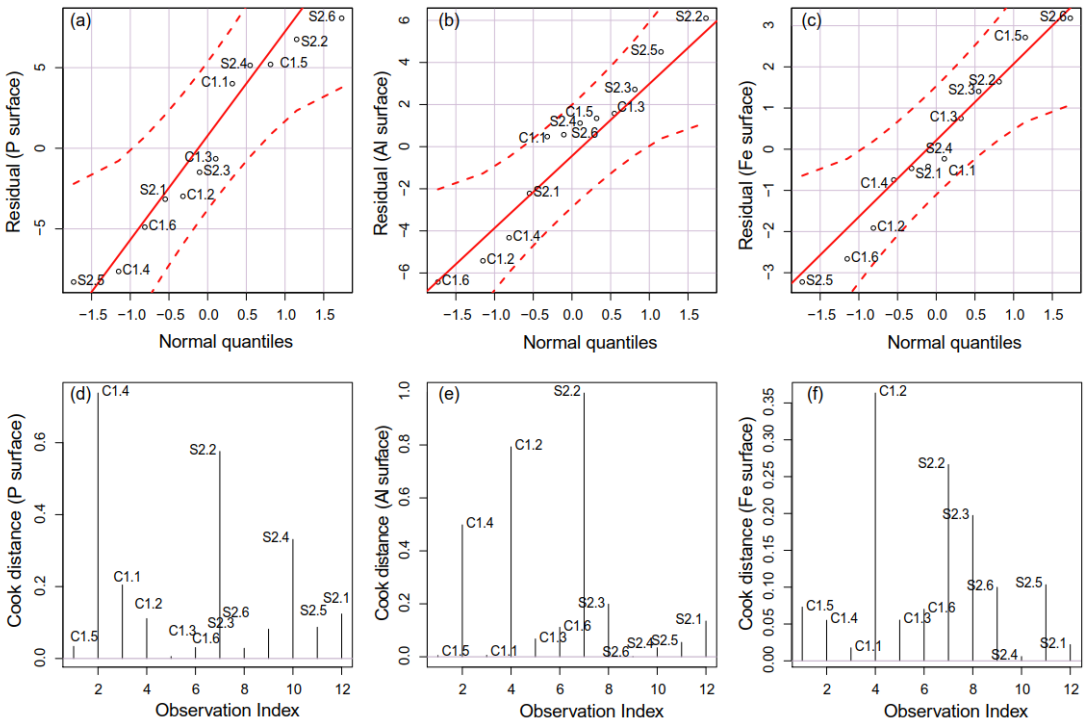

Figure S3. Analysis of model residual value and identification of outliers based on the Cook distance in the experiment domain for surface model of P (a,d), Al (b,e) and Fe (c,f).

Nature of phosphorus-products obtained from silicon-rich and silicon-free solutions:

Recovery of phosphorus from both silicon-rich and silicon-free leachate solution was investigated. A silicon-rich solution was obtained by leaching fly ash with 2M of hydrochloric acid (HCl). The properties of the leachate solution were well described in our previous study[3]. Phosphorus was recovered from the silicon-rich solution at pH 3.5 by addition of 1M NaOH. Silicon free leachate solution is the solution used in this study. Fig. S4 shows the fraction of analytes in P-product obtained from Si-free and Si-rich solution.

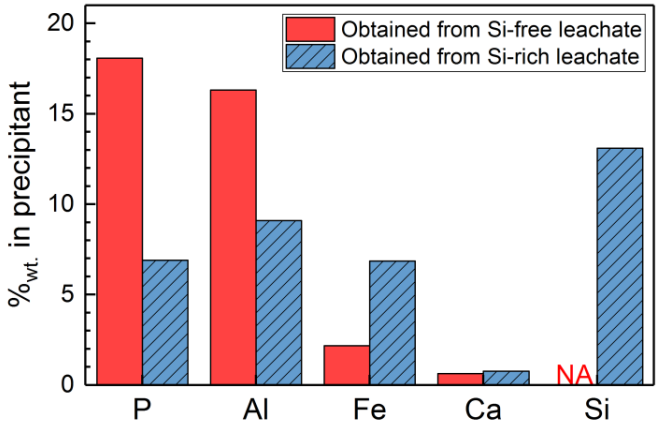

Figure S4. Comparison of phosphorus products obtained from Si-free and Si-rich solution

References:

[1] I. Puigdomenech, MEDUSA and HYDRA: Software for Chemical Equilibrium Calculations, Dept. of Inorganic Chemistry, Royal Institute of Technology (KTH), Stockholm, Sweden

[2] R. Leardi, Experimental design in chemistry: A tutorial, Analytica'Chimica Acta 652 (1) (2009) 161 – 172, fundamental and Applied Analytical Science. A Special Issue In Honour of Alan Townshend. doi:https://doi.org/10.1016/j.aca.2009.06.015.

[3] R. Budhathoki, A. Väisänen, Acid leaching of siliceous fly ash from 370 industrial-scale CFB-boiler in the context of phosphorus recovery –Part I: Removal of silicon from leachate solutions by silica gel precipitation, Hydrometallurgy.

Paper IV

SUSTAINABLE CONVERSION OF $AlPO_4$ DERIVED FROM BIOMASS FLY ASH INTO STRUVITE BY HYDROMETALLURGICAL METHODS

by
Roshan Budhathoki
Ari Väisänen
Manu Lahtinen

Manuscript

Sustainable conversion of $AlPO_4$ derived from biomass fly ash into struvite by hydrometallurgical methods

Roshan Budhathoki*, Ari Väisänen, Manu Lahtinen

Department of Chemistry, Renewable Natural Resources and Chemistry of Living Environment, University of Jyväskylä, P.O. Box 35, FI-40014 Jyväskylä, Finland

Abstract

This paper presents a green perspective to convert aluminium phosphate procured from biomass fly ash to struvite. The conversion process is divided into three steps: dissolution of $AlPO_4$ in phosphoric acid solution, sorption of cationic impurities by a strong acidic cation exchange resin (CER) and struvite precipitation. The effect of phosphoric acid concentration on P extraction and CER dosage on metals adsorption were investigated. Results showed that 0.5 molar concentration of phosphoric acid was sufficient to dissolve 99% of P and use of Amberlite IR120 H^+ resin at 0.6 g/mL dosage facilitated 99.8 and 97.1% removal of Al and Fe from the solution. Purified solution with elevated P content was recirculated for dissolution of $AlPO_4$ solids: this offered a green approach that limits the use of fresh phosphoric acid solution. Over 99% of P in the purified solution was precipitated at pH 9.5 using equimolar concentration of Mg:N:P (1:1:1). Highly crystalline and pure struvite precipitates comprised of heavy metal at low concentrations (Zn, Cr and Pb < 40 mg/kg).

Keywords: Phosphorus recovery, Fly ash utilization, Struvite precipitation, Cation exchange

1. Introduction

Utilization of limited natural phosphate minerals, apatite, for phosphorus (P) production presents a great threat to sustainable supply of affordable phosphorus in the coming years [1, 2]. Recycling of phosphorus from viable secondary sources is increasingly becoming a stimulating approach for P conservation. In this context, ash residues obtained from sewage sludge, municipal solid-waste, animal manure, biomass and etc. have emerged out as a potential source of phosphorus [3, 4, 5, 6]. Particularly, precipitation based P-recovery methods have emphasized on obtaining Ca-P precipitate due to its higher solubility in water and suitability as chemical fertilizer [7, 8]. Despite the lack of commercial values as a raw material for P-industry, phosphorus recovery as Al/Fe-P solids still provides an assurance to the phosphorus sustainability. However, new use of recycled iron/aluminium phosphate and/or its conversion to phosphorus compounds with more usability and value need to be developed [9].

Conversion of Fe/Al-P compounds to struvite (MAP, $MgNH_4PO_4 \cdot 6\,H_2O$) is a promising option, as it can be directly used as a fertilizer which exhibits comparable fertilization potentiality to commercial fertilizer. The slow release of both ammonia and phosphorus in soil is particularly beneficial for plant availability [10, 11]. The conversion method commences with dissolution of Fe/Al-P compounds in either acidic or basic medium, as their solubility in neutral regimes is negligible [12]. Irrespective of the dissolution media, the separation of metals impurities from the P-rich leachate is essential prior to struvite precipitation.

Precipitation, solvent extraction, adsorption and cation exchange are some of the established hydrometallurgical techniques that efficiently remove metal ions from phosphoric acid solution. Addition of organophosphorous reagent to precipitate organo-metallic complexes of Al and Fe showed promising results with efficiency up to 99 and 93% for removal of Fe and Al, respectively [13]. On the other hand, addition of silica-fluoride based precipitating reagents for removal of the precipitate entails considerable loss of phosphate [14]. The extraction capacity and selectivity during solvent extraction of either phosphoric acid or cationic impurities (Al^{3+}, Fe^{3+} and/or etc.) decrease in relation with increasing impurity concentration [15, 16]. Adsorption based purification of phosphoric acid has its own limits in industrial application due to decreasing sorption efficiency with increasing adsorbate concentration [17]. Ion exchange techniques, in contrast, offer better advantages as being economical, recyclable and having high selectivity for specific ions [18]. Strong acidic styrene type cation exchange resins showed feasible sorption behaviour for removal of Al and Fe ions from phosphoric acid solution with respective efficiency up to 84 and 78% [19, 20].

Struvite precipitation reaction may be described as:

$$Mg^{2+} + NH_4{}^{+} + PO_4{}^{3-} \longrightarrow MgNH_4PO_4 \cdot 6\,H_2O \qquad (1)$$

The extend of struvite precipitation and nature of precipitates depend on supersaturation, temperature, co-existing ions or impurities and solution pH [21]. Temperature primarily impacts the solubility of MAP and solution supersaturation, which in turn affects the MAP crystal growth [22]. MAP precipitation at

*Corresponding author
Email address: roshan.budhathoki@jyu.fi (Roshan Budhathoki)

a pH range of 8-9.5, equal molar concentration of Mg^{2+}, NH_4^+ and PO_4^{3-} ions at room temperature was identified feasible for efficient recovery of phosphorus as struvite [23, 24, 25].

This study aims to identify a sustainable method to convert aluminium phosphate, obtained from biomass fly ash in our previous study, to struvite. The leachability of $AlPO_4$ solid in phosphoric acid solutions were investigated. Metal ion impurities were removed via cation exchange mechanism with a strong acidic styrene based resin and the sorption behaviour was evaluated. Prospects of recirculation of purified solution for $AlPO_4$ dissolution were explored in order to minimize the use of fresh phosphoric acid. Finally, Mg and NH_4 sources were added in purified P-rich solution for struvite precipitation and quality of the precipitates were evaluated.

2. Experimental

2.1. Materials

Synthetic $AlPO_4$ containing 18.9% P, 16% Al and 1.5% Fe (concentration in similar range to that of precipitated $AlPO_4$) was used in leaching and metal removal studies. While $AlPO_4$ derived from biomass fly ash, in our earlier study, was employed in struvite precipitation study [6].

2.2. Dissolution experiment

0.1, 0.5 and 1 M of phosphoric acid were prepared from an analytical grade 85% H_3PO_4 from EMSURE®. The constant LS ratio of 40, in this study, ensures the Al concentration in the range of 3 - 5 g/L and styrene based cation exchange resin exhibited favourable adsorption of Al at that concentration [19]. 1 g of $AlPO_4$ was dissolved in 40 mL of 0.1, 0.5 and 1 M H_3PO_4 with the aid of magnetic stirrer at 500 rpm for 1 h. LS ratio of 40 mL/g was also employed during recirculation of diluted-purified solution for solid dissolution and P-rich solutions containing Al and Fe as main impurities were obtained.

2.3. Removal of Al and Fe with cation exchange resin

Amberlite® IR120 H^+ form (AIR-120H), a strongly-acidic cation exchange resin (CER), was used to remove metal cations from the P-rich solution. AIR-120H was identified as an effective and inexpensive material to remove high concentration of Al and Fe ions from neutral to mildly acidic solution [26]. CER dosage of 0.01 to 0.5 g/mL was investigated. Required mass of CER was added to 10 mL of P-rich solution during optimization studies, while 50 mL was used in removal of Al^{3+} and Fe^{3+} ions followed by struvite precipitation. The slurry of CER and P-rich solution were stirred with a magnetic stirrer at 200 rpm for 1 h.

2.4. Struvite recovery experiment

Two batch experiments were performed; (i) fresh 0.5 M phosphoric acid was used to obtain P-rich solution from $AlPO_4$, while (ii) purified P-rich solution was diluted to maintain 0.5 molar concentration of phosphoric acid and employed for dissolution. Al^{3+} and Fe^{3+} ions were removed at CER dosage of 0.6 g/mL. pH of P-rich solutions were first raised to 8 by addition of 1 M NaOH. Then, Mg^{2+} and NH_4^+ sources were added in a stoichiometric concentration (Mg^{2+}:NH_4^+:PO_4^{3-}=1:1:1). $MgCl_2 \cdot 6\,H_2O$ and NH_4Cl were obtained from Sigma-Aldrich and used as source of Mg^{2+} and NH_4^+ ions. At last, the pH of solutions were raised to 9.5 and struvite precipitates were obtained and evaluated.

2.5. Analytical methods

1 ml of each solution, filtered through 0.45 μm syringe filter, was diluted and elemental composition was determined with inductively coupled plasma optical emission spectrometry (ICP-OES PerkinElmer Optima 8300). Bruker Quantax400 EDS coupled with Zeiss EVO-50XVP and Bruker Alpha Platinum-ATR were employed respectively for SEM and infra-red analysis of precipitates. An X–ray powder diffraction analysis was done with a PANalytical X'Pert Pro diffractometer in Bragg-Berentano geometry with Johansson-type monochromor (Cu $K_{\alpha 1}$ radiation; 1.5406 Å with power settings 45 kV, 40 mA). Each, lightly mortar ground, sample was prepared into a sample cavity of routine steel-made sample holder. The data was recorded from a spinning sample by X'Celerator detector in the 2θ-range of 3–70^o with a step size of 0.017^o and counting times of 60 s per step. The diffraction data were analyzed using program PANalytical HighScore Plus v. 4.7 with PDF4+ database.

3. Results and discussion

3.1. Solubility of Al-P solids in phosphoric acid solution

Dissolution of Al-P solids in varying concentration of phosphoric acid was performed and its response is presented in Fig. 1. 0.5 M of H_3PO_4 at LS ratio of 40 mL/g and 1 h extraction allowed total digestion of Al, Fe and P. The dissolution efficiency (η) was estimated with Eq.2.

$$\eta_A(\%) = \frac{C^L_{(mg/L)}}{C^A_{(mg/kg)}} \times \frac{V^L_{(mL)}}{W^{AlPO_4}_{(g)}} \times 100 \quad (2)$$

where $C^L_{(mg/L)}$ is concentration of analyte A (Al, Fe and P) in P-rich solution, $C^A_{(mg/kg)}$ concentration of analytes A in solid, $V^L_{(mL)}$ volume of leaching reagent and $W^{AlPO_4}_{(g)}$ is the weight of solid used during leaching. A known concentration of P (in 0.5 M phosphoric acid solution) was subtracted from the measured P concentration for determination of its dissolution efficiency.

3.2. Removal of Al and Fe with cation exchange resin

The feasibility of Al^{3+} and Fe^{3+} removal with AIR-120H, a strongly cation exchange resin, from P-rich solution obtained with 0.5 M H_3PO_4 were studied with varying CER dosage at retention time of 1 h (Fig. 2(a)). Minimum contact time of 30 min was required to remove Al and Fe in the concentration range of 1000 mg/L with AIR-120H from synthetic solution [26]. Due to higher concentration of metal ion impurities, retention time of 1 h was employed in this study. CER dosage of 0.35 g/mL was found suitable for removal of 99% of Al^{3+} ions, while CER

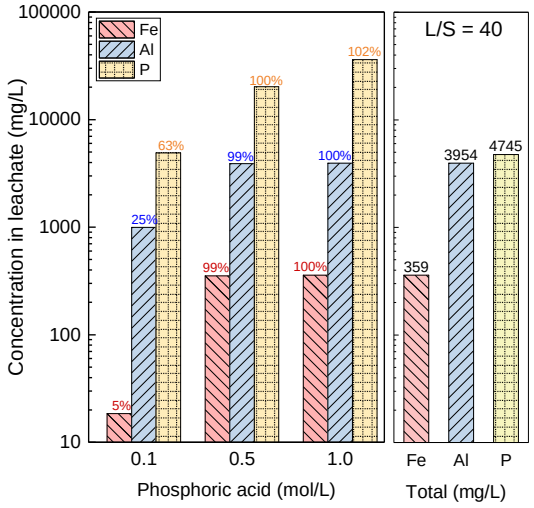

Figure 1: Effect of phosphoric acid concentration on dissolution behaviour of synthetic $AlPO_4$ at LS ratio of 40 mL/g and extraction time of 1 h.

dosage of 0.5 is required to remove both Al^{3+} and Fe^{3+} ions from the P-rich solution.

The adsorption mechanism of Al^{3+} and Fe^{3+} ions on AIR-120H resin was also investigated using Langmuir and Freundlich adsorption isotherms. The Langmuir isotherm is based on theoretical principle that assumes the uptake of metal ions occurs on a homogeneous surface by monolayer sorption. The Freundlich isotherm, in contrast, assumes sorption of metal ions in a heterogeneous surface of adsorbate's monolayer [27]. The sorption isotherm model provides an explication for the behaviour of adsorbate species between the liquid and solid phases [28].

Eq. 3 and 4 represent a general form of the Langmuir and Freundlich isotherm;

$$q_e = \frac{x}{m} = \frac{q_{max} b C_e}{(1 + bC_e)} \tag{3}$$

$$q_e = K_f C_e^{1/n} \tag{4}$$

where q_e (mg/g) is the quantity of solute adsorbed per weight unit of adsorbent at equilibrium, C_e (mg/L) is the concentration of solute remaining in the solution. q_{max} and b are Langmuir adsorption capacity and energy, while K_f and $1/n$ are Freundlich constant for adsorption capacity and intensity of sorption. These constant parameters are obtained from slopes and intercepts of the linear relationship as described in Eq. 5 and 6 (Fig. 2(b-e)). The result depicts that Freundlich isotherm provides a better fit to experimental data for Al sorption with correlation regression coefficient (R^2) value of 0.989, while Langmuir isotherm provides better fit for Fe ions with R^2 value of 0.932.

$$\text{Langmuir isotherm}: \frac{1}{q_e} = \left(\frac{1}{q_{max} b}\right)\frac{1}{C_e} + \frac{1}{q_{max}} \tag{5}$$

$$\text{Freundlich isotherm}: \log q_e = \left(\frac{1}{n}\right)\log C_e + \log K_f \tag{6}$$

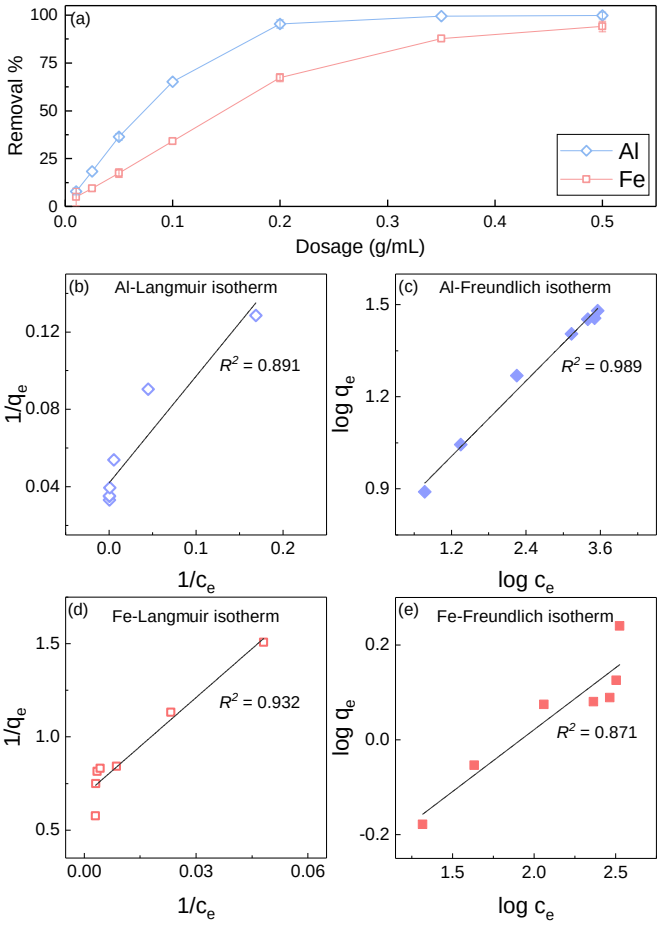

Figure 2: Effect of AIR-120H dosage on the removal efficiency of Al^{3+} and Fe^{3+} (a), Langmuir and Freundlich isotherm plot of aluminium (b-c) and iron (d-e).

Table 1: Langmuir and Freundlich isotherm parameters of Eq. 5 and 6 for sorption of Al and Fe with AIR-120H.

Metal	Langmuir isotherm				Freundlich isotherm		
	b	q_{max}	R_L	R^2	n	K_f	R^2
Al	0.076	23.87	0.0033	0.891	4.89	5.765	0.989
Fe	0.039	1.45	0.0672	0.932	3.83	0.316	0.871

Langmuir and Freundlich constants are listed in Table 1. The separation factor (R_L) from Langmuir isotherm aids to explicate the affinity of sorption between the adsorbate and sorbent. This can be derived as $R_L = 1/(1 + bC_0)$. The R_L value indicates the behaviour of sorption to be irreversible ($R_L = 0$), favourable ($0 < R_L < 1$), linear ($R_L = 1$) or unfavourable ($R_L < 1$) [29]. Likewise, the model parameter n in Freundlich isotherm, at $1 < n < 10$, suggests the beneficial sorption behaviour [30].

Therefore, styrene divinylbenzene based strong cation exchange resin (Amberlite IR120 H^+) showed favourable and

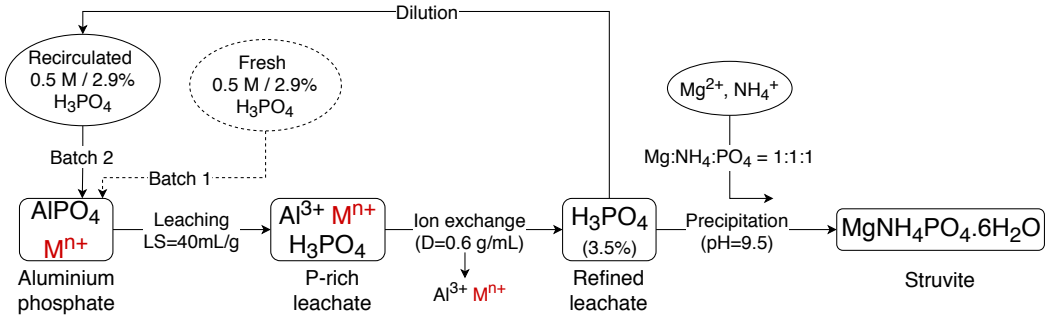

Figure 3: Process flow sheet for precipitation of struvite from P-rich solution obtained with fresh and recirculated 0.5 M phosphoric acid solution. M^{n+} represent metal impurities.

Table 2: Summary of conversion of aluminium phosphate to struvite showing concentration of various elements at different stages with their respective efficiencies in batch 1 (use of pristine 0.5 M phosphoric acid) and batch 2 (use of refined solution with 0.5 M phosphoric acid) experiments.

Element	$AlPO_4$ precipitates (mg/kg)	P-rich solution Leaching: LS = 40 mL/g		Refined P-rich solution Ion exchange: Dosage = 0.6 g/mL		Supernatant Precipitation: pH = 9.5	
		Batch 1 (mg/L)	Batch 2 (mg/L)	Batch 1 (mg/L)	Batch 2 (mg/L)	Batch 1 (mg/L)	Batch 2 (mg/L)
P	180090	19970 (99.5)[a]	19950 (99.1)	18420 (92.3)	18540 (92.9)	105.7 (99.4)	115.2 (99.3)
Al	160300	3990 (99.6)	3965 (98.9)	9.0 (99.8)	10.1 (99.7)	-	-
Fe	20010	493 (98.5)	485 (99.2)	14.5 (97.1)	15.2 (96.9)	-	-
Ca	6300	155 (98.2)	158 (100.3)	-	-	-	-
Mg	1180	29 (98.2)	29 (96.6)	-	-	-	-

[a] Values in "( )" represent efficiency in % of each process (extraction/removal), - = not detected (<LOD)

beneficial sorption behaviour and was found suitable to remove metal ions in high concentrations form the phosphoric acid leachate solution. At the given concentration, 4 g/L of Al and 0.5 g/L of Fe in the P-rich solution, adsorption of Al ions occurred in a heterogeneous surface, while uptake of Fe ions proceeded on homogeneous surface of AIR-120H resin by monolayer sorption.

3.2.1. Recirculation of refined solution for P-extraction

The $H_3PO_4\%_{(wt.)}$ content in fresh 0.5 M phosphoric acid was estimated to be 2.9%. It was increased to 3.5% after dissolution of $AlPO_4$ at LS ratio of 40, which accounts an increment by a factor of 1.21. At the given process parameter, 84% of refined P-rich solution was recirculated. This can be improved either by lowering the LS ratio or using CER with higher sorption capacity. However, the earlier process requires higher dosage of CER due to elevated concentration of metal impurities. Fig. 3 illustrates a green approach to convert aluminium phosphate to struvite by using recirculated refined solution. Similar leaching and metal ion removal efficacies in fresh (batch 1) and purified (batch 2) P-rich solution were observed (Table 2).

3.3. Struvite precipitation

The P-rich solution, obtained from biomass fly ash derived $AlPO_4$, comprised of major cationic impurities (Al and Fe) in high concentration and trace elements with toxic characteristics in minor concentration. AIR-120H was also shown to be capable of removing heavy metals (Cr, Cu, Ni, Pb and Zn) from aqueous solution [27, 31, 32]. Therefore, a CER dosage of 0.6 g/mL was employed to remove most of the cationic impurities. Table 2 depicts that at 0.6 g/mL of CER was sufficient to remove 99 and 97% of Al and Fe, respectively and possibly other metals ions including heavy metals to some extent. Concentration of other cationic impurities were below the detective limit (with ICP-OES) in the purified solution.

The P-rich solutions free from cationic impurities widen the scope of P recovery as pure high-grade phosphoric acid with further purification and concentration via evaporation. However, this study focuses on P recovery as struvite while the earlier is scheduled for future investigation. Lack of competing and co-existing ions in the refined solution ensure impurities free precipitates [33]. In addition, equimolar ratio of $Mg^{2+}/NH_4^+/PO_4^{3-}$ (1:1:1) at pH 9.5 was identified efficient for precipitation of the soluble phosphorus as struvite [34, 35]. In this study, addition of Mg^{2+} and NH_4^+ sources and precipitation at 9.5 contributed to 99% of P recovery in batch 1 and 2.

The efficiency of the proposed conversion process in batch 1 and 2 is estimated to be 91.3 and 91.5% respectively. The net efficiency is derived with Eq. 7:

$$\eta_{\text{net}} = \eta_{\text{D}} \times \eta_{\text{CER}} \times \eta_{\text{PPT}} \tag{7}$$

where η_{D}, η_{CER} and η_{PPT} represent dissolution, ion exchange and precipitation efficiencies, respectively.

3.4. Struvite characterization

3.4.1. Elemental analysis

Elemental composition of precipitates estimated with ICP-OES is presented in Table 3. The Mg/P ratio in the precipitates from batch 1 and 2 was found to be 0.773 and 0.777, which closely resembles the theoretical ratio of 0.785 in pure struvite. A slight elevation in the concentration of Fe, Al, Zn, Cr and Pb in batch 2 precipitate was also noticed and is attributed to their accumulation during recirculation of purified solution for dissolution purpose.

Table 3: Elemental composition of batch 1 and 2 precipitates.

Element (mg/kg)	P	Mg	Fe	Al	Zn	Cr	Pb
Batch 1	125000	96600	100.4	85.8	35.1	12.3	7.0
Batch 2	125850	97820	105.1	70.0	39.3	13.2	8.1

3.4.2. X-ray Diffraction

Results from XRD analysis confirm the presence of struvite ($MgNH_4PO_4 \cdot 6\,H_2O$) as a dominant crystalline phase for all precipitates as shown in Fig. 4. Search match routines revealed high scored match to struvite structure (PDF4 ref: 015-0762) in all three patterns. Only very few weak diffraction peaks remain unindexed and additional phase analysis did not reveal unambiguous match to any candidates due to the low number of and low intensities of the remaining unindexed peaks. Between batch 1 and 2 struvite, the intensities observed for the (110), (020), (011) and (211) reflections differ for each other. This is attributed to preferred orientation and the elongation of crystals in respective plane.[36]

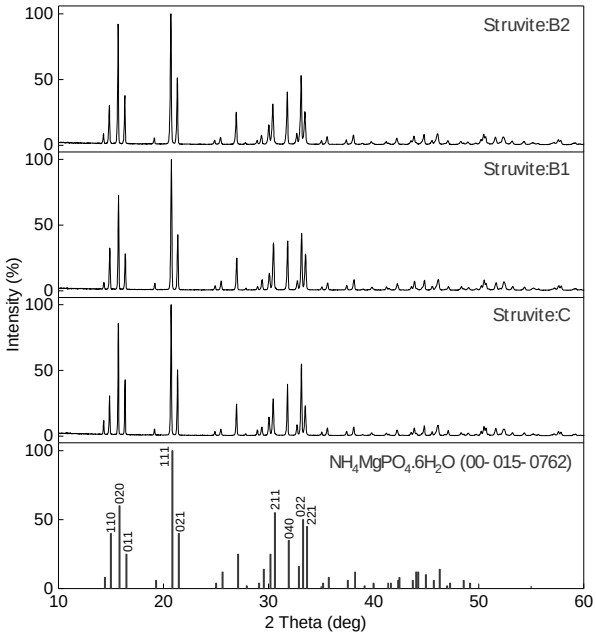

Figure 4: X-ray diffraction pattern showing the crystalline nature of the precipitates obtained at pH 9.5 from batch 1-2 (Struvite:B1-B2), synthetic solution (Struvite:C) and standard struvite.

3.4.3. Infrared spectroscopy analysis

A comparison of ATR IR spectra of precipitates to synthetic compound (Struvite:C) is presented in Fig. 5, which reveals similarities in the position of absorbance peaks and their intensities. Peaks 1-4 (3800-2200 cm^{-1}) were attributed to O−H and N−H stretching. Peaks 5-7 at 1675, 1610 and 1432 cm^{-1} were assigned to NH_4^+ bending vibrations. Peaks 8, 9-11 (980-565 cm^{-1}) were attributed respectively to stretching and bending vibrations of PO_4^{3-}, while peak 12 at 460 cm^{-1} was ascribed to Mg−O stretching [37]. The spectral peaks from this study were also compared to reported peaks from other study and presented in Table 4 [38].

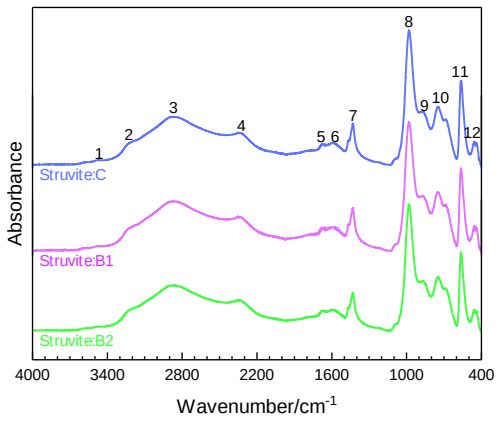

Figure 5: Infrared absorption-spectra of struvite precipitated from batch 1-2 (Struvite:B1-B2), synthetic solution (Struvite:C). The numbered peaks corresponds to assigned IR active functional group in Table 4.

Table 4: Comparison of the observed and reported absorption peaks of struvite [38].

Peak number	Observed value (cm^{-1})	Reported value (cm^{-1})	Bonds/vibrations
1	3475	3480	OH, NH stretching
2	3245	3256	OH, NH stretching
3	2870	2943	OH, NH stretching
4	2345	2353	OH, NH stretching
5	1675	1683	NH_4^+ $\nu 4$ bending
6	1610	1615	NH_4^+ $\nu 4$ bending
7	1432	1439	NH_4^+ $\nu 2$ bending
8	980	1004	PO_4^{3-} $\nu 3$ stretching
9	885	896	PO_4^{3-} $\nu 4$ bending
10	755	761	PO_4^{3-} $\nu 2$ bending
11	565	570	PO_4^{3-} $\nu 2$ bending
12	460	459	Mg-O stretching

Comparison of the spectra also facilitated to investigate the effect of recirculation on the nature of precipitates. Similarities in the spectral position and their intensity suggest that recirculation of refined P-rich solution do not affect the concentration and position of IR active functional group of the struvite precipitates.

3.4.4. SEM analysis

Fig. 6 and 7(a-c) displays the photographic and SEM images of precipitates obtained from synthetic sample (Struvite:C), batch 1 (Struvite:B1) and batch 2 (Struvite:B2) at pH 9.5. The

Figure 6: Precipitated struvite precipitates from (a) synthetic solution (Struvite:C) and (b-c) batch 1-2 (Struvite:B1-B2).

morphology of white-granular struvite precipitates depict orthorhombic structure that grow further into the form of tubular particles and fractal aggregates. In the absence of coexisting salts, the granulated particles was found to form compact and hard aggregates [33]. Chen et al. described the mechanism for aggregate growth which initiates with collision of orthorhombic crystals of struvite to form aggregates. With further growth, cluster-cluster aggregation dominates the evolution and formation of fractal aggregates with elongated shape and rougher occurs [39].

The appearances and morphology of struvite precipitates obtained from batch 1 and 2 were similar. Thus, recirculation of purified solution did not indicate to impose any threat to morphology of the precipitates.

4. Conclusion

In summary, we reported a green/sustainable approach to convert aluminium phosphate obtained from biomass fly ash to struvite, a slow releasing fertilizer. Over 99% of P was dissolved from $AlPO_4$ solids by 0.5 M H_3PO_4 at LS ratio of 40 mL/g. The P-rich solutions containing Al and Fe as major cationic impurities were purified by the use of a strong acidic cation exchange resin (Amberlite IR120 H^+) at 0.6 g/mL of dosage. This facilitated the removal of Al and Fe ions up to 99.8 and 97.1%, respectively. 84% of purified P-rich solution was recirculated to dissolve Al–P solids. Similar efficacies in the dissolution and metal impurities removal process in fresh and recirculated leaching reagents were observed. The cationic impurity free P-rich solutions were precipitated at pH 9.4 at equimolar concentration of $Mg^{2+}/NH_4{}^+/PO_4{}^{3-}$ (1:1:1). Highly-pure white-crystalline struvite precipitates were obtained with heavy metal (Zn, Cr and Pb) concentrations accounting less than 40 mg/kg. Procuring struvite from biomass fly ash is seen as a sustainable P recycling method which promotes conservation of natural resources used for fertilizer production.

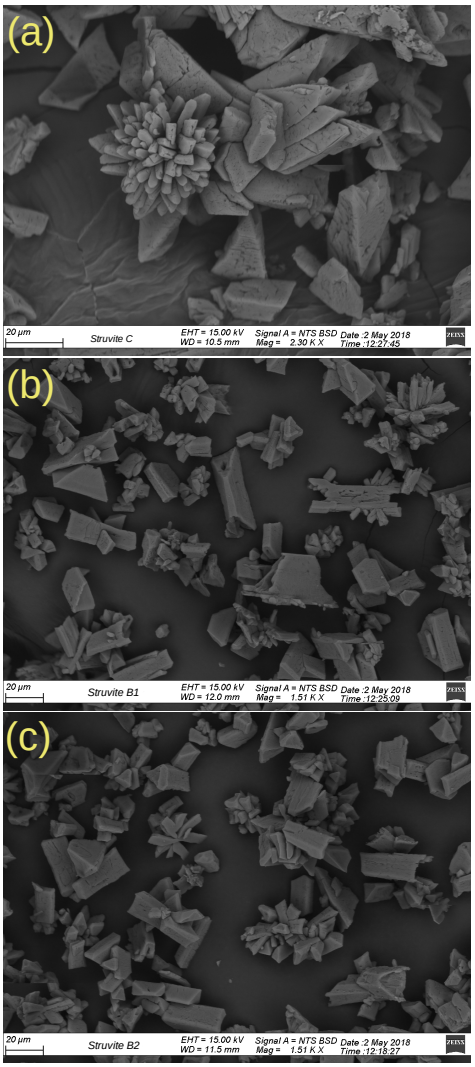

Figure 7: SEM images of struvite precipitates from (a) synthetic solution (Struvite:C), (b) batch 1 (Struvite:B1) and (c) batch 2 (Struvite:B2).

References

[1] J. Cooper, R. Lombardi, D. Boardman, C. Carliell-Marquet, The future distribution and production of global phosphate rock reserves, Resources, Conservation and Recycling 57 (Supplement C) (2011) 78 – 86. doi:https://doi.org/10.1016/j.resconrec.2011.09.009.

[2] B. K. Mayer, L. A. Baker, T. H. Boyer, P. Drechsel, M. Gifford, M. A. Hanjra, P. Parameswaran, J. Stoltzfus, P. Westerhoff, B. E. Rittmann, Total value of phosphorus recovery, Environmental Science & Technology 50 (13) (2016) 6606–6620, pMID: 27214029. doi:10.1021/acs.est.6b01239.

[3] S. Donatello, D. Tong, C. Cheeseman, Production of technical grade phosphoric acid from incinerator sewage sludge ash (issa), Waste Management 30 (8) (2010) 1634 – 1642. doi:https://doi.org/10.1016/j.wasman.2010.04.009.

[4] Y. Kalmykova, K. K. Fedje, Phosphorus recovery from municipal solid waste incineration fly ash, Waste Management 33 (6) (2013) 1403 – 1410. doi:https://doi.org/10.1016/j.wasman.2013.01.040.

[5] K. Kuligowski, T. G. Poulsen, Phosphorus and zinc dissolution from thermally gasified piggery waste ash using sulphuric acid, Bioresource Technology 101 (14) (2010) 5123 – 5130. doi:https://doi.org/10.1016/j.biortech.2010.01.143.

[6] R. Budhathoki, A. Väisänen, M. Lahtinen, Selective recovery of phosphorus as $AlPO_4$ from silicon-free CFB-derived fly ash leachate, Hydrometallurgy 178 (2018) 30 – 36. doi:https://doi.org/10.1016/j.hydromet.2018.03.025.

[7] K. Kaikake, T. Sekito, Y. Dote, Phosphate recovery from phosphorus-rich solution obtained from chicken manure incineration ash, Waste Management 29 (3) (2009) 1084 – 1088. doi:https://doi.org/10.1016/j.wasman.2008.09.008.

[8] L. Fang, J. shan Li, S. Donatello, C. Cheeseman, Q. Wang, C. S. Poon, D. C. Tsang, Recovery of phosphorus from incinerated sewage sludge ash by combined two-step extraction and selective precipitation, Chemical

Engineering Journal 348 (2018) 74 – 83. doi:https://doi.org/10.1016/j.cej.2018.04.201.

[9] M. Takahashi, S. Kato, H. Shima, E. Sarai, T. Ichioka, S. Hatyakawa, H. Miyajiri, Technology for recovering phosphorus from incinerated wastewater treatment sludge, Chemosphere 44 (1) (2001) 23 – 29, iCUPCT. doi:https://doi.org/10.1016/S0045-6535(00)00380-5.

[10] C. Plaza, R. Sanz, C. Clemente, J. M. Fernández, R. González, A. Polo, M. F. Colmenarejo, Greenhouse evaluation of struvite and sludges from municipal wastewater treatment works as phosphorus sources for plants, Journal of Agricultural and Food Chemistry 55 (20) (2007) 8206–8212, pMID: 17877411. doi:10.1021/jf071563y.

[11] S. Antonini, M. A. Arias, T. Eichert, J. Clemens, Greenhouse evaluation and environmental impact assessment of different urine-derived struvite fertilizers as phosphorus sources for plants, Chemosphere 89 (10) (2012) 1202 – 1210. doi:https://doi.org/10.1016/j.chemosphere.2012.07.026.

[12] J. C. Brosheer, F. A. Lenfesty, J. F. Anderson, Solubility in the system aluminum phosphate-phosphoric acid-water, Journal of the American Chemical Society 76 (23) (1954) 5951–5956. doi:10.1021/ja01652a016.

[13] N. Abdennebi, K. Benhabib, C. Goutaudier, M. Bagane, Removal of aluminium and iron ions from phosphoric acid by precipitation of organometallic complex using organophosphorous reagent, Journal of Materials and Environmental Science 8 (2) (2017) 557–565.

[14] J. R. Lehr, A. W. Frazier, J. P. Smith, Phosphoric acid impurities, precipitated impurities in wet-process phosphoric acid, Journal of Agricultural and Food Chemistry 14 (1) (1966) 27–33. doi:10.1021/jf60143a009.

[15] F. Ruiz, A. Marcilla, A. M. Ancheta, Purification of Wet Process Phosphoric Acid by Solvent Extraction with Propyl Ethers, Solvent Extraction and Ion Exchange 5 (6) (1987) 1141–1150. doi:10.1080/07366298708918613.

[16] C. Ming, L. Jun, J. Yang, L. Jianhong, Z. Xinhua, Y. Defang, Efficient solvent extraction of phosphoric acid with dibutyl sulfoxide, Journal of Chemical Technology & Biotechnology 93 (2) (2017) 467–475. doi:10.1002/jctb.5377.

[17] W. Hamza, C. Chtara, M. Benzina, Purification of industrial phosphoric acid (54%) using fe-pillared bentonite, Environmental Science and Pollution Research 23 (16) (2016) 15820–15831. doi:10.1007/s11356-015-5557-5.

[18] C. Shen, Y. Chang, L. Fang, M. Min, C. H. Xiong, Selective removal of copper with polystyrene-1,3-diaminourea chelating resin: synthesis and adsorption studies, New J. Chem. 40 (2016) 3588–3596. doi:10.1039/C5NJ02703A.

[19] C. Tang, Y. Qiu, Y. Wang, X. Wang, Z. Zhang, L. Yang, Kinetic studies on Al³⁺removal from phosphoric acid by cation exchange resin, Canadian Journal of Chemical Engineering 9999 (2017) 1–11. doi:10.1002/cjce.23070.

[20] Q. Wang, J. shan Li, P. Tang, L. Fang, C. S. Poon, Sustainable reclamation of phosphorus from incinerated sewage sludge ash as value-added struvite by chemical extraction, purification and crystallization, Journal of Cleaner Production 717–725doi:10.1016/j.jclepro.2018.01.254.

[21] S. Agrawal, J. S. Guest, R. D. Cusick, Elucidating the impacts of initial supersaturation and seed crystal loading on struvite precipitation kinetics, fines production, and crystal growth, Water Research 252–259doi:10.1016/j.watres.2018.01.002.

[22] X. Zhang, J. Hu, H. Spanjers, J. B. van Lier, Struvite crystallization under a marine/brackish aquaculture condition, Bioresource Technology 218 (2016) 1151 – 1156. doi:https://doi.org/10.1016/j.biortech.2016.07.088.

[23] A. N. Kofina, P. G. Koutsoukos, Spontaneous precipitation of struvite from synthetic wastewater solutions, Crystal Growth and Design 5 (2) (2005) 489–496. doi:10.1021/cg049803e.

[24] G. Jia, H. Zhang, J. Krampe, T. Muster, B. Gao, N. Zhu, B. Jin, Applying a chemical equilibrium model for optimizing struvite precipitation for ammonium recovery from anaerobic digester effluent, Journal of Cleaner Production 297–305doi:10.1016/j.jclepro.2017.01.116.

[25] A. Gunay, D. Karadag, I. Tosun, M. Ozturk, Use of magnesit as a magnesium source for ammonium removal from leachate, Journal of Hazardous Materials 156 (1) (2008) 619 – 623. doi:https://doi.org/10.1016/j.jhazmat.2007.12.067.

[26] M. E. Goher, A. M. Hassan, I. A. Abdel-moniem, A. H. Fahmy, M. H. Abdo, S. M. El-sayed, Removal of aluminum , iron and manganese ions from industrial wastes using granular activated carbon and Amberlite IR-120H, The Egyptian Journal of Aquatic Research (2) 155–164. doi:10.1016/j.ejar.2015.04.002.

[27] P. Meshram, S. K. Sahu, B. D. Pandey, V. Kumar, T. R. Mankhand, Removal of Chromium(III) from the Waste Solution of an Indian Tannery by Amberlite IR 120 Resin, International Journal of Nonferrous Metallurgy (October) 32–41. doi:10.4236/ijnm.2012.13005.

[28] M. M. Ghoneim, H. S. El-Desoky, K. M. El-Moselhy, A. Amer, E. H. A. El-Naga, L. I. Mohamedein, A. E. Al-Prol, Removal of cadmium from aqueous solution using marine green algae, ulva lactuca, The Egyptian Journal of Aquatic Research 40 (3) (2014) 235 – 242. doi:https://doi.org/10.1016/j.ejar.2014.08.005.

[29] K. R. Hall, L. C. Eagleton, A. Acrivos, T. Vermeulen, Pore- and solid-diffusion kinetics in fixed-bed adsorption under constant-pattern conditions, Industrial & Engineering Chemistry Fundamentals 5 (2) (1966) 212–223. doi:10.1021/i160018a011.

[30] K. Kadirvelu, C. Namasivayam, Agricutural by-product as metal adsorbent: Sorption of lead(ii) from aqueous solution onto coirpith carbon, Environmental Technology 21 (10) (2000) 1091–1097. doi:10.1080/09593330.2000.9618995.

[31] P. Dr. Waleed Mohammad Salih, H. Gzar, N. Falah Hassan, Sorption of Lead, Zinc and Copper from Simulated Wastewater by Amberlite IR-120 Resin, Journal of Engineering 18 (2012) 1042–1054.

[32] P. E. Franco, M. T. Veit, C. E. Borba, G. da Cunha Gonçalves, M. R. Fagundes-Klen, R. Bergamasco, E. A. da Silva, P. Y. R. Suzaki, Nickel(II) and Zinc(II) removal using Amberlite IR-120 resin: Ion exchange equilibrium and kinetics, Chemical Engineering Journal 221 (2013) 426 – 435. doi:https://doi.org/10.1016/j.cej.2013.02.006.

[33] Y. J. Shih, R. R. M. Abarca, M. D. G. de Luna, Y. H. Huang, M. C. Lu, Recovery of phosphorus from synthetic wastewaters by struvite crystallization in a fluidized-bed reactor: Effects of pH, phosphate concentration and coexisting ions, Chemosphere 466–473doi:10.1016/j.chemosphere.2017.01.088.

[34] S. H. Lee, R. Kumar, B. H. Jeon, Struvite precipitation under changing ionic conditions in synthetic wastewater: Experiment and modeling, Journal of Colloid and Interface Science 93–102doi:10.1016/j.jcis.2016.04.013.

[35] S. Wu, S. Zou, G. Liang, G. Qian, Z. He, Enhancing recovery of magnesium as struvite from landfill leachate by pretreatment of calcium with simultaneous reduction of liquid volume via forward osmosis, Science of the Total Environment 137–146doi:10.1016/j.scitotenv.2017.08.038.

[36] A. A. Rouff, Sorption of chromium with struvite during phosphorus recovery, Environmental Science and Technology 46 (22) (2012) 12493–12501. doi:10.1021/es302296m.

[37] V. Stefov, B. Šoptrajanov, I. Kuzmanovski, H. Lutz, B. Engelen, Infrared and Raman spectra of magnesium ammonium phosphate hexahydrate (struvite) and its isomorphous analogues. III. Spectra of protiated and partially deuterated magnesium ammonium phosphate hexahydrate, Journal of Molecular Structure 752 (1) (2005) 60 – 67. doi:https://doi.org/10.1016/j.molstruc.2005.05.040.

[38] C. C. Su, R. R. M. Abarca, M. D. G. de Luna, M. C. Lu, Phosphate recovery from fluidized-bed wastewater by struvite crystallization technology, Journal of the Taiwan Institute of Chemical Engineers (5) 2395–2402. doi:10.1016/j.jtice.2014.04.002.

[39] Z. Ye, Y. Shen, X. Ye, Z. Zhang, S. Chen, J. Shi, Phosphorus recovery from wastewater by struvite crystallization: Property of aggregates, Journal of Environmental Sciences (China) 26 (5) (2014) 991–1000. doi:10.1016/S1001-0742(13)60536-7.
URL http://dx.doi.org/10.1016/S1001-0742(13)60536-7

DEPARTMENT OF CHEMISTRY, UNIVERSITY OF JYVÄSKYLÄ
RESEARCH REPORT SERIES

1. Vuolle, Mikko: Electron paramagnetic resonance and molecular orbital study of radical ions generated from (2.2)metacyclophane, pyrene and its hydrogenated compounds by alkali metal reduction and by thallium(III)trifluoroacetate oxidation. (99 pp.) 1976
2. Pasanen, Kaija: Electron paramagnetic resonance study of cation radical generated from various chlorinated biphenyls. (66 pp.) 1977
3. Carbon-13 Workshop, September 6-8, 1977. (91 pp.) 1977
4. Laihia, Katri: On the structure determination of norbornane polyols by NMR spectroscopy. (111 pp.) 1979
5. Nyrönen, Timo: On the EPR, ENDOR and visible absorption spectra of some nitrogen containing heterocyclic compounds in liquid ammonia. (76 pp.) 1978
6. Talvitie, Antti: Structure determination of some sesquiterpenoids by shift reagent NMR. (54 pp.) 1979
7. Häkli, Harri: Structure analysis and molecular dynamics of cyclic compounds by shift reagent NMR. (48 pp.) 1979
8. Pitkänen, Ilkka: Thermodynamics of complexation of 1,2,4-triazole with divalent manganese, cobalt, nickel, copper, zinc, cadmium and lead ions in aqueous sodium perchlorate solutions. (89 pp.) 1980
9. Asunta, Tuula: Preparation and characterization of new organometallic compounds synthesized by using metal vapours. (91 pp.) 1980
10. Sattar, Mohammad Abdus: Analyses of MCPA and its metabolites in soil. (57 pp.) 1980
11. Bibliography 1980. (31 pp.) 1981
12. Knuuttila, Pekka: X-Ray structural studies on some divalent 3d metal compounds of picolinic and isonicotinic acid N-oxides. (77 pp.) 1981
13. Bibliography 1981. (33 pp.) 1982
14. 6th National NMR Symposium, September 9-10, 1982, Abstracts. (49 pp.) 1982
15. Bibliography 1982. (38 pp.) 1983
16. Knuuttila, Hilkka: X-Ray structural studies on some Cu(II), Co(II) and Ni(II) complexes with nicotinic and isonicotinic acid N-oxides. (54 pp.) 1983
17. Symposium on inorganic and analytical chemistry May 18, 1984, Program and Abstracts. (100 pp.) 1984
18. Knuutinen, Juha: On the synthesis, structure verification and gas chromatographic determination of chlorinated catechols and guaiacols occuring in spent bleach liquors of kraft pulp mill. (30 pp.) 1984
19. Bibliography 1983. (47 pp.) 1984
20. Pitkänen, Maija: Addition of BrCl, B_2 and Cl_2 to methyl esters of propenoic and 2-butenoic acid derivatives and ^{13}C NMR studies on methyl esters of saturated aliphatic mono- and dichlorocarboxylic acids. (56 pp.) 1985
21. Bibliography 1984. (39 pp.) 1985
22. Salo, Esa: EPR, ENDOR and TRIPLE spectroscopy of some nitrogen heteroaromatics in liquid ammonia. (111 pp.) 1985

23. Humppi, Tarmo: Synthesis, identification and analysis of dimeric impurities of chlorophenols. (39 pp.) 1985
24. Aho, Martti: The ion exchange and adsorption properties of sphagnum peat under acid conditions. (90 pp.) 1985
25. Bibliography 1985 (61 pp.) 1986
26. Bibliography 1986. (23 pp.) 1987
27. Bibliography 1987. (26 pp.) 1988
28. Paasivirta, Jaakko (Ed.): Structures of organic environmental chemicals. (67 pp.) 1988
29. Paasivirta, Jaakko (Ed.): Chemistry and ecology of organo-element compounds. (93 pp.) 1989
30. Sinkkonen, Seija: Determination of crude oil alkylated dibenzothiophenes in environment. (35 pp.) 1989
31. Kolehmainen, Erkki (Ed.): XII National NMR Symposium Program and Abstracts. (75 pp.) 1989
32. Kuokkanen, Tauno: Chlorocymenes and Chlorocymenenes: Persistent chlorocompounds in spent bleach liquors of kraft pulp mills. (40 pp.) 1989
33. Mäkelä, Reijo: ESR, ENDOR and TRIPLE resonance study on substituted 9,10-anthraquinone radicals in solution. (35 pp.) 1990
34. Veijanen, Anja: An integrated sensory and analytical method for identification of off-flavour compounds. (70 pp.) 1990
35. Kasa, Seppo: EPR, ENDOR and TRIPLE resonance and molecular orbital studies on a substitution reaction of anthracene induced by thallium(III) in two fluorinated carboxylic acids. (114 pp.) 1990
36. Herve, Sirpa: Mussel incubation method for monitoring organochlorine compounds in freshwater recipients of pulp and paper industry. (145 pp.) 1991
37. Pohjola, Pekka: The electron paramagnetic resonance method for characterization of Finnish peat types and iron (III) complexes in the process of peat decomposition. (77 pp.) 1991
38. Paasivirta, Jaakko (Ed.): Organochlorines from pulp mills and other sources. Research methodology studies 1988-91. (120 pp.) 1992
39. Veijanen, Anja (Ed.): VI National Symposium on Mass Spectrometry, May 13-15, 1992, Abstracts. (55 pp.) 1992
40. Rissanen, Kari (Ed.): The 7. National Symposium on Inorganic and Analytical Chemistry, May 22, 1992, Abstracts and Program. (153 pp.) 1992
41. Paasivirta, Jaakko (Ed.): CEOEC'92, Second Finnish-Russian Seminar: Chemistry and Ecology of Organo-Element Compounds. (93 pp.) 1992
42. Koistinen, Jaana: Persistent polychloroaromatic compounds in the environment: structure-specific analyses. (50 pp.) 1993
43. Virkki, Liisa: Structural characterization of chlorolignins by spectroscopic and liquid chromatographic methods and a comparison with humic substances. (62 pp.) 1993
44. Helenius, Vesa: Electronic and vibrational excitations in some

biologically relevant molecules. (30 pp.) 1993

45. Leppä-aho, Jaakko: Thermal behaviour, infrared spectra and x-ray structures of some new rare earth chromates(VI). (64 pp.) 1994
46. Kotila, Sirpa: Synthesis, structure and thermal behavior of solid copper(II) complexes of 2-amino-2- hydroxymethyl-1,3-propanediol. (111 pp.) 1994
47. Mikkonen, Anneli: Retention of molybdenum(VI), vanadium(V) and tungsten(VI) by kaolin and three Finnish mineral soils. (90 pp.) 1995
48. Suontamo, Reijo: Molecular orbital studies of small molecules containing sulfur and selenium. (42 pp.) 1995
49. Hämäläinen, Jouni: Effect of fuel composition on the conversion of fuel-N to nitrogen oxides in the combustion of small single particles. (50 pp.) 1995
50. Nevalainen, Tapio: Polychlorinated diphenyl ethers: synthesis, NMR spectroscopy, structural properties, and estimated toxicity. (76 pp.) 1995
51. Aittola, Jussi-Pekka: Organochloro compounds in the stack emission. (35 pp.) 1995
52. Harju, Timo: Ultrafast polar molecular photophysics of (dibenzylmethine)borondifluoride and 4-aminophthalimide in solution. (61 pp.) 1995
53. Maatela, Paula: Determination of organically bound chlorine in industrial and environmental samples. (83 pp.) 1995
54. Paasivirta, Jaakko (Ed.): CEOEC'95, Third Finnish-Russian Seminar: Chemistry and Ecology of Organo-Element Compounds. (109 pp.) 1995
55. Huuskonen, Juhani: Synthesis and structural studies of some supramolecular compounds. (54 pp.) 1995
56. Palm, Helena: Fate of chlorophenols and their derivatives in sawmill soil and pulp mill recipient environments. (52 pp.) 1995
57. Rantio, Tiina: Chlorohydrocarbons in pulp mill effluents and their fate in the environment. (89 pp.) 1997
58. Ratilainen, Jari: Covalent and non-covalent interactions in molecular recognition. (37 pp.) 1997
59. Kolehmainen, Erkki (Ed.): XIX National NMR Symposium, June 4-6, 1997, Abstracts. (89 pp.) 1997
60. Matilainen, Rose: Development of methods for fertilizer analysis by inductively coupled plasma atomic emission spectrometry. (41 pp.) 1997
61. Koistinen, Jari (Ed.): Spring Meeting on the Division of Synthetic Chemistry, May 15-16, 1997, Program and Abstracts. (36 pp.) 1997
62. Lappalainen, Kari: Monomeric and cyclic bile acid derivatives: syntheses, NMR spectroscopy and molecular recognition properties. (50 pp.) 1997
63. Laitinen, Eira: Molecular dynamics of cyanine dyes and phthalimides in solution: picosecond laser studies. (62 pp.) 1997
64. Eloranta, Jussi: Experimental and theoretical studies on some

quinone and quinol radicals. (40 pp.) 1997

65. Oksanen, Jari: Spectroscopic characterization of some monomeric and aggregated chlorophylls. (43 pp.) 1998
66. Häkkänen, Heikki: Development of a method based on laser-induced plasma spectrometry for rapid spatial analysis of material distributions in paper coatings. (60 pp.) 1998
67. Virtapohja, Janne: Fate of chelating agents used in the pulp and paper industries. (58 pp.) 1998
68. Airola, Karri: X-ray structural studies of supramolecular and organic compounds. (39 pp.) 1998
69. Hyötyläinen, Juha: Transport of lignin–type compounds in the receiving waters of pulp mills. (40 pp.) 1999
70. Ristolainen, Matti: Analysis of the organic material dissolved during totally chlorine-free bleaching. (40 pp.) 1999
71. Eklin, Tero: Development of analytical procedures with industrial samples for atomic emission and atomic absorption spectrometry. (43 pp.) 1999
72. Välisaari, Jouni: Hygiene properties of resol-type phenolic resin laminates. (129 pp.) 1999
73. Hu, Jiwei: Persistent polyhalogenated diphenyl ethers: model compounds syntheses, characterization and molecular orbital studies. (59 pp.) 1999
74. Malkavaara, Petteri: Chemometric adaptations in wood processing chemistry. (56 pp.) 2000
75. Kujala Elena, Laihia Katri, Nieminen Kari (Eds.): NBC 2000, Symposium on Nuclear, Biological and Chemical Threats in the 21st Century. (299 pp.) 2000
76. Rantalainen, Anna-Lea: Semipermeable membrane devices in monitoring persistent organic pollutants in the environment. (58 pp.) 2000
77. Lahtinen, Manu: *In situ* X-ray powder diffraction studies of Pt/C, CuCl/C and Cu_2O/C catalysts at elevated temperatures in various reaction conditions. (92 pp.) 2000
78. Tamminen, Jari: Syntheses, empirical and theoretical characterization, and metal cation complexation of bile acid-based monomers and open/closed dimers. (54 pp.) 2000
79. Vatanen, Virpi: Experimental studies by EPR and theoretical studies by DFT calculations of α-amino-9,10-anthraquinone radical anions and cations in solution. (37 pp.) 2000
80. Kotilainen, Risto: Chemical changes in wood during heating at 150-260 °C. (57 pp.) 2000
81. Nissinen, Maija: X-ray structural studies on weak, non-covalent interactions in supramolecular compounds. (69 pp.) 2001
82. Wegelius, Elina: X-ray structural studies on self-assembled hydrogen-bonded networks and metallosupramolecular complexes. (84 pp.) 2001
83. Paasivirta, Jaakko (Ed.): CEOEC'2001, Fifth Finnish-Russian Seminar: Chemistry and Ecology of Organo-Element Compounds. (163 pp.) 2001
84. Kiljunen, Toni: Theoretical studies on spectroscopy and

atomic dynamics in rare gas solids. (56 pp.) 2001

85. Du, Jin: Derivatives of dextran: synthesis and applications in oncology. (48 pp.) 2001
86. Koivisto, Jari: Structural analysis of selected polychlorinated persistent organic pollutants (POPs) and related compounds. (88 pp.) 2001
87. Feng, Zhinan: Alkaline pulping of non-wood feedstocks and characterization of black liquors. (54 pp.) 2001
88. Halonen, Markku: Lahon havupuun käyttö sulfaattiprosessin raaka-aineena sekä havupuun lahontorjunta. (90 pp.) 2002
89. Falábu, Dezsö: Synthesis, conformational analysis and complexation studies of resorcarene derivatives. (212 pp.) 2001
90. Lehtovuori, Pekka: EMR spectroscopic studies on radicals of ubiquinones Q-*n*, vitamin K_3 and vitamine E in liquid solution. (40 pp.) 2002
91. Perkkalainen, Paula: Polymorphism of sugar alcohols and effect of grinding on thermal behavior on binary sugar alcohol mixtures. (53 pp.) 2002
92. Ihalainen, Janne: Spectroscopic studies on light-harvesting complexes of green plants and purple bacteria. (42 pp.) 2002
93. Kunttu, Henrik, Kiljunen, Toni (Eds.): 4th International Conference on Low Temperature Chemistry. (159 pp.) 2002
94. Väisänen, Ari: Development of methods for toxic element analysis in samples with environmental concern by ICP-AES and ETAAS. (54 pp.) 2002
95. Luostarinen, Minna: Synthesis and characterisation of novel resorcarene derivatives. (200 pp.) 2002
96. Louhelainen, Jarmo: Changes in the chemical composition and physical properties of wood and nonwood black liquors during heating. (68 pp.) 2003
97. Lahtinen, Tanja: Concave hydrocarbon cyclophane B-prismands. (65 pp.) 2003
98. Laihia, Katri (Ed.): NBC 2003, Symposium on Nuclear, Biological and Chemical Threats – A Crisis Management Challenge. (245 pp.) 2003
99. Oasmaa, Anja: Fuel oil quality properties of wood-based pyrolysis liquids. (32 pp.) 2003
100. Virtanen, Elina: Syntheses, structural characterisation, and cation/anion recognition properties of nano-sized bile acid-based host molecules and their precursors. (123 pp.) 2003
101. Nättinen, Kalle: Synthesis and X-ray structural studies of organic and metallo-organic supramolecular systems. (79 pp.) 2003
102. Lampiselkä, Jarkko: Demonstraatio lukion kemian opetuksessa. (285 pp.) 2003
103. Kallioinen, Jani: Photoinduced dynamics of $Ru(dcbpy)_2(NCS)_2$ – in solution and on nanocrystalline titanium dioxide thin films. (47 pp.) 2004
104. Valkonen, Arto (Ed.): VII Synthetic Chemistry Meeting and XXVI Finnish NMR Symposium. (103 pp.) 2004

105. Vaskonen, Kari: Spectroscopic studies on atoms and small molecules isolated in low temperature rare gas matrices. (65 pp.) 2004
106. Lehtovuori, Viivi: Ultrafast light induced dissociation of $Ru(dcbpy)(CO)_2I_2$ in solution. (49 pp.) 2004
107. Saarenketo, Pauli: Structural studies of metal complexing schiff bases , Schiff base derived *N*-glycosides and cyclophane π-prismands. (95 pp.) 2004
108. Paasivirta, Jaakko (Ed.): CEOEC'2004, Sixth Finnish-Russian Seminar: Chemistry and Ecology of Organo-Element Compounds. (147 pp.) 2004
109. Suontamo, Tuula: Development of a test method for evaluating the cleaning efficiency of hard-surface cleaning agents. (96 pp.) 2004
110. Güneş, Minna: Studies of thiocyanates of silver for nonlinear optics. (48 pp.) 2004
111. Ropponen, Jarmo: Aliphatic polyester dendrimers and dendrons. (81 pp.) 2004
112. Vu, Mân Thi Hong: Alkaline pulping and the subsequent elemental chlorine-free bleaching of bamboo (*Bambusa procera*). (69 pp.) 2004
113. Mansikkamäki, Heidi: Self-assembly of resorcinarenes. (77 pp.) 2006
114. Tuononen, Heikki M.: EPR spectroscopic and quantum chemical studies of some inorganic main group radicals. (79 pp.) 2005
115. Kaski, Saara: Development of methods and applications of laser-induced plasma spectroscopy in vacuum ultraviolet. (44 pp.) 2005
116. Mäkinen, Riika-Mari: Synthesis, crystal structure and thermal decomposition of certain metal thiocyanates and organic thiocyanates. (119 pp.) 2006
117. Ahokas, Jussi: Spectroscopic studies of atoms and small molecules isolated in rare gas solids: photodissociation and thermal reactions. (53 pp.) 2006
118. Busi, Sara: Synthesis, characterization and thermal properties of new quaternary ammonium compounds: new materials for electrolytes, ionic liquids and complexation studies. (102 pp.) 2006
119. Mäntykoski, Keijo: PCBs in processes, products and environment of paper mills using wastepaper as their raw material. (73 pp.) 2006
120. Laamanen, Pirkko-Leena: Simultaneous determination of industrially and environmentally relevant aminopolycarboxylic and hydroxycarboxylic acids by capillary zone electrophoresis. (54 pp.) 2007
121. Salmela, Maria: Description of oxygen-alkali delignification of kraft pulp using analysis of dissolved material. (71 pp.) 2007
122. Lehtovaara, Lauri: Theoretical studies of atomic scale impurities in superfluid ^{4}He. (87 pp.) 2007
123. Rautiainen, J. Mikko: Quantum chemical calculations of structures, bonding, and spectroscopic properties of some sulphur and selenium iodine cations. (71 pp.) 2007
124. Nummelin, Sami: Synthesis, characterization, structural and

retrostructural analysis of self-assembling pore forming dendrimers. (286 pp.) 2008

125. Sopo, Harri: Uranyl(VI) ion complexes of some organic aminobisphenolate ligands: syntheses, structures and extraction studies. (57 pp.) 2008
126. Valkonen, Arto: Structural characteristics and properties of substituted cholanoates and *N*-substituted cholanamides. (80 pp.) 2008
127. Lähde, Anna: Production and surface modification of pharmaceutical nano- and microparticles with the aerosol flow reactor. (43 pp.) 2008
128. Beyeh, Ngong Kodiah: Resorcinarenes and their derivatives: synthesis, characterization and complexation in gas phase and in solution. (75 pp.) 2008
129. Välisaari, Jouni, Lundell, Jan (Eds.): Kemian opetuksen päivät 2008: uusia oppimisympäristöjä ja ongelmalähtöistä opetusta. (118 pp.) 2008
130. Myllyperkiö, Pasi: Ultrafast electron transfer from potential organic and metal containing solar cell sensitizers. (69 pp.) 2009
131. Käkölä, Jaana: Fast chromatographic methods for determining aliphatic carboxylic acids in black liquors. (82 pp.) 2009
132. Koivukorpi, Juha: Bile acid-arene conjugates: from photoswitchability to cancer cell detection. (67 pp.) 2009
133. Tuuttila, Tero: Functional dendritic polyester compounds: synthesis and characterization of small bifunctional dendrimers and dyes. (74 pp.) 2009
134. Salorinne, Kirsi: Tetramethoxy resorcinarene based cation and anion receptors: synthesis, characterization and binding properties. (79 pp.) 2009
135. Rautiainen, Riikka: The use of first-thinning Scots pine (*Pinus sylvestris*) as fiber raw material for the kraft pulp and paper industry. (73 pp.) 2010
136. Ilander, Laura: Uranyl salophens: synthesis and use as ditopic receptors. (199 pp.) 2010
137. Kiviniemi, Tiina: Vibrational dynamics of iodine molecule and its complexes in solid krypton - Towards coherent control of bimolecular reactions? (73 pp.) 2010
138. Ikonen, Satu: Synthesis, characterization and structural properties of various covalent and non-covalent bile acid derivatives of N/O-heterocycles and their precursors. (105 pp.) 2010
139. Siitonen, Anni: Spectroscopic studies of semiconducting single-walled carbon nanotubes. (56 pp.) 2010
140. Raatikainen, Kari: Synthesis and structural studies of piperazine cyclophanes – Supramolecular systems through Halogen and Hydrogen bonding and metal ion coordination. (69 pp.) 2010
141. Leivo, Kimmo: Gelation and gel properties of two- and three-component Pyrene based low molecular weight organogelators. (116 pp.) 2011
142. Martiskainen, Jari: Electronic energy transfer in light-harvesting complexes isolated from *Spinacia oleracea* and from three

photosynthetic green bacteria *Chloroflexus aurantiacus*, *Chlorobium tepidum*, and *Prosthecochloris aestuarii*.(55 pp.) 2011

143. Wichmann, Oula: Syntheses, characterization and structural properties of [O,N,O,X´] aminobisphenolate metal complexes. (101 pp.) 2011
144. Ilander, Aki: Development of ultrasound-assisted digestion methods for the determination of toxic element concentrations in ash samples by ICP-OES. (58 pp.) 2011
145. The Combined XII Spring Meeting of the Division of Synthetic Chemistry and XXXIII Finnish NMR Symposium. Book of Abstracts. (90 pp.) 2011
146. Valto, Piia: Development of fast analysis methods for extractives in papermaking process waters. (73 pp.) 2011
147. Andersin, Jenni: Catalytic activity of palladium-based nanostructures in the conversion of simple olefinic hydro- and chlorohydrocarbons from first principles. (78 pp.) 2011
148. Aumanen, Jukka: Photophysical properties of dansylated poly(propylene amine) dendrimers. (55 pp.) 2011
149. Kärnä, Minna: Ether-functionalized quaternary ammonium ionic liquids – synthesis, characterization and physicochemical properties. (76 pp.) 2011
150. Jurček, Ondřej: Steroid conjugates for applications in pharmacology and biology. (57 pp.) 2011
151. Nauha, Elisa: Crystalline forms of selected Agrochemical actives: design and synthesis of cocrystals. (77 pp.) 2012
152. Ahkola, Heidi: Passive sampling in monitoring of nonylphenol ethoxylates and nonylphenol in aquatic environments. (92 pp.) 2012
153. Helttunen, Kaisa: Exploring the self-assembly of resorcinarenes: from molecular level interactions to mesoscopic structures. (78 pp.) 2012
154. Linnanto, Juha: Light excitation transfer in photosynthesis revealed by quantum chemical calculations and exiton theory. (179 pp.) 2012
155. Roiko-Jokela, Veikko: Digital imaging and infrared measurements of soil adhesion and cleanability of semihard and hard surfaces. (122 pp.) 2012
156. Noponen, Virpi: Amides of bile acids and biologically important small molecules: properties and applications. (85 pp.) 2012
157. Hulkko, Eero: Spectroscopic signatures as a probe of structure and dynamics in condensed-phase systems – studies of iodine and gold ranging from isolated molecules to nanoclusters. (69 pp.) 2012
158. Lappi, Hanna: Production of Hydrocarbon-rich biofuels from extractives-derived materials. (95 pp.) 2012
159. Nykänen, Lauri: Computational studies of Carbon chemistry on transition metal surfaces. (76 pp.) 2012
160. Ahonen, Kari: Solid state studies of pharmaceutically important molecules and their derivatives. (65 pp.) 2012

161. Pakkanen, Hannu: Characterization of organic material dissolved during alkaline pulping of wood and non-wood feedstocks (76 pp.) 2012
162. Moilanen, Jani: Theoretical and experimental studies of some main group compounds: from closed shell interactions to singlet diradicals and stable radicals. (80 pp.) 2012
163. Himanen, Jatta: Stereoselective synthesis of Oligosaccharides by *De Novo* Saccharide welding. (133 pp.) 2012
164. Bunzen, Hana: Steroidal derivatives of nitrogen containing compounds as potential gelators.(76 pp.) 2013
165. Seppälä, Petri: Structural diversity of copper(II) amino alcohol complexes. Syntheses, structural and magnetic properties of bidentate amino alcohol copper(II) complexes. (67 pp.) 2013
166. Lindgren, Johan: Computational investigations on rotational and vibrational spectroscopies of some diatomics in solid environment. (77 pp.) 2013
167. Giri, Chandan: Sub-component self-assembly of linear and non-linear diamines and diacylhydrazines, formulpyridine and transition metal cations. (145 pp.) 2013
168. Riisiö, Antti: Synthesis, Characterization and Properties of Cu(II)-, Mo(VI)- and U(VI) Complexes With Diaminotetraphenolate Ligands. (51 pp.) 2013
169. Kiljunen, Toni (Ed.): Chemistry and Physics at Low Temperatures. Book of Abstracts. (103 pp.) 2013
170. Hänninen, Mikko: Experimental and Computational Studies of Transition Metal Complexes with Polydentate Amino- and Aminophenolate Ligands: Synthesis, Structure, Reactivity and Magnetic Properties. (66 pp.) 2013
171. Antila, Liisa: Spectroscopic studies of electron transfer reactions at the photoactive electrode of dye-sensitized solar cells. (53 pp.) 2013
172. Kemppainen, Eeva: Mukaiyama-Michael reactions with α-substituted acroleins – a useful tool for the synthesis of the pectenotoxins and other natural product targets. (190 pp.) 2013
173. Virtanen, Suvi: Structural Studies Of Dielectric Polymer Nanocomposites. (49 pp.) 2013
174. Yliniemelä-Sipari, Sanna: Understanding The Structural Requirements for Optimal Hydrogen Bond Catalyzed Enolization – A Biomimetic Approach.(160 pp.) 2013
175. Leskinen, Mikko V: Remote β-functionalization of β'-keto esters (105 pp.) 2014
176. 12th European Conference on Research in Chemistry Education (ECRICE2014). Book of Abstracts. (166 pp.) 2014
177. Peuronen, Anssi: N-Monoalkylated DABCO-Based N-Donors as Versatile Building Blocks in Crystal Engineering and Supramolecular Chemistry. (54 pp.) 2014
178. Perämäki, Siiri: Method development for determination and recovery of rare earth elements from industrial fly ash. (88 pp.) 2014

179. Chernyshev, Alexander, N.: Nitrogen-containing ligands and their platinum(IV) and gold(III) complexes: investigation and basicity and nucleophilicity, luminescence, and aurophilic interactions. (64 pp.) 2014
180. Lehto, Joni: Advanced Biorefinery Concepts Integrated to Chemical Pulping. (142 pp.) 2015
181. Tero, Tiia-Riikka: Tetramethoxy resorcinarenes as platforms for fluorescent and halogen bonding systems. (61 pp.) 2015
182. Löfman, Miika: Bile acid amides as components of microcrystalline organogels. (62 pp.) 2015
183. Selin, Jukka: Adsorption of softwood-derived organic material onto various fillers during papermaking. (169 pp.) 2015
184. Piisola, Antti: Challenges in the stereoselective synthesis of allylic alcohols. (210 pp.) 2015
185. Bonakdarzadeh, Pia: Supramolecular coordination polyhedra based on achiral and chiral pyridyl ligands: design, preparation, and characterization. (65 pp.) 2015
186. Vasko, Petra: Synthesis, characterization, and reactivity of heavier group 13 and 14 metallylenes and metalloid clusters: small molecule activation and more. (66 pp.) 2015
187. Topić, Filip: Structural Studies of Nano-sized Supramolecular Assemblies. (79 pp.) 2015
188. Mustalahti, Satu: Photodynamics Studies of Ligand-Protected Gold Nanoclusters by using Ultrafast Transient Infrared Spectroscopy. (58 pp.) 2015
189. Koivisto, Jaakko: Electronic and vibrational spectroscopic studies of gold-nanoclusters. (63pp.) 2015
190. Suhonen, Aku: Solid state conformational behavior and interactions of series of aromatis oligoamide foldamers. (68 pp.) 2016
191. Soikkeli, Ville: Hydrometallurgical recovery and leaching studies for selected valuable metals from fly ash samples by ultrasound-assisted extraction followed by ICP-OES determination. (107 pp.) 2016
192. XXXVIII Finnish NMR Symposium. Book of Abstracts. (51 pp.) 2016
193. Mäkelä, Toni: Ion Pair Recognition by Ditopic Crown Ether Based bis-Urea and Uranyl Salophen Receptors. (75 pp.) 2016
194. Lindholm-Lehto, Petra: Occurrence of pharmaceuticals in municipal wastewater treatment plants and receiving surface waters in Central and Southern Finland. (98 pp.) 2016
195. Härkönen, Ville: Computational and Theoretical studies on Lattice Thermal conductivity and Thermal properties of Silicon Clathrates (89 pp.) 2016
196. Tuokko, Sakari: Understanding selective reduction reactions with heterogeneous Pd and Pt:climbing out of the black box (85 pp.) 2016
197. Nuora, Piia: Monitapaustutkimus LUMA-Toimintaan liittyvissä oppimisympäristöissä tapahtuvista kemian oppimiskokemuksista (171 pp.) 2016

198. Kumar, Hemanathan: Novel Concepts on The Recovery of By-Products from Alkaline Pulping (61 pp.) 2016
199. Arnedo-Sánchez, Leticia: Lanthanide and Transition Metal Complexes as Building Blocks for Supramolecular Functional Materials (227 pp.) 2016
200. Gell, Lars: Theoretical Investigations of Ligand Protected Silver Nanoclusters (134 pp.) 2016
201. Vaskuri, Juhani: Oppiennätyksistä opetussuunnitelman perusteisiin - lukion kemian kansallisen opetussuunnitelman kehittyminen Suomessa vuosina 1918-2016 (314 pp.) 2017
202. Lundell Jan, Kiljunen Toni (Eds.): 22nd Horizons in Hydrogen Bond Research. Book of Abstracts. 2017
203. Turunen, Lotta: Design and construction of halogen-bonded capsules and cages. (61 pp.) 2017
204. Hurmalainen, Juha: Experimental and computational studies of unconventional main group compounds: stable radicals and reactive intermediates. (88 pp.) 2017
205. Koivistoinen Juha: Non-linear interactions of femtosecond laser pulses with graphene: photo-oxidation, imaging and photodynamics. (68 pp.) 2017
206. Chen, Chengcong: Combustion behavior of black liquors : droplet swelling and influence of liquor composition. (39 pp.) 2017
207. Mansikkamäki, Akseli: Theoretical and Computational Studies of Magnetic Anisotropy and Exchange Coupling in Molecular Systems. 2018, 190 p. (+included articles).
208. Tatikonda, Rajendhraprasad: Multivalent N-donor ligands for the construction of coordination polymers and coordination polymer gels (62 pp.) 2018